12-18-2014

Resistive Heating and Electrochromic Devices Using PET, Nylon, and Spandex Fabrics Treated With PEDOT:PSS

Whitney M. Kline
University of Connecticut - Storrs, whitney.kline@uconn.edu

Resistive Heating and Electrochromic Devices Using PET, Nylon, and Spandex Fabrics Treated With PEDOT:PSS

Whitney M. Kline, Ph.D.

University of Connecticut, 2014

Abstract

Conductive fabrics have the potential to transform the textile industry with technological innovations that include self-warming clothing, adaptive camouflage, and biomimetics. Further understanding of the construction and properties of conductive fabric may one day realize the full potential of these applications. Herein, a poly(ethylene terephthalate) (PET) synthetic leather substrate was treated with dimethyl sulfoxide (DMSO) doped poly(3,4-ethylenedioxythiophene):poly(styrenesulfonate) (PEDOT:PSS) and was found to exhibit low sheet resistance and high thermal stability. A study that measured the resistance versus the concentration of conductive material found that saturation was achieved after the addition of only 1 wt. % doped PEDOT:PSS. The treated PET reached sheet resistances as low as 2 Ω/sq. and was capable of resistive heating, and reached a maximum temperature of 150°C in less than two minutes when a 5 V potential was applied. Additionally, the fabric was soaked in water and resistively heated, self-drying in approximately 8 minutes. In another series of experiments, a stretchable electrochromic fabric device (EFD) was demonstrated by utilizing an oligomeric urethane/ionic liquid electrolyte system.

This EFD was capable of 50% deformation while still retaining its ability to change color upon the application of a potential difference. The electrochromic material used was a soluble alkylsilane-containing precursor polymer that was spray-coated onto the conductive fabric substrates, and was oxidatively converted chemically with a solution of $FeCl_3$. All of the work contained within were proof of concept experiments that may one day help realize the commercialization in such applications.

Resistive Heating and Electrochromic Devices Using PET, Nylon, and Spandex Fabrics Treated With PEDOT:PSS

Whitney M. Kline

B. Sc., Georgia Institute of Technology, 2010

A Dissertation

Submitted in Partial Fulfillment of the

Requirements for the Degree of

Doctor of Philosophy

at the

University of Connecticut

2014

APPROVAL PAGE

Doctor of Philosophy Dissertation

Resistive Heating and Electrochromic Devices Using PET, Nylon, and Spandex Fabrics Treated With PEDOT:PSS

Presented by:

Whitney M. Kline, B.Sc.

Major Advisor _____

Gregory Sotzing

Associate Advisor _____

Douglas Adamson

Associate Advisor _____

Anson Ma

Associate Advisor _____

Montgomery Shaw

Associate Advisor _____

Puxian Gao

University of Connecticut

2014

Dedicated to my family.

December 15, 2014

Acknowledgements

It is with great pleasure that I get to thank all of those who helped me in this achievement. With your advice, help, and encouragement, I was able to overcome the challenges of graduate school, and I would not be here without your support.

First and foremost, I would like to express my gratitude to my advisor, Professor Gregory Sotzing, for his guidance and motivation. His style of advisement gave me the freedom to explore my own ideas and has helped me grow as an independent scientist. With his wealth of knowledge in conducting polymers, he provided me with constructive criticisms and directed my research. I also appreciate his willingness to include his students in business meetings and discuss intellectual property as I believe this has helped prepare me for the real world. I would like to thank my associate advisors, Professors Douglas Adamson, Anson Ma, Montgomery Shaw, Rampi Ramprasad, and Puxian Gao for their suggestions and feedback, especially during my proposal and data defense.

The Sotzing research group has made my time in graduate school unforgettable and I am grateful to them all. I would like to extend my thanks to Dr. Robert Lorenzini, for collaborating with me on multiple manuscripts, and to Felicia Brodeur, for assisting me with electrochromic fabric devices. I would also like to acknowledge the other members of my group, especially Jose Santana, Amrita Kumar, Yumin Zhu, Xiaozheng Zhang, and Rui Ma for their feedback and help.

I’d like to thank the Institute of Material Science and the associates program, the electronics shop, and the machine shop. Laura Pinatti, JoAnne Ronzello, Gary Lavigne, Mark Dudley, Roger Ristau, and Lichun Zhang are always there to help and offer suggestions.

List of Figures

List of Tables

Table of Contents

Chapter 2: Experimental Methods

Chapter 3: Reverse Engineering Fabric

Chapter 4: Preparing and Characterizing Conductive Fabric

Chapter 5: Resistive Heating of Conductive Fabric

Chapter 6: Electrochromic Fabric Devices

Chapter 1: Introduction

1.1 Background

1.1.1 The Discovery and Development of Conductive Polymers

Polymers are one of the most widely used materials in the world, with applications ranging from containers to clothing. They are known to be electrical and thermal insulators, and are used as such in electrical and electronic applications which can take advantage of their very high resistivities. Two examples of this type of application are coatings for wires and cases for electrical equipment. These properties were thought to be true of all polymers, until the late twentieth century, when the first conductive polymer was discovered.

Poly(acetylene), a conjugated polymer with semi-conductor properties, was first made in 1958 by Natta and his work force and conducted electricity between $7x10^{-11}$ and $7x10^{-3}$ S/m. In 1967, by accident, Hideki Shirakawa added 1000 times too much catalyst and discovered the result was a metallic looking film which conducted electricity and turned out to be trans-poly(acetylene). By adjusting the reaction conditions, the cis and trans form of the polymer could be controlled. Alan MacDiarmid and his co-worker Alan Heeger were investigating optical properties of metallic looking polymers and had discovered that oxidation of the polymers led to physical changes. They invited Shirakawa to their laboratory and the three of them subsequently began investigating the different isomers of poly(acetylene). In 2000, the Nobel Prize in Chemistry was awarded jointly to Alan Heeger, Alan MacDiarmid and Hideki Shirakawa “for the discovery

and development of conductive polymers."[1] Because of their initial labors, the field of conductive polymers is today an important field of research for chemists and physicists.

In order for a polymer to be electrically conductive, it must imitate a metal in that it must have free electrons. Therefore, a conductive polymer must have alternating single and double bonds, such as seen in Figure 1.1. Such a bond pattern allows for the resonance stabilization of charges formed during doping.

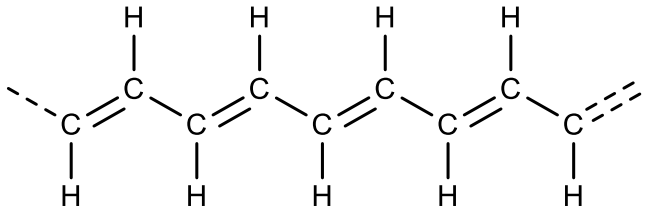

Figure 1.1: Expanded structure of poly(acetylene) depicting the alternating double and single bonds.

For conductivity to occur, electrons must either be removed from the polymer (oxidation), or inserted into the material (reduction). This process is known as doping. Two types of doping for poly(acetylene) are:

Oxidation with a halogen (p-doping)

$$(CH_n) + \frac{3x}{2} I \rightarrow (CH_n)^+ + I_3^-$$

Reduction with alkali metal (n-doping)

$$(CH_n) + xNa \rightarrow (CH_n)^{x-} + xNa^+$$

Doping poly(acetylene) by using the halogen method transforms the polymer into a good conductor by causing electrons to be removed from the polymer

creating a stable radical cation. In its original form, polyacetylene has the conductive properties of a semiconductor, whereas doped polyacetylene has the conductive properties comparable to good conductors such as copper and silver.[2] However, when a conductive polymer is subjected to increasing temperature, the conductivity increases, unlike metals, which have decreasing conductivity with increasing temperature. This behavior is because conductive polymers act like semiconductors. When energy from heat is added to the material, electrons are able to move from the valence band to the conduction band. A metal (conductor) already has electrons in the conduction band, so when heat is added the electrons move in a less organized pattern thus decreasing conductivity.

Applications for conductive polymers include anti-static substances for photographic film, corrosion inhibitors, compact capacitors, anti static coatings, electromagnetic shielding for computers (smart windows), transistors, light emitting diodes, lasers used in flat televisions, solar cells, and displays in cell phones.

1.1.2 Conductivity and Sheet Resistance

Conductivity is the ability of a material to conduct an electric current and has the SI unit Siemens per meter (S/m). To measure conductivity of a solid material, the sample is typically placed between two plates that act as electrodes. A voltage is applied to the sample and the current is measured. Using Ohm's Law and the geometry of the cell, the resistance, resistivity and conductivity can be calculated (Section 2.2.8). Unless otherwise stated, it is assumed that the

measurement was made at standard temperature (25°C) since conductivity is also temperature dependent. The conductivity of a material depends on the number of charge carriers (electrons) and their mobility. In a metal, it is assumed that all outer electrons are free to carry charge and the impedance to mobility is due to electron collisions. For an insulator, the electrons are tightly bound so that there is high resistance to charge flow. Factors that affect conductivity include the density of charge carriers, their mobility, the direction, the presence of doping materials, and temperature.

1.1.3 Conductivity in Thin Films & Fabric

The current industry standard for measuring the conductivity of thin films uses a 4-point probe method in a linear array, in which a current is applied to the two outer probes and the voltage is measure from the two inner probes. A commonly reported measurement is the sheet resistance of thin films, which also uses this 4-point probe method. The sheet resistance (R_S) is related to resistance as demonstrated in Equation 1.1.

$$R_s = R\frac{W}{L} \qquad \text{Equation 1.1}$$

The sheet resistance is a method of standardization of resistance measurements by implementing a geometric factor. Basically, for any size of thin film, the sheet resistance should remain constant. In order to minimize error, the thickness of the film and the diameter of the electrodes should be much smaller than the distance between the electrodes. Sheet resistance is reported in Ω/sq, to differentiate it from resistance because it has been geometrically standardized.

Surface resistivity is a commonly reported value for plastics since environmental factors, such as humidity, can cause quick changes in behavior. Surface resistance is the resistance of a material to the flow of electrical current across its surface. Mostly, surface resistivity is reported according to the standard ASTM D257. In this method, the electrodes are placed on the same surface and the resistance is measured. The width and length are used to convert the resistance to resistivity, according to Equation 1.2.

$$\rho = R\frac{A}{L} \qquad \text{Equation 1.2}$$

This measurement is two dimensional, contrasting with volume resistivity.

1.1.4 Electron Band Theory

According to band theory, the electrical properties of a semiconductor are determined by electronic structure in which electrons move between discrete energy states called bands. The highest occupied band is called the valence band, and the lowest unoccupied band is called the conduction band. The energy difference between these bands is called the band gap. Electrons need a certain energy to occupy a band and require more energy to move from the valence band to the conduction band. Additionally, since neither empty nor fully bands carry electricity, bands need to be partially filled in order to be electrically conducting. Figure 1.2 depicts the band gap difference between metals, insulators, and semiconductors. Metals have partially filled energy bands, allowing for high conductivities. In contrast, insulators and semiconductors have either completely full or completely empty energy bands. Most polymers are insulators and have full valence bands and empty conduction bands, which

are separated by a wide band gap. Conjugated polymers, however, have a narrow band gap characteristic of semiconductors and doping can alter the band structure by either removing an electron from the valence band (p-doping) or adding an electron to the conduction band (n-doping).

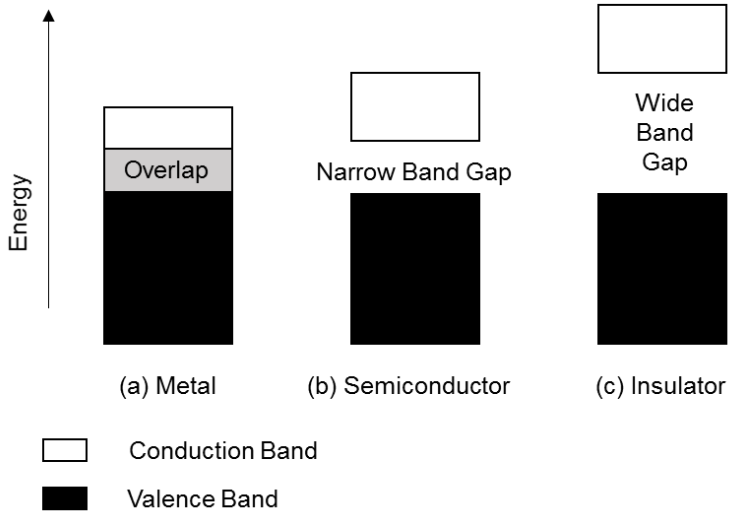

Figure 1.2: A schematic representation of energy gaps in (a) metal (b) insulator and (c) semiconductor.

1.1.5 Doping

The conductivity of a polymer can be greatly increased by doping with either an oxidative/reductive substituent or a donor/acceptor radical. Doping agents are either strong oxidizing agents or strong reducing agents and can be either neutral molecules or inorganic salts. Doping is usually quantitative; the carrier concentration is directly proportional to the dopant concentration.[3] Polymers may be doped by using a number of techniques: gaseous doping, solution doping, electrochemical doping, self-doping, radiation-induced doping, and ion-exchange doping. Due to convenience and low cost,

gaseous, solution and electrochemical doping are the most common doping methods.

Doping is accomplished by electrochemical oxidation (p-doping) or reduction (n-doping) or exposing the conjugated polymer to a charge transfer agent (dopant) in the gas or solution phase. For gaseous doping, the polymer is exposed to vapor phase dopant in vacuum. For solution doping, the dopant is dissolved in a solvent.

Traditionally doped conducting polymers involve charge movement and so during electrochemical cycling between neutral and ionic states, ions must migrate in the bulk polymer, limiting the rate at which cycling can occur. A self-doped conducting polymer is advantageous over traditionally doped polymers in that the response time is decreased. This type of doped polymer also is supposed to maintain a stable, doped state for longer periods of time and can have conductivity on the order of 1 S/cm. Some applications for this type are battery electrodes, conductive layers in electrochromic displays, semiconductor devices, field-effect transistors, and schottky diodes.

There is a distinct difference between doping a conjugated polymer, such as PEDOT and doping a conductive polymer, such as PEDOT:PSS. The doping of PEDOT is referred to as primary doping and is used to describe the addition of a material to a conjugated polymer which leads to a strong increase in the conductivity, like the addition of PSS to PEDOT. Secondary doping, as defined by MacDiarmid, refers to an additive that further increases the conductivity of an already doped polymer by up to several orders of magnitude, as is the case

with the addition of DMSO to PEDOT:PSS.[4] The main difference between the two is that primary doping is reversible, while secondary doping is permanent and remains even after the additive is removed. For the work described using PEDOT:PSS herein, a secondary dopant is the technical term for the solvents that will be added to increase conductivity. The conductivity of PEDOT:PSS can be greatly increased by the addition of a secondary dopant, such as dimethyl sulfoxide (DMSO). This dopant induces a conformational change in the PEDOT chains; untreated PEDOT:PSS has both coil and linear (expanded coil) conformations, whereas treated PEDOT:PSS has a greater amount of linear chains. The conformational change results in greater mobility of the charge carrier, therefore increasing conductivity (Fig 1.3). The secondary dopant, which is highly polar, interacts with the charged polymer chains and causes them to rearrange irreversibly into a form that is more thermodynamically favorable.

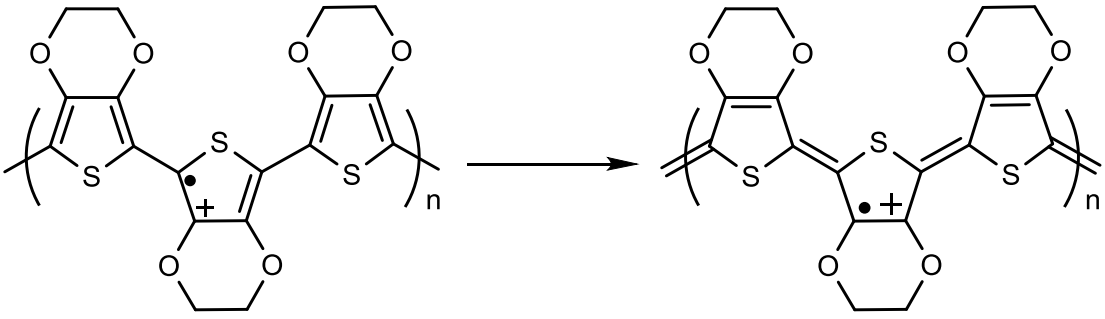

Benzoid Structure Quinoid Structure

Figure 1.3: Depiction of the conformational change in doped PEDOT.

Dopants also play an important role in the stabilization of conductive polymers. A dopant may improve the stability of a conductive polymer in atmospheric air, or it may make a polymer more resistant to oxygen or water, etc. Only small amounts of dopant are needed in order to achieve large increases in conductivity in polymers, which is similar to the doping of inorganic semiconductors. However, the two vary mechanistically in that doping an organic polymer involves only the partial oxidation or reduction of the polymer. Since poly(acetylene) was one of the first conducting polymers, it has been studied extensively, and the doping characteristics for poly(acetylene) have been applied to other conjugated polymers as well.[5]

1.1.6 PEDOT:PSS

Poly(3,4-ethylenedioxythiophene)-polystyrenesulfonic acid (PEDOT:PSS) has been one of the most successful conjugated polymers due to its advantageous properties such as high stability in its p-doped form, high conductivity, aqueous solution processing, ease of film formation, and good transparency.[6] PEDOT by itself is difficult to work with because it is insoluble in all common solvents and oxidizes quickly in air. While oxidizing PEDOT can increase the conductivity, over-oxidization drastically reduces the conductivity values most likely because of degradation of the polymer. The problem with insolubility of PEDOT in water was solved by using a water-soluble polyelectrolyte, poly(styrene sulfonic acid) (PSS), as the charge balancing dopant during polymerization. The combination of the two is known as PEDOT:PSS (Figure 1.4). It is worth noting that the concentration of PSS can be changed within the PEDOT:PSS solution;

monomers of PEDOT may range from having no monomer on the chain being oxidized up to approximately one third of the monomers
being oxidized. The extra charge induced by the oxidization from PSS is delocalized across the chain, resulting in a change in electronic density of the sulfur atoms in PEDOT.

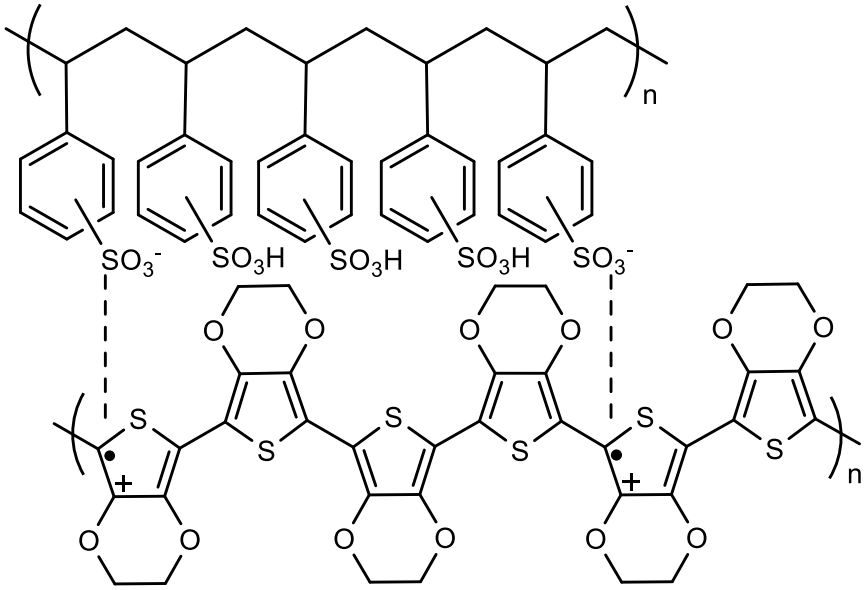

Figure 1.4: Depiction of PEDOT and the interaction between PEDOT and PSS.

Polymerization of PEDOT can be divided into two separate polymerization reactions:

a) Oxidative chemical polymerization of the EDOT monomer - Chemical polymerization of EDOT derivatives can be carried out using several methods and oxidants. The most useful method involves the polymerization of EDOT in an aqueous polyelectrolyte (most likely PSS) solution at room temperature using $Na_2S_2O_8$ as the oxidizing agent. The resulting aqueous solution is dark blue PEDOT:PSS.

b) Electrochemical Polymerization of EDOT Derivatives - This method requires only small amounts of EDOT monomer and has a short polymerization time. The electrochemical polymerization results in the formation of a sky-blue doped PEDOT film at the anode.

This work uses one of the most conductive forms (Clevios PH1000) for fabric to maximize the conductivity and minimize the resistance of the fabrics. CleviosPH1000 has a solid content between 1-1.3 % in water, a ratio of PEDOT:PSS of 1:2.5, a viscosity at 20°C of 30 mPas, a particle size of 30 nm, and conductivity reported up to 1000 S/cm after doping with 5% DMSO.[7]

1.2 Resistive Heating

1.2.1 Introduction

Resistive heating was first studied by James Prescott Joule in 1841 and is sometimes referred to as Joule heating. Joule immersed a length of wire in a fixed amount of water and measured the temperature rise as a result of a known current flowing through the wire for a 30 minute period. By varying the current and the length of the wire he deduced that the heat produced was proportional to the square of the current multiplied by the electrical resistance of the wire.

1.2.2 Fundamentals

When an electric current flows through a material that has resistance, it creates heat. Although, resistive heating does not occur in superconducting materials because these materials have zero electrical resistance in the superconducting state. Resistive heating is the result of friction created by microscopic phenomena such as retarding forces and collisions involving the moving particles

that form the current (usually electrons) and the atomic ions that make up the body of the conductor. Charged particles in an electric circuit are accelerated by an electric field but give up some of their kinetic energy each time they collide with an ion. The increase in the kinetic or vibrational energy of the ions manifests itself as heat and a rise in the temperature of the conductor. Hence energy is transferred from the electrical power supply to the conductor and any materials with which it is in thermal contact. In other words, the heat corresponds to the work done by the charge carriers in order to travel to a lower potential.

This heat generation may be intended by design, such as a heating appliance (a toaster, a hair dryer, an electric space heater, a coffee percolator, or an electric blanket). Such appliances consist of a conductor with a resistance chosen to produce the desired amount of resistive heating. In other cases, resistive heating may be undesirable (a power line, which is supposed to transmit energy, not dissipate it or an electrical transformer). In this case, the diversion of energy is often referred to as resistive loss.

The amount of heat dissipated in an object with some resistance is measured in terms of power, or the energy per unit time. Thus, power is the rate at which energy is being converted into heat inside a conductor. Power is calculated by Equation 1.3 or 1.4, where *P* is the power, *I* is the current through the resistor, *V* is the voltage drop across the resistor, and *R* is the resistance.

$$P = I \times V \qquad \text{Equation 1.3}$$

$$P = I^2 \times R \qquad \text{Equation 1.4}$$

Resistance heaters most commonly take the form of a coil, helix, or specifically designed resistive wire embedded in or wound on a heat resistant, insulating substance. Most resistive heating elements are of this type with materials such as an alloy of nickel and chrome being a common metal combination and a high-alumina ceramic being a common insulator. A nickel chrome 60% alloy can withstand temperatures of up to 1000°C without sagging or deforming. Although resistive heating is common and obviously beneficial, when uncontrolled, it can severely damage or even destroy an appliance and may lead to an electrical fire. Additionally, Resistors create electrical noise, called Johnson-Nyquist noise. The relationship between Johnson-Nyquist noise and resistive heating is explained by the fluctuation-dissipation theorem. This theorem was originally formulated by Harry Nyquist in 1928, but later proven by Herbert Callen and Theodore A. Welton in 1951. The fluctuation-dissipation theorem relies on the assumption that the response of a system in thermodynamic equilibrium to a small applied force is the same as its response to a spontaneous fluctuation. Therefore, the theorem connects the linear response relaxation of a system from a prepared non-equilibrium state to its statistical fluctuation properties in equilibrium. The theorem says that when there is a process that dissipates energy, turning it into heat, there is a reverse process related to thermal fluctuations. For example, if an electrical current is running through a wire loop containing a resistor, the current will rapidly go to zero due to the resistance because resistance dissipates electrical energy and turns it into heat. The wire loop in actuality has a small and rapidly fluctuation current caused by the thermal fluctuations from electrons and

atoms in the resistor. This fluctuation is Johnson noise, which converts heat energy into electrical energy, or the reverse of resistance.

1.2.3 Relating to Fabric

There have been many studies detailing the effectiveness of resistive heating in response to hypothermia.[8,9,10] A study comparing passive warming to resistive heating covered patients with a carbon fiber blanket and a wool blanket and in the resistive heating group, the carbon fiber blanket was heated. Mean body core temperature decreased 0.4°C/hr. for passive warming, and increased 0.8°C/hr. with resistive heating.[11] In our case, resistive heating fabric was of interest for the potential to remove the oven curing step in the manufacture of shoes. Internal curing using resistive heating isn't a new concept and has even been reported from another group at the University of Connecticut.[12] However, our method of resistive heating is much different than most because it uses a conductive polymer (PEDOT:PSS) infused fabric instead of a metal based resistive heater.

1.3 Electrochromic Fabric Devices (EFDs)[13]

1.3.1 Introduction

As our primate ancestors gradually shed their characteristic body hair, they developed a need for a protective layer against cold winters, insects, thorns, UV rays, etc. The genetic divergence of body louse (*Pediculus humanus humanus*) from head louse (*P. humanus capitis*) suggests that humans have been wearing clothing for 30,000 – 114,000 years.[14] Over time, the advantages our ancestors enjoyed by wearing rudimentary clothing made from fur, leaves, grass, and leather evolved into the multi-billion dollar textile industry we know today. Even

though there have been vast improvements in our materials and methods of manufacturing, imagine if you were to step into a time machine as you currently are – it is a safe bet that a Mesopotamian would be more interested in your smartphone than your t-shirt. The stage is set for the next generation of textile materials that will be as aesthetically pleasing as they are functional. Electrochromism is the ability of a material to change color when a potential difference is applied. The first electrochromic device (ECD) was described in 1969, when it was discovered that thin films of WO_3 reversibly changed color.[15] Since then, synthetic research efforts have yielded a diverse array of materials spanning the entire visible spectrum, and the various components of ECDs have been further refined and optimized. With these advancements, along with progress in processable conductive polymers, teams are working towards electrochromic color changing textiles for various industrial and academic applications. From cutting-edge fashion to medical diagnostic indicators embedded in clothing, the possibilities for such textiles are as infinite as the imagination.

1.3.2 Electrochromic Device History & Fundamentals

1.3.2.1 Transmissive Window-Type Devices

There are two main types of transmissive ECDs, single layer (Figure 1.5) and dual layer; these devices differ depending on the use of one or two electrochromic layers. They share the following fundamental components: films of a conductive material deposited on a substrate (the working and counter electrodes), a film of EC material (or two films, one on each electrode), and a

layer of electrolyte material. Epoxy and other sealants[16] are used to ensure the electrolyte material does not leak from the device. The conductive material carries the charge from a power source to the EC material, and, like the substrates used, are typically optically transparent. The electrolyte material ensures completion of the circuit by facilitating the transfer of ions between electrodes. The application of a potential difference, typically in the range of -3 – +3 V, changes either the π or d-electron state of the EC material and induces a color change. Electrochromic materials can switch between two colors, between multiple colorings under different potentials,[17] or between colored & colorless. There are three main classes of electrochromic materials, namely organic small molecules, (viologens,[18, 19, 20, 21] pendant oligothiophenes[22, 23]) inorganics,[24, 25, 26] and organic polymers. This review will focus solely on the latter.

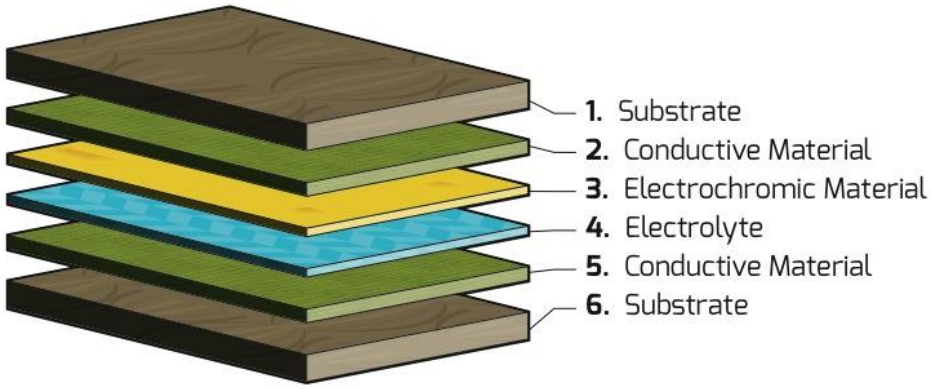

Figure 1.5: Illustration of a single layer ECD. [27]

Organic electrochromic polymers (OEPs) are highly conjugated systems with band gaps commonly ranging from 0.5 – 3.0 eV, and have several advantages over inorganics. These include multiple colorations with the same material, tuneability of the band gap, high stability, good coloration efficiency, rapid

switching times, high flexibility and relatively low cost.[28] Due to their rigid, aromatic structures, OEPs are typically not soluble or processable, and therefore have to be polymerized directly on the substrate in order to build an ECD.[29, 30] This limitation can be mitigated with the use of precursor EC polymers[31] or solubilizing substituents.[32, 33]

1.3.2.2 Reflective-Type Devices

Reflective ECDs are now ubiquitous, albeit barely noticeable to the uninitiated observer – many major automobile manufacturers are equipping new cars with electrochromic antiglare mirrors.[34] These mirrors are made with the traditional ECD architecture, and utilize two EC materials in a dual-layer ECD; the anodically colored species is a derivative of thiazine, and the cathodically colored species is a viologen.[35] A mirrored surface is placed behind the EC materials, which allows less light to reflect back at the driver as the transmissivity changes. These products are typically controlled with a photosensor, requiring no input from the driver for operation. Due to the lack of transparency of textile materials, all EFDs to date are reflective in nature.

1.3.2.3 Electrochromic Device Assembly & The Electrolyte Layer

OEPs have historically been deposited onto substrates by electropolymerization in an electrolyte/organic solvent bath before the aforementioned layers of ECDs are actually assembled. Assembly entails deposition of EC material, combining the electrodes, introducing the electrolyte material and hermetically sealing the device. Proper sealing is usually achieved with electrochemically-inert epoxies, rubbers, or acrylics,[36] and is absolutely essential for good device performance.

The electrolyte material must be physically contained within the device, and EC materials are prone to oxidation from the air and sensitive to moisture and other environmental contaminants.[3] The assembly process has been simplified with the development of in-situ polymerization:[37] With this method, all of the materials are combined, the device is sealed, and the EC monomer is electropolymerized within the ECD in one step.

Thakur et al. have published a comprehensive review covering electrolyte materials for ECDs.[38] The ionic medium to complete the circuit between the electrodes can be liquid, gel, or solid. Specific examples include poly(ethylene glycol) and poly(propylene oxide) salt solutions/crosslinked matrices and ionic liquids.[39] The ideal electrolyte material is easily processed, porous (to facilitate charge transfer and avoid a short circuit), possesses reasonable mechanical strength, is relatively impervious to temperature changes, and is not reactive to other materials within the device.

1.3.2.4 Conductive Materials for Window Type Devices

Owing to its low resistivity (1×10^{-4} Ω/cm, sometimes reported lower), optical transparency and ease of manufacture, thin films of indium tin oxide (ITO) are the most common conductive material used in ECDs.[40] ITO thin films have been made by sputtering methods,[41, 42, 43, 44] electron beam evaporation,[45] sol-gel processes,[46, 47] and electron-enhanced ion plating,[48] among others. Materials that have also been successfully utilized in ECDs include graphene[49] and poly(3,4-ethylenedioxythiophene) (PEDOT).[50] Groups are currently enhancing the conductive properties of ITO with multilayer films,[51] and improving the optical

properties of ITO with the use of antireflective coatings.[52] Because of the high costs, global scarcity of indium,[53] and technological challenges of manufacturing defect-free coatings on plastics, teams are exploring alternatives to ITO, including other metal oxide films.[54]

1.3.3 A Variety of Functionalities and Colors

Color mixing will be necessary to build a library of colors for various applications. We have published a method of high-throughput screening for the copolymerization of EC monomers.[55] In this work, two substituted propylenedioxythiophene monomers were allowed to diffuse into a polyelectrolyte matrix. After the saturation point was reached, the monomers were polymerized upon the application of a potential difference. With some calculations based on the diffusion of the monomers in the electrolyte, the feed ratio to reliably reproduce copolymers with the observed color can be elucidated. Using our methodology and the various basic colors that are plotted in Figure 1.6, any color could theoretically be generated. More thorough descriptions of the variety of available colors have been published.[56, 57]

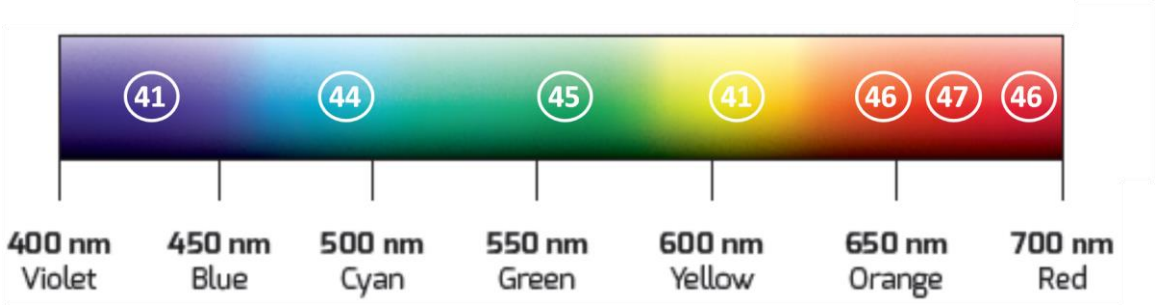

Figure 1.6 – EC polymer perceived color, in reduced states. Oxidized states have varying transmissivity. References: purple[41], blue[58], green[59], yellow[41], orange[60], orange-red[61], and red[46]. [62]

1.3.4 Transition to Textiles: Conductive Polymers

Most traditional ECDs are made using ITO-coated pieces of glass or polyethylene terephthalate (PET). The process of applying ITO to a substrate is time and resource intensive, as advanced sputter-coating techniques and infrastructure are required. In terms of conductive textiles, many CPs have been used as conductive materials, including polythiophenes,[63, 64] polypyrroles,[65, 66] polyaniline,[67, 68] and PEDOT.[69, 70, 71] To design an EFD conducive to commercial production, a CP that is easily applied to fabric and textile substrates is needed. Commercially available aqueous dispersions of PEDOT, polyaniline and polypyrrole are available and can coat a substrate in CP by simply drop casting and drying in an oven below 80°C.

The optical properties of CPs are dependent on their bandgaps.[72] All CPs are potentially electrochromic; CPs with bandgaps greater than 3eV are colorless and transparent in their undoped form, and CPs with bandgaps less than 1.5 eV are absorbing in the undoped form, but relatively transparent in the doped form.[73] Secondary dopants are an important component of conductive polymers, and teams are working towards increasing their electrical conductivity and stability.[74] A list of the conductivities of common polymers, as well as a thorough review of conductive polymers in textiles has been published.[75]

1.3.5 Electrochromic Color Changing Textiles & Fibers

The field of electrochromic color changing textiles has produced some reports of proof-of-concept devices in the literature. There are, however, myriad patents suggesting in passing that the scope of various electrochromic technologies can

be extended to include exotic substrates, including cotton, natural and synthetic fabrics,[76, 77] paper, glass, wood, leather,[78] among others.[79] Large firms are rapidly moving to patent the electrochromic fabric space; Nike has recently patented the concept of utilizing EC materials to change the color of a pair of sneakers using a smartphone app.[80] The University of Connecticut spin-off company Alphachromics, Inc. is obtaining patents on electrochromic fabric.

Paper was the first textile treated with a redox colorant. The phrase “blueprint” originated from a common method of mass-producing documents, which tinged the paper with the characteristically blue redox colorant Prussian blue. In this process, which was invented in 1842,[81] paper was impregnated with potassium ferricyanide and ammonium ferric citrate to form Prussian brown. When exposed to light, Prussian brown generated Prussian blue through redox processes. In 1843, an early facsimile machine was patented, where Prussian blue was generated by electro-oxidative consumption as an iron stylus passed over paper impregnated with potassium ferrocyanide. [82] The first report on truly electrochromic color change (based on the application of current) in a fibrous material was in 1942, when “electrolytic writing paper” was developed by the impregnation of paper with WO_3 or MoO_3, and color change was induced by the use of a stylus-like electrode.[83]

Nearly five decades later, the first modern EFDs began to emerge. The simplest type of EFD, namely one that uses a conductive polymer that also happens to be EC in nature, was demonstrated in 1991 by Kuhn et al. by polymerizing aniline and pyrrole onto fabrics.[84] For the remainder of this review, only papers with

EFDs explicitly discussing EC properties will be considered, with special consideration given to the use of an EC material in addition to a conductive polymer.

1.3.5.1 Hybrid EFDs

In 2006, a hybrid ITO/fabric EFD (hEFD) was demonstrated by Leclerc et al. using a commercially available “conductive textile” as one of the electrodes, and a piece of ITO-coated PET as the other (Figure 1.7).[85] In this work, the EC materials, poly(thiophene–*b*– 4-butyltriphenylamine) (PTBuTPA) and poly(3,6-dimethoxy-9,9-dihexylfluorene–*b*– 4-butyltriphenylamine) (PFBuTPA) were spray-coated onto ITO-coated plastic, and therefore were not impregnated into the actual fabric. Both materials operated between -1.1 and +2.2 V. PTBuTPA switched between yellow and green, and PFBuTPA switched between green and reddish-brown. It was noted that the fabric could not handle any additional potential below -1.1 V, and that switching speeds were too slow for display applications. However, the coloring was very strong for a fabric-based device. Xin et al. made a hEFD in 2013 with a polyaniline-coated piece of ITO/PET as one electrode, and a copper coated piece of fabric as the other.[86] The copper electrodes had an average resistance of 0.04 Ω/sq. The hEFD changes between black and brown between -1.0 - +1.0 V (Figure 1.8) After 15 switching cycles, deleterious effects on the color swing were observed.

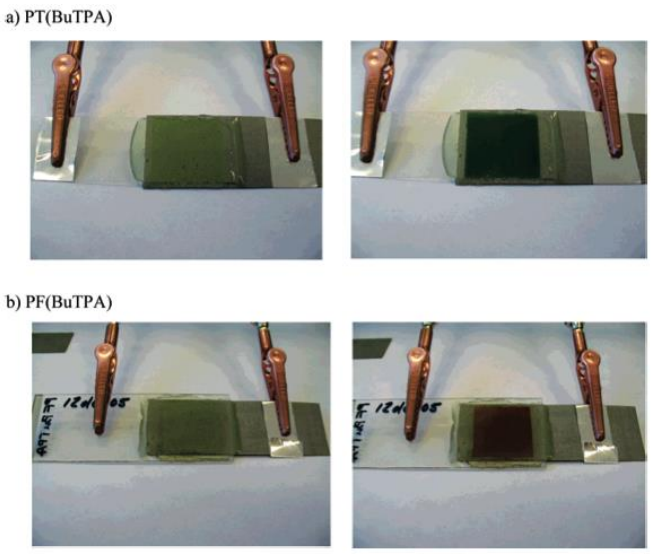

Figure 1.7: The first hEFD by Leclerc et al, 2006. Top: poly(thiophene–*b*– 4-butyltriphenylamine) Bottom: poly(3,6-dimethoxy-9,9-dihexylfluorene–*b*– 4-butyltriphenylamine)

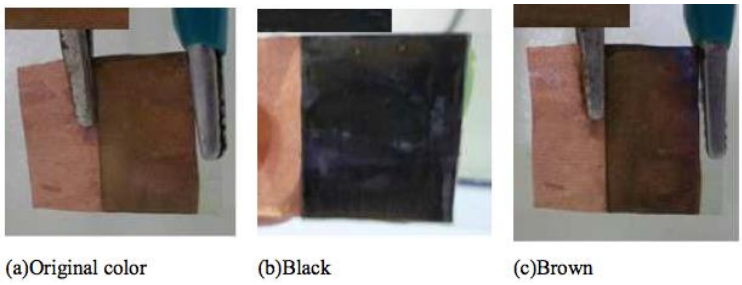

Figure 1.8: hEFD made with polyaniline on ITO/PET and copper coated fabric.

Also in 2013, Kelly et al. soaked PET and viscose (cellulose xanthate) nonwoven materials treated by screen printing with carbon black/silver in aniline, and chemically polymerized directly on the substrates.[87, 88] Conductivities ranged from 0.007 – 0.066 S/cm and 0.035 – 0.103 S/cm, respectively. After building an hEFD with the aforementioned substrates as the bottom electrodes and PET/ITO films as the upper electrode (Figure 1.9), it switched from dark gray/green to blue

with the application of -3 V, but only lasted for a maximum of 10 charging/discharging cycles. This is an extension of their work from 2011, which employed Prussian blue as both the EC material and electrolyte (Figure 1.10).[89] Kelly has been using this method for conductive fabrics since as early as 2007.[90]

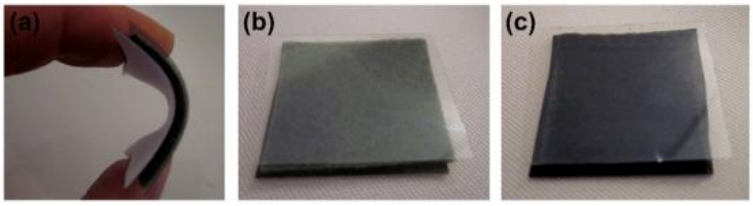

Figure 1.9: Flexible hEFD containing viscose–PAn composite (a); before (b); and after (c) the application of -3 V for 1 min.

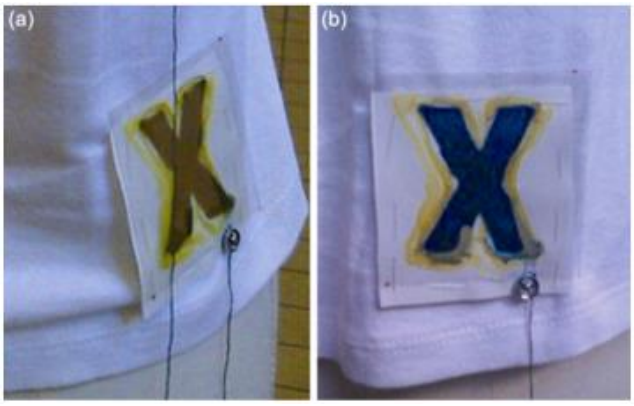

Figure 1.10: Flexible hEFD based on the previously aforementioned screen printing on fabric, using Prussian blue as the EC material.

1.3.5.2 Single-Substrate EFDs

In 2009, Li et al. prepared a single-substrate EFD (ssEFD) by polymerizing EDOT onto a PET textile via an “in-situ” chemical oxidative conversion method, switching from dark blue to light blue when the applied potential changed from -0.42 V – 0 V to 0 V – +1.0 V (conductivity = 2.67 × 10^{-2} S/cm; resistance = 1.6 ×

10^4 Ω/cm^2).[91] In the same year, this group used a similar method to make a ssEFD using polyaniline (PANI) on cotton textile (conductivity of 1.13×10^{-3} S/cm, resistance of 1.6×10^5 Ω/cm^2) that switched between yellow-green (-0.45 V – +0.3 V), and dark green (+0.3 V – +10 V).[92] In each of these reports, it was observed through SEM that a continuous film had developed across the fabrics, consisting of nanoparticles of ~100 nm and ~50-100 nm for PEDOT/PET and PANI/conductive cotton, respectively.

2011 ushered in the development of a ssEFD by coating polyester fabrics with aniline and chemically oxidizing with potassium peroxydisulfate.[93] Cases et al. reported color changing from lime green at -1 V to dark green at +2 V (Figure 1.11). Two samples of the PANI fabric were doped with HSO_4^- and Cl^-, and had surface resistivities of 1,500 and 19,000 Ω/sq., respectively.

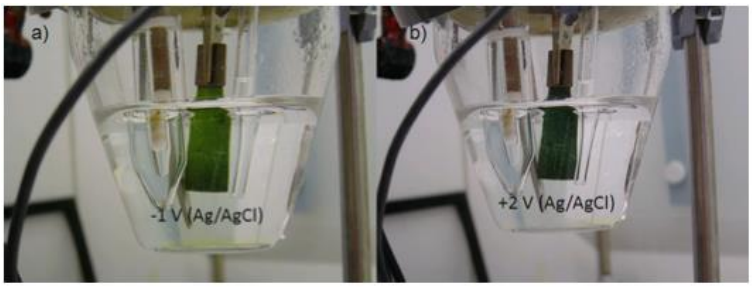

Figure 1.11: Polyester conducting fabric/PANI doped with HSO_4^-.

One year later, Mokhtari et al. made a ssEFD by soaking polyester fabric with 3-methylthiophene for 24 hr. and oxidatively converting to polymer with ferric chloride. They observed electrochromic behavior (red to yellow) under an applied voltage of +12 V.[94]

1.3.5.3 All-Organic EFD

In 2010, our research group first published in this area when we constructed an all-organic EFD using a stretchable spandex that was soaked in PEDOT:PSS,[95, 96] and spray-coated with an EC silane-containing precursor polymer (Figure 1.12).[97] The maximum conductivity achieved by multiple dipping cycles in PEDOT:PSS was 1.71 S/cm. The precursor polymer was converted at +1.1 V in an electrolyte bath to yield poly(EDOT–*b*–thiophene–*b*–EDOT), an EC that changed from blue in the oxidized state to red in the reduced state.[21] To ensure device continuity during deformation events, a stretchable polyurethane-based electrolyte[98] was utilized in later experiments.

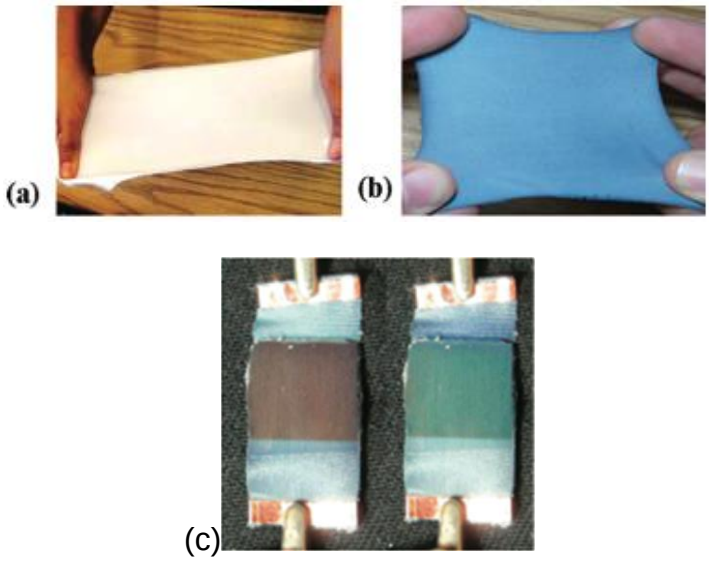

Figure 1.12: (a) unsoaked, (b) PEDOT:PSS impregnated stretchable spandex, (c) all organic true EFD

1.3.5.4 Electrochromic "Yarn"

Although not technically an EFD, in 2009 Takamatsu et al. created a stretchable helical "yarn" out of 2.1 mm × 20 mm strips of traditional PEDOT/PET film ECDs,

which could be knitted into a woven fabric-like material towards wearable displays.[99] (Figure 1.13) These devices utilized ionic liquid as the electrolyte, and switched from light blue to dark blue at –3 V. A single piece of helically wound yarn was capable of a stretch ratio of 1.41 before the device mechanically failed.

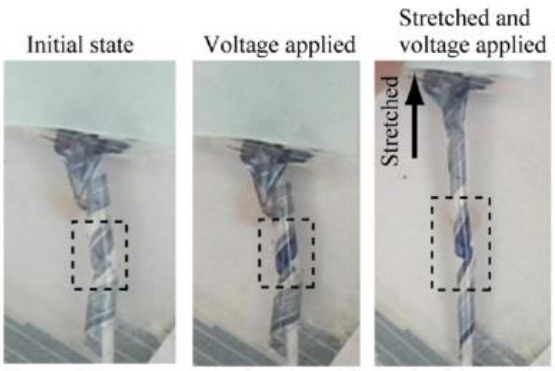

Figure 1.13: PEDOT:PSS/PET ECD cut into small yarn-like strips can be woven into a fabric-like material.

1.3.6 A Look Forward – Optimization and Applications

1.3.6.1 Difficulty Precedes Ease

Despite the exciting recent advances in the field of EFDs, there remain a number of hurdles that must be overcome before commercialization becomes viable. Below, five major problems are described and coupled with potential solutions.

1) Inherent Stability

As mentioned in the EFD section, many of the devices described in the literature did not fare well with multiple charging and discharging cycles. No long-term study on the stability of EFDs has been published, however, some traditional ECDs have performed one million switching cycles.[100] Instability in electrochromic devices can have at least four sources: mechanical,

electrochemical, chemical, and photochemical.[101] Mechanical damage can occur from mistreatment, or defects in the thin films during manufacturing. Electrochemical damage can occur from overpolarization,[102] as voltage is not uniform across a large surface. Irreversible electrochemical processes include aggregation, dimerization, and non-electrochemical oxidation. The mechanisms of degradation of EC materials in the presence of air and light have been studied.[103] Ultra-pure EC and EFD materials could mediate this somewhat, as well as UV protectant coatings, dried & degassed materials, and proper sealing.

2) Washability, Longevity

Both ECDs and EFDs demand delicate handling, and are especially sensitive to water and mechanical stress. Attempting to stick an unprotected EFD into a washing machine full of surfactant and hot water would almost surely lead to its destruction. Urethane coatings and other methods of encapsulation will be necessary to make EFDs impervious to the elements, including temperature and moisture fluctuations[104] and submersion in water, and will also provide chemical resistance against common household agents and detergents.

3) Consumer & manufacturing safety

CPs and their monomers are relatively safe according to material safety data sheets, so long as they are not accidently introduced into the eye or ingested. Electrolyte materials (salts, ionic liquids) vary greatly, but are generally innocuous. Glycols can be used as safe liquid electrolyte media. Typically, EC coatings are thin and require a commensurately small amount of material. Many

CPs are doped with harmful agents, including strong acids and organic solvents. The previously mentioned encapsulating agents could mitigate this limitation.

4) Sluggish switching speeds

Switching speeds in ECDs generally occur within a second or two, whereas switching speeds in EFDs are significantly longer. The switching speed is proportional to the conductivity of the electrodes in the device; a metal-based hEFD switches much faster than an all-organic EFD.[82] For certain applications (automotive interiors, clothing) slow switching speed may not be an issue. In thiophene-based EC materials, switching speeds have been tied to the bulkiness of substituents on the alkylenedioxy bridge.[105]

5) Contrast/optical brightness remains low for EFDs

Ideally, the conductive and EC polymers used in an EFD would be colorless. A hindrance to successful and customizable EFDs is the inherent color most conductive polymers possess. Even with the recent advances in graphene processing, the inherent black color makes carbon materials ineligible for this application. We published in this journal in 2011, showing how soaking various colored fabrics in an aqueous dispersion of PEDOT:PSS impacted the color and saturation of the electrochromic fabric (Figure 1.14).[106] Thin coatings of PEDOT:PSS can be optically transparent, [107, 108] but may not provide the necessary conductivity to switch the EFD. Thin coatings of ITO and other inorganic conductors could theoretically be sprayed onto textile materials, which should provide enough conductivity to alleviate this problem.

Figure 1.14: The effects of PEDOT:PSS on the color of base colored textile.

Another variable that has a deleterious effect on the optical brightness is light scattering. Most fabrics exhibit high surface roughness, which in turn maximizes the light scattered away from the observer. Electrospinning techniques could be used to obviate this limitation by generating smooth, continuous films of EC polymer.[109]

1.3.6.2 Potential Applications – Not Just for Fashionistas

A field that would likely adapt naturally to utilize EFDs is the fashion industry. Every article of clothing one wears could potentially be made electrochromic, with shoes being the easiest place to start (good mechanical stability, ability to store battery and delicate components in a rubber sole). Other industries that might adopt EFD technologies for their aesthetic value include furniture, automotive seats, carpet and wallpaper. In terms of functional applications, one can imagine medical diagnostic equipment embedded into clothing. Examples include a color change to indicate abnormal blood sugar levels for diabetics and a color change when the battery of a pacemaker is low. As was previously mentioned, Nike

currently holds a patent for a color change on an element of a shoe based on the number of miles run.

1.4 References

[1] http://www.nobelprize.org/nobel_prizes/chemistry/laureates/2000/press.html

[2] J. Tsukamoto, A. Takahashi, K. Kawasaki, *Japanese Journal of Applied Physics,* 1990, **29**, 125

[3] D. Kumar, R. C. Sharma, *Eur. Polym. J.*, 1998, **34**, No. 8, 1053-1060

[4] A. G. MacDiarmid, A. J. Epstein, *Synth. Met.,* 1994, **65**, 103-106

[5] A. G. MacDiarmid, R. J. Mammone, R. B. Kaner, S. J. Porter, R. Pethig, A. J. Heeger, D. R. Rosseinsky, *Phil Trans R Soc A,* 1985, **314**, 3.

[6] S. K. M. Jonnson, J. Birgerson, X. Crispin, G. Greczynski, W. Osikowicz, A. W. Denier van der Gon, W. R. Salaneck, M. Fahlman, *Synthetic Metals,* 2003, **139** , 1-10

[7] A. Elschner, S. Kirchmeyer, W. Lovenich, U. Merker, K. Reuter, 2011, *PEDOT Principles and Applications of an Intrinsicaly Conductive Polymer,* CRC Press, Boca Raton, FL

[8] Matsuzaki, Y.; et. al.; *British Journal of Anaesthesia* **90** (2003) 689-691.

[9] Perl, T.; et. al.; *Minerva Anestesiologica* **74** (2008) 687-690.

[10] Negishi, C.; et. al.; *Anesth. Analg.* **96** (2003) 1683-1687.

[11] Kober, A.; et.al.; *Mayo Clin. Proc* **76** (2001) 369-375.

[12] Ramakrishnan, B.; Zhu, L.; Pitchumani, R.; *ASME* **122** (2000) 124.

[13] Kline, W.M.; Lorenzini, R.G.; Sotzing, G.A. *Color. Technol.* 2014, 130, 1-8

[14] R Kittler, M Kayser and M Stoneking, *Current Biology*, **13** (2003) 1414.

[15] S K Deb, *Appl. Opt. Suppl*., **3** (1969) 192.

[16] H J Byker, *Electrochim. Acta,* 46 (2001) 2015.

[17] G A Sotzing, J L Reddinger, A R Katritzky, J Soloducho, R Musgrave, J R Reynolds and P J Steel, *Chem. Mater.,* **9** (1997) 1578.

[18] P M S Monk, The Viologens: Physicochemical Properties, Synthesis and Applications of the Salts of 4,4'-Bipyridine, J. Wiley & Sons, Chichester, 1998.

[19] R Cinnsealach, G Boschloo, S N Rao and D Fitzmaurice, *Sol. Energ. Mat. Sol. C.,* **55** (1998) 215.

[20] X W Sun and J X Wang, *Nano Letters,* **8** (2008) 1884.

[21] D G Kurth, J P López and W A Dong, *Chem. Commun.,* **16** (2005) 2119.

[22] Y Ohsedo, I Imae, Y Shirota, *Poly. Sci. Part B: Polym. Phys.* **41** (2003) 2471.

[23] I Imae, K Nawa, Y Ohsedo, N Noma and Y Shirota, *Macromolecules,* **30** (1997) 380.

[24] C G Granqvist, *Sol. Energ. Mat. Sol. C.,* **60** (2000) 201.

[25] S K Deb, *Sol. Energ. Mat. Sol. C.,* **92** (2008) 245.

[26] E Avendaño, L Berggren, G A Niklasson, C G Granqvist and A Azens, *Thin Solid Films,* **496** (2006) 30.

[27] Billy Shore Design, www.billyshore.com

[28] G Sonmez and F Wudl, *J. Mat. Chem*., **15** (2005) 20.

[29] D Baran, A Balan, S Celebi, B Meana Esteban, H Neugebauer, N S Sariciftci and L Toppare, *Chem. Mater*., **22** (2010) 2978.

[30] B C Thompson, Y Kim, T D McCarley and J R Reynolds, *J. Am. Chem. Soc.,* **128** (2006) 12714.

[31] M A Invernale, J G Bokria, M Ombaba, K R Lee, D M D Mamangun and G A Sotzing, *Polymer*, **51** (2010) 378.

[32] A Cirpan, A A Argun, C R G Grenier, B D Reeves, J R Reynolds *J. Mater. Chem.* **13** (2003) 2422

[33] P Shi, C M Amb, A L Dyer, J R Reynolds *ACS Appl. Mater. Interfaces* **4** (2012) 6512

[34] US patent 4902108

[35] J Zmija and M J Malachowski, *J. of Ach. in Mat. and Man. Eng..* **48** (2011) 14.

[36] C Xu, X Kong, L Liu, F Su, S Kim and M Taya, *Proc. SPIE-INT. Soc. Opt. Eng.* (2006) 6168.

[37] M A Invernale, Y Ding, D M D Mamangun, M S Yavuz and G A Sotzing, *Adv. Mat*., **22** (2010) 1379.

[38] V K Thakur, G Ding, J Ma, P S Lee and X Lu, *Adv. Mat.,* **24** (2012) 4071.

[39] W Lu, A G Fadeev, B Qi, E Smela, B R Mattes, J Ding and M Forsyth, *Science*, **297** (2002) 983.

[40] C G Granqvist and A Hultåker, *Thin Solid Films*, **411** (2002) 1.

[41] D Kim, M Park and G Lee, *Surf. Coat. Technol.,* **201** (2006) 927.

[42] F El Akkad, A Punnoose and G Prabu, *Appl. Phys. A,* **71** (2000) 157.

[43] L Meng and M P Dos Santos, *Thin Solid Films,* **303** (1997) 151.

[44] T Minami, H Sonohara, T Kakumu and S Takata, *Thin Solid Films,* **270** (1995) 37.

[45] H R Fallah, M Ghasemi, A Hassanzadeh and H Steki, *Mater. Res. Bull.,* **42** (2007) 487.

[46] C Su, T Sheu, Y Chang, M Wan, M Feng and W Hung, *Synth. Met.,* **153** (2005) 9.

[47] S R Ramanan, *Thin Solid Films,* **389** (2001) 207.

[48] S Takaki, K Matsumoto and K Suzuki, *Appl. Surf. Sci., **33/34*** (1988) 919.

[49] L Zhao, L Zhao, Y Xu, T Qiu, L Zhi and G Shi, *Electrochim. Acta*, **55** (2009) 491.

[50] A A Argun, A Cirpan and J R Reynolds, *Adv. Mat.,* **15** (2003) 1338.

[51] K H Choi, J Y Kim, Y S Lee and H J Kim, *Thin Solid Films,* **341** (1999) 152.

[52] B Chiou and J Tsai, *J. Mater. Sci. - Mater. Electron.,* **10** (1999) 491.

[53] S K Moore, "Supply Risk, Scarcity and Cellphones – The Data" *IEEE Spectrum*, 1 Mar 2008. http://spectrum.ieee.org/telecom/wireless/supply-risk-scarcity-and-cellphones

[54] T Minami, *Semicond. Sci. Technol.,* **20** (2005) S35-S44

[55] F A Alamer, M T Otley, Y Ding and G A Sotzing, *Adv. Mat.* (2013) DOI: 10.1002/adma.201302729

[56] P M Beaujuge, J R Reynolds, *Chem. Rev.* **110** (2010) 268.

[57] C M Amb, A L Dyer, J R Reynolds, *Chem. Mater.* **23** (2001) 397.

[58] P M Beaujuge, S V Vasilyeva, S Ellinger, T D McCarley and J R Reynolds, *Macromolecules* **42** (2009) 3694.

[59] G Sonmez, H B Sonmez, C K F Shen, R W Jost, Y Rubin and F Wudl, *Macromolecules,* **38** (2005) 669.

[60] A L Dyer, M R Craig, J E Babiarz, K Kiyak and J R Reynolds, *Macromolecules,* **43** (2010) 4460.

[61] T Ikeda and M Higuchi, *Langmuir,* **27** (2011) 4184.

[62] Billy Shore Design, www.billyshore.com

[63] D Knittel and E Schollmeyer, *Synt. Met.* **159** (2009) 1433.

[64] D Das, K Sen, A Saraogi and S Maity, *J. Appl. Polym. Sci.,* **116** (2010) 3555.

[65] D Kincal, A Kumar, A D Child and J R Reynolds, *Synt. Met.* **92** (1998) 53.

[66] K W Oh, H J Park and S H Kim, *J. Appl. Poly. Sci.,* **88** (2003) 1225.

[67] G E Collins and L J Buckley, *Synt. Met.* **78** (1996) 93.

[68] N Onar, A C Aksit, M F Ebeoglugil, I Birlik, E Celik and I Ozdemir, *J. Appl. Poly. Sci.* **114** (2009) 2003.

[69] W A Daoud, J H Xin and Y S Szeto, *Sens. Actuators, B,* **109** (2005) 329.

[70] H K Kim, M S Kim, S Y Chun, Y H Park, B S Jeon, J Y Lee and S H Kim, *Mol. Cryst. Liq. Crys.,* **405** (2003) 161.

[71] K H Hong, K W Oh, and T J Kang, *J. Appl. Poly. Sci.* **97** (2005) 1326.

[72] A O Patil, A J Heeger and F Wudl, *Chem. Rev.* **88** (1988) 183.

[73] R J Mortimer, A L Dyer and J R Reynolds, *Displays* **27** (2006) 2.

[74] N Romyen, S Thongyai, P Praserthdam and G A Sotzing, *J. Mater. Sci. - Mater. Electron.* **24** (2013) 2897.

[75] O Ala and Q Fan, *Research Journal of Textile & Apparel*, **13** (2009) 51.

[76] US Patent 7,618,680

[77] US Patent 6,456,418

[78] US Patent 7,420,727

[79] US Patent 2013/0010346

[80] US Patent 8,474,146

[81] P M S Monk, R J Mortimer and D R Rosseinsky, Electrochhromism and Electrochromic Devices, Cambridge University Press, Cambridge, 2007.

[82] Bain, A. UK Patent 9745, 27th May 1843

[83] P. Talmay, US Patents 2,281,013 (1942) and 2,319,765 (1943)

[84] R V Gregory, W C Kimbrell and H H Kuhn, *Journal of Coated Fabrics* **20** (1991) 167.

[85] S Beaupré, J Dumas and M Leclerc, *Chem. Mater.* **18** (2006) 4011.

[86] Q Zhang, B Xin and L Lin, *Advanced Materials Research* **651** (2013) 77.

[87] F M Kelly, L Meunier, C Cochrane and V Koncar, *Displays* **34** (2013) 1.

[88] F M Kelly, L Meunier, C Cochrane and V Koncar, *J. Display Technol.* **9** (2013) 626.

[89] L Meunier, F M Kelly, C Cochrane and V Koncar, *Indian J. Fibre Text.* **36** (2011) 429.

[90] F M Kelly, J H Johnston, T Borrmann and M J Richardson, *Eur. J. Inorg. Chem.* (2007) 5571.

[91] X Li, G Zhao, J Qian and Z Fu, *Chem. J. Chinese U.,* **30** (2009) 1052.

[92] X Li, J Qian and Z Fu, *Journal of Beijing Institute of Clothing Technology (Natural Science Edition),* **29** (2009) 12.

[93] J Molina, M F Esteves, J Fernández, J Bonastre, F Cases, *Eur. Polym. J.* **47** (2011) 2003.

[94] J Mokhtari and M Nouri, *Fibers and Polymers,* **13** (2012) 139

[95] Y Ding, M A Invernale and G A Sotzing, *ACS Appl. Mater. Inter.* **2** (2010) 1588.

[96] US Patent 8,178,629

[97] M A Invernale, Y Ding and G A Sotzing, *ACS Appl. Mater. Inter.* **2** (2010) 296.

[98] US Patent 2012/224,247

[99] S Takamatsu, K Matsumoto and I Shimoyama, Stretchable yarn of display elements. Paper presented at the *Proceedings of the IEEE MEMS,* 2009, 1023-1026

[100] W Lu, A G Fadeev, B Qi, B R Mattes *Synt. Met.* **135-136** (2003) 139-140.

[101] R D Rauh, *Electrochim. Acta,* **44** (1999) 3165.

[102] K. Doblhofer and K Rajeshwar, T Skotheim, R L Elsenbaumer and J.R. Reynolds, Handbook of Conducting Polymers, Marcel Dekker, Inc, New York, 1998.

[103] J Jensen, M V Madsen, F C Krebs *J. Mater. Chem. C* **1** (2013) 4826

[104] T Taka, *Synt. Met*. **55-57** (1993) 5014.

[105] A Kumar, D M Welsh, M C Morvant, F Piroux, K A Abboud and J R Reynolds, *Chem. Mater*., **10** (1998) 896.

[106] M A Invernale, Y Ding and G A Sotzing, *Color. Techno.* **127** (2011) 167.

[107] Q Pei, G Zuccarello, M Ahlskog and O Inganäs, *Polymer* **35** (1994) 1347.

[108] X Crispin, F L E Jakobsson, A Crispin, P C M Grim, P Andersson, A Volodin and M Berggren, *Chem. Mater.* **18** (2006) 4354.

[109] S Y Jang, V Seshadri, M S Khil, A Kumar, M Marquez, P T Mather and G A Sotzing, *Adv. Mater*. **17** (2005) 2177.

Chapter 2: Experimental Methods

2.1 Materials

2.1.1 List of Materials Used

1-butyl-3-methylimidazolium hexafluorophosphate (BMIMPF6, Sigma Aldrich) Hexamethylene diisocyanate (HDI), poly(tetrahydrofuran), M_n = 2000g/mol (Poly(THF)), hydroquinone, 4,4'-biphenol, Dimethylacetamide (DMAc), n-butyllthium (2.6M in hexanes), ethylenedioxythiophene, 2,5-dibromothiophene, tetrahydrofuran, dichloro(1,3-bisphenylphosphino)propane)nickel, magnesium bromide ethyl etherate, n-pentane, dichloromethane (DCM), iron(III) chloride, acetonitrile (ACN), dimethylsulfoxide (DMSO), 1-butyl-3-metyhlimidazolum hexafluorophosphate (BMIM), Orgacon S300, lithium trifluoromethane sulfonate, propylene carbonate, and polyethyleneglycol diacrylate (Mn = 700) were purchased from Sigma Aldrich. Dichlorodioctylsilane was purchased from Gelest, and was distilled before use. Adhesive copper tape from Newark, D-Sorbitol from ACROS, Clevios PH1000 PEDOT:PSS was purchased from Heraeus. The PET and Nylon fabrics were generously donated. The Lycra spandex was donated by Lubrizol, and the stretchable polyester fabric was cut from commercially available trouser socks purchased from a big box retailer.

2.1.2 Formulations

UV Curable Polymer Electrolyte "Normal Gel"

This gel electrolyte was made according to previous publications. The mixture contains 5 g of propylene carbonate, 5 g of poly(ethylene glycol) diacrylate (Mn = 700), 1 g of lithium trifluoromethanesulfonate, and 17.5 mg of 2,2-dimethoxy-2-

phenylacetophenone (DMPAP). The fastest method to mix the normal gel is to add the salt, initiator and PC and then sonicate (about 15 minutes). After fully mixed, add the PEGDA and sonicate briefly. The electrolyte is a colorless liquid before exposure to UV. Once exposed to 365 nm UV light, the electrolyte becomes a crosslinked transparent gel.

UV Curable Polymer Electrolyte "Stretchable Gel"

This gel electrolyte is a variation of the normal gel described above. The mixture contains 3 g propylene carbonate, 7 g PEGMA, 1 g lithium trifluoromethanesulfonate, and 17.5 mg of 2,2-dimethoxy-2-phenylacetophenone.

Polyurethane Electrolyte

125 mg of polyurethane was first dissolved in 1.25 mL DMAc, followed by the addition of 20 mg of BMIM (to make a 0.1 M mixture).

PEDOT:PSS

Orgacon S300 and Heraeus Clevios PH1000 were used as received and doped with dimethyl sulfoxide (DMSO) or Ethylene Glycol.

2.2 Characterization Techniques

2.2.1 Thermal Analysis (Thermogravimetric Analysis & Differential Scanning Calorimetry)

Thermogravimetric analysis (TGA) and differential scanning calorimetry (DSC) were primarily used in the initial determination of fabric compositions. TGA was used to determine the degradation temperature of each fabric. All TGA measurements were executed on a TA Instruments Q500, and data was

examined using TA Universal Analysis software. Oxygen was chosen as the sample gas and all samples were heated at a rate of 10°C/min.

DSC was used to determine the glass transition temperature and melting temperature of each of the fabrics. DSC measurements were conducted on either a TA Instruments Q100 or Q20, using nitrogen as the sample gas. The typical heating and cooling rates were 10°C/min. The samples were first heated to just below the degradation temperature, as determined by TGA, in order to clear the thermal history. The samples were then cooled to the limits of the instrument and the glass and melting temperatures were recorded on the following heating cycle. Data was examined using TA Universal Analysis software.

2.2.2 Optical Analysis (ATR IR Spectroscopy)

Attenuated total reflection (ATR) is a sampling technique that was used in conjunction with infrared spectroscopy (IR) in order to determine the fiber chemical compositions. Results were run through a commercial database to obtain the polymer. The Japanese government maintained SDBS[110] and this text[111] were used for additional analysis assistance.

2.2.3 Optical Microscopy

A Nikon Metaphot microscope was used for optical microscopy.

2.2.4 Electron Microscopy

All Field emission scanning electron microscopy (FESEM) was done using a JEOL JSM-6330F. All samples were sputter coated with a thin layer of Au/Pd prior to imaging, which is needed for non-conductive samples to be visible in the

electron microscope. Film thickness values from FESEM were determined using ImageJ software.

2.2.5 Mechanical Analysis

Stress/strain data was obtained with a dynamic mechanical analyzer (TA Instruments DMA 2980).

2.2.6 Cyclic Voltammetry (CV)

Cyclic voltammetry (CV) is a widely used technique for determining electrochemical information. For a new conjugated polymer, CV is used to measure the oxidation and reduction potentials, which can then be used to polymerize the monomer electrochemically. These values are also used as guidelines when cycling the polymer between the oxidized and reduced states to observe color change.

2.2.7 Chronocoulometry (CC)

The determined oxidation potential from CV can be used to electropolymerize an electroactive monomer in electrochromic devices. In this technique, the change in potential is kept very small in order to keep the potential almost constant during the polymerization process. This technique is also used to cycle between a positive and negative potential to observe the electrochromic change.

2.2.8 Sheet Resistance

In the beginning of this work, resistances were measured using a two point probe. In this technique, current is sent through one probe and exits the other and the voltage drop is measured between the probes. The resistance (R) is then calculated using Ohm's Law (Equation 2.1),

$$R = \frac{V}{I}$$ Equation 2.1

where *V* is the voltage and *I* is the current. Resistance is related to resistivity (ρ) by Equation 2.2.

$$R = \rho \frac{L}{A} = \rho \frac{L}{tW}$$ Equation 2.2

where *L* is the length, *A* is the cross-sectional area, *t* is the thickness, and *W* is the width. The sheet resistance (R_S) is related by Equation 2.3.

$$R = Rs \frac{L}{W}$$ Equation 2.3

and can be calculated according to Equation 2.4.

$$R_s = \frac{\rho}{t}$$ Equation 2.4

However, this method does not account for contact resistance, which can be the same magnitude as the sheet resistance. In order to avoid contact resistance, a four-line probe was used to measure the sheet resistance of conductive fabrics, and was fabricated previously in our group.[112] (Figure 2.1). This technique uses four electrode contacts spaced evenly apart. The current is applied to the outer two probes and the voltage is measured between the inner two probes with a high impedance voltmeter. In our lab, current was applied to the outer two copper wires using a Keithley 224 Programmable Current Source and voltage was measured using a Keithley 196 System Digital Multimeter. The distance between each of the copper lines is 0.35cm. The red rubber piece is placed on top of the sample to keep the surface from being damaged. The top acrylic plate screws on for constant pressure.

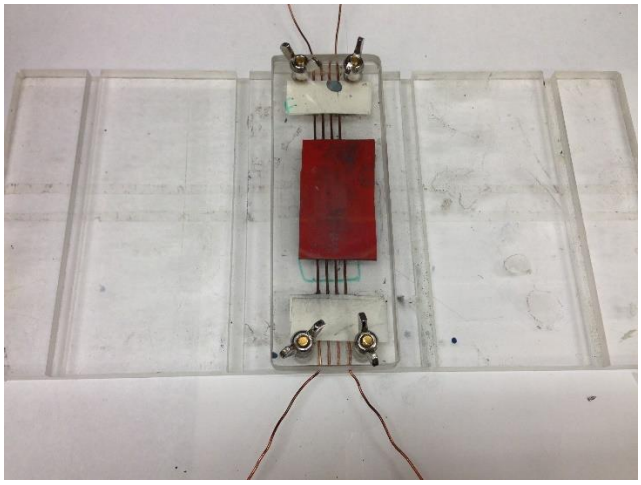

Figure 2.1: The four-line probe.

2.2.9 Colorimetry

A PhotoResearch PR-670 colorimeter with a 10° standard observer angle and a measurement range of 360 to 860nm in 1nm intervals was used for color measurement. The EFD was mounted in a black box that was illuminated with a D65 standard illuminant light. Reported values for the color were in the L*u*v* color space.

2.2.10 Ionic Conductivity

An Agilent 4284A precision LCR meter was used for measuring ionic conductivity of the polyurethane electrolytes. The measuring container is shown in Figure 2.2.

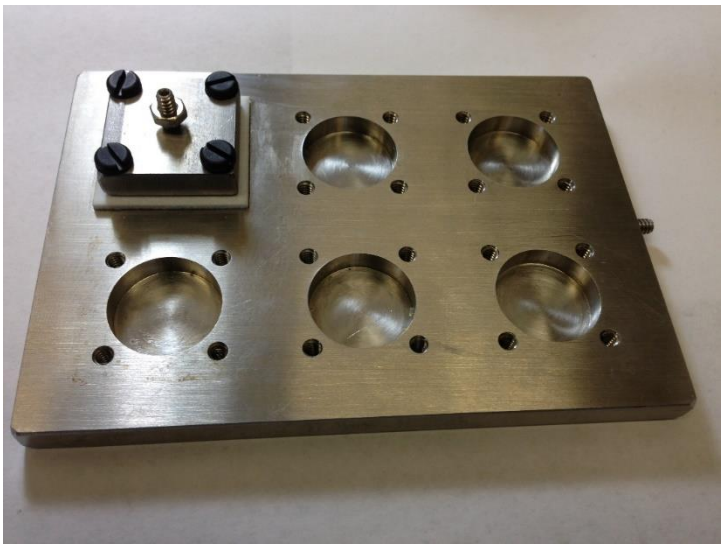

Figure 2.2: Cell used for ionic conductivity of electrolytes.

Each cell has a diameter of 2 cm and a depth of 5.442 mm. The electrolyte is poured into the cell and a Teflon spacer is used to separate the bottom plate from the top. Impedance (*Z)* and Degrees (Θ) were measured and used to calculate ionic conductivity as per Equation 2.5,

$$\sigma = \frac{L}{AR} \qquad \text{Equation 2.5}$$

where σ is the ionic conductivity, *L* is the sample thickness, *A* is the sample area, and *R* is the resistance. When Θ is close to zero, *R* can be considered the same as *Z.*

2.3 References

[110] Spectral Database for Organic Compounds, SDBS. Maintained by the National Institute of Advanced Industrial Science and Technology (AIST), Japan. http://sdbs.db.aist.go.jp/sdbs/

[111] Pretsch, Ernö, Bühlmann, Phillippe and Badertscher, Martin. *Structure*

Determination of Organic Compounds: Springer Berlin, Heidelberg, 2009.

[112] Hiremath, R. K.; Rabinal, M. K.; Mulimani, B. G. Review of Scientific Instruments.

2006, 77, 126106.

Chapter 3: Reverse Engineering Fabric

3.1 Introduction

The fabrics contained within this work were all obtained commercially. As such, very little was known about the chemical composition, additives, or properties of the fabrics. Characterization techniques described in Chapter 2 were employed in order to better understand each fabric.

3.2 Grey PET (Synthetic Leather)

The grey PET was described as an unfinished synthetic leather backing with a 0.75 mm thickness. See Figure 3.14 for a visual comparison of the grey and white PET.

3.2.1 Attenuated Total Reflectance Fourier Transform Infrared Spectroscopy (ATR FTIR)

Traditionally, the IR beam must be passed through the sample, which causes problems in sample preparation for liquids and solids because the intensity of the spectral features is determined by the sample thickness. For ATR FTIR, the crystal is placed in contact with the sample surface and the IR beam is directed through the crystal, creating an evanescent wave from the internal reflectance. The crystal must be optically dense and have a higher refractive index than the sample for this technique to work or the light will be transmited rather than internally reflected in the crystal. Additionally, there must be good contact between the sample and the crystal surface because the wave only protrudes a few microns beyond the crystal surface and into the sample.[1] The resulting ATR

FTIR spectra (Figure 3.1) was analyzed using a commercial database and a match was found for PET. The absorption bands at 3100-2800 cm^{-1} are attributed to aromatic and aliphatic –C-H bond stretching, 1720 cm^{-1} to the ester carbonyl bond stretching, 1300 cm^{-1} to the ester group stretching, and 1100 cm^{-1} to the methylene group.

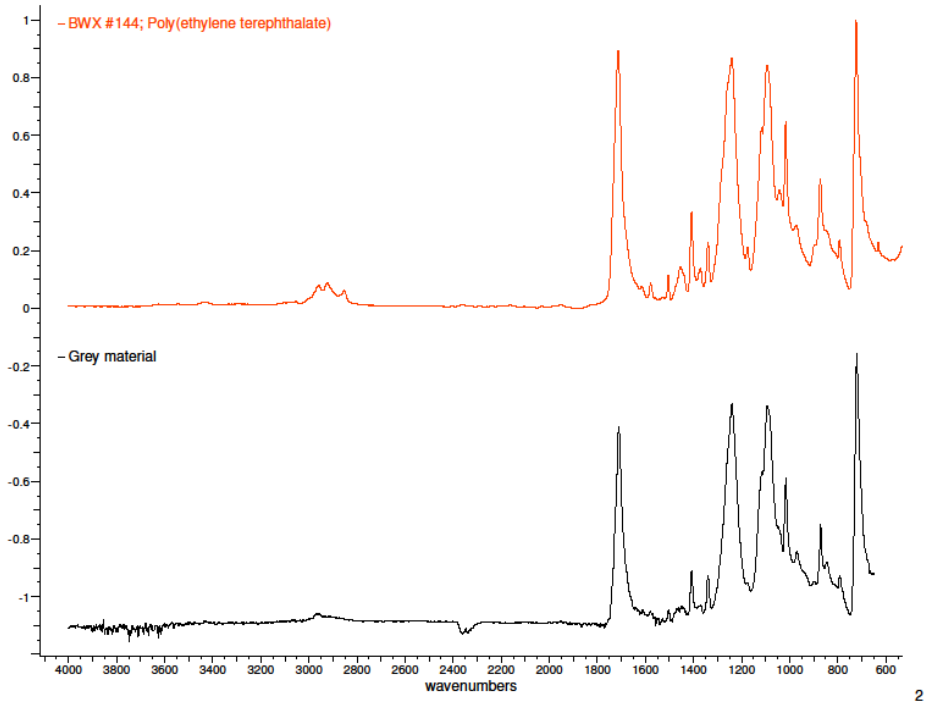

Figure 3.1: ATR FTIR comparison of grey leather and commercial PET.

3.2.2 Thermal Analysis

3.2.2.1 Thermogravimetric Analysis (TGA)

The degradation temperature at 3% weight loss in oxygen was 313°C. See Figure 3.15 for a comparison between the white and grey PET degradation curves.

3.2.2.2 Differential Scanning Calorimetry (DSC)

DSC was run for the grey PET at 10°C/min in nitrogen. The first heating cycle revealed an endothermic peak at 150°C that disappeared upon a second heating cycle and so was likely due to stresses in the material from manufacturing. The melting point, as recorded on the second heating, was 238°C. The first and second heating cycles are shown in Figure 3.2.

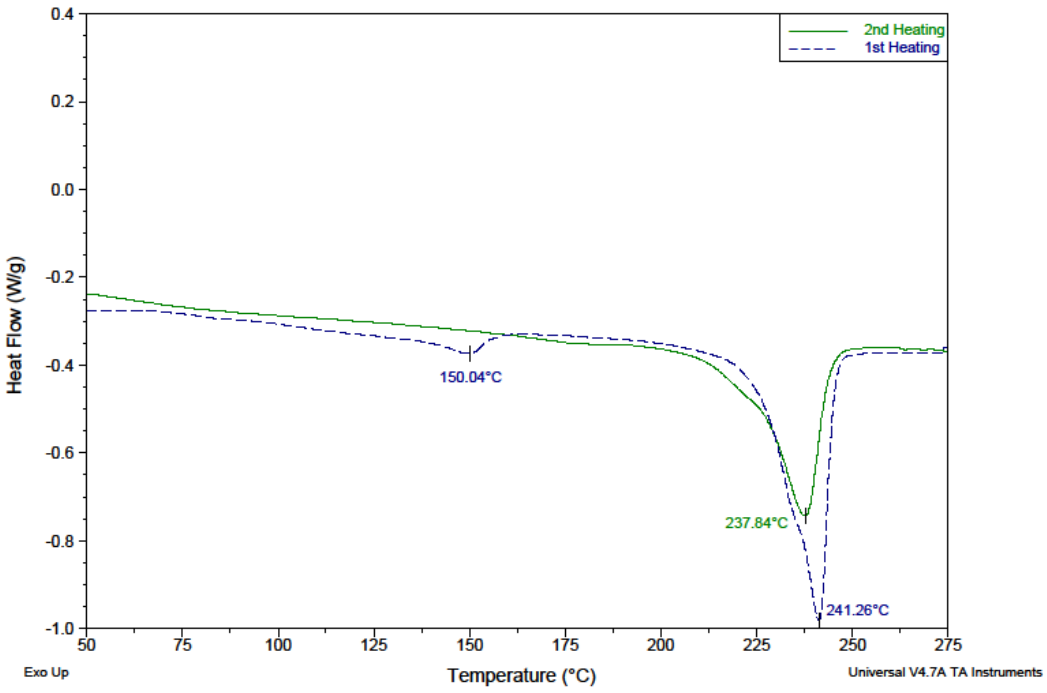

Figure 3.2: First and second heating cycles for grey PET.

The glass transition temperature was determined from the second heating to be about 64°C and was very broad (Figure 3.3).

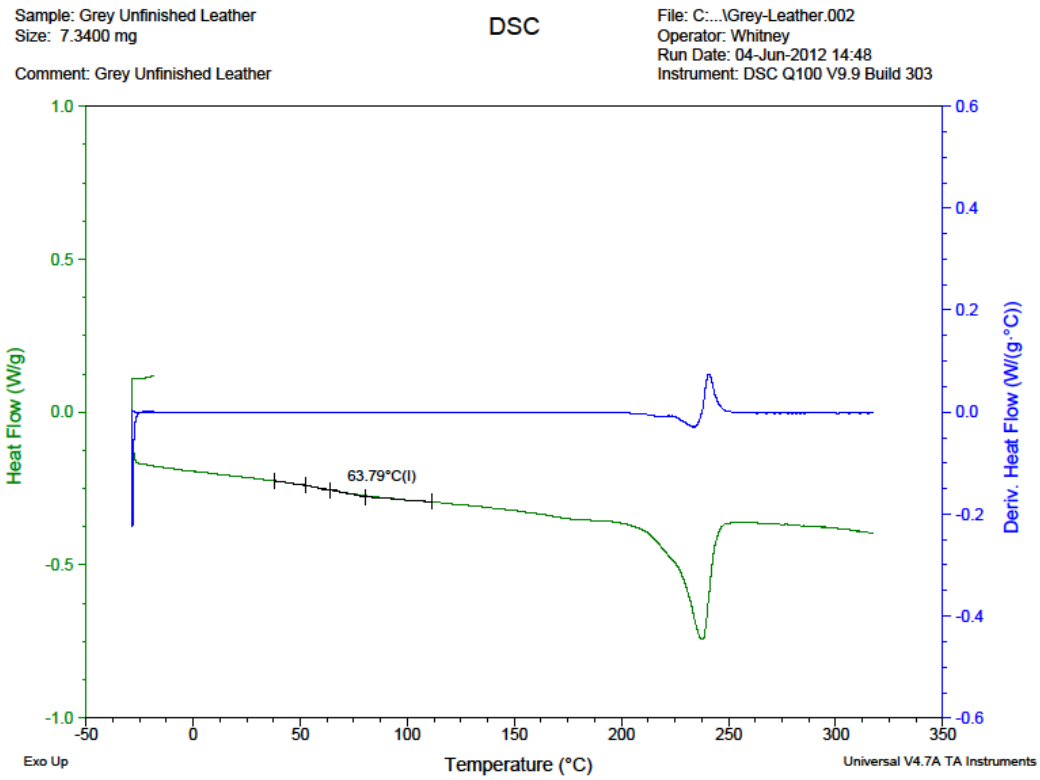

Figure 3.3: Determination of glass transition in grey PET.

3.2.2.3 Thermal Comparison to Commercial PET

The thermal data compared to that of commercial PET can be seen in Table 3.1.

Material	T_d (°C)	T_g (°C)	T_m (°C)
Grey PET	313	64	238
Commercial PET	~320	67-81	>250

.

Table 3.1: Thermal analysis of fabric PET vs commercial PET.

PET held isothermal at 310°C did not significantly decompose, however it did start to decompose at 320°C.[2]

3.2.3 Elemental Analysis

For additional confirmation that the leathers were PET, elemental analysis was performed. According to the structure of PET (Figure 3.4), there are 4 oxygens, 10 carbons, and 8 hydroges, yielding a theoretical molecular weight of 192 g/mol. The theoretical and experimental analysis results are shown in Table 3.2.

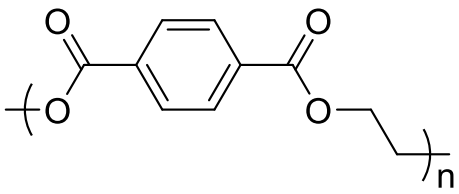

Figure 3.4: Structure of PET.

Element	Experimental	Theoretical
Carbon	60%	62.5%
Hydrogen	4%	4.2%
Nitrogen	0%	0%

Table 3.2: Experimental and theoretical elemental analysis

3.2.4 Gas Chromatography Mass Spectrometry (GC-MS)

Trace amounts of water, DMSO, propylene carbonate, BHT, and some aromatic compounds were found in the untreated fabric. See Section 4.2.2.3 for a comparison of the results between untreated and treated grey PET as well as the GC-MS trace.

3.2.5 Optical Microscope

Optical microscope images were not detailed enough to help determine characteristics of the fabric. The dark spots on the 5x images are from the microscope lens.

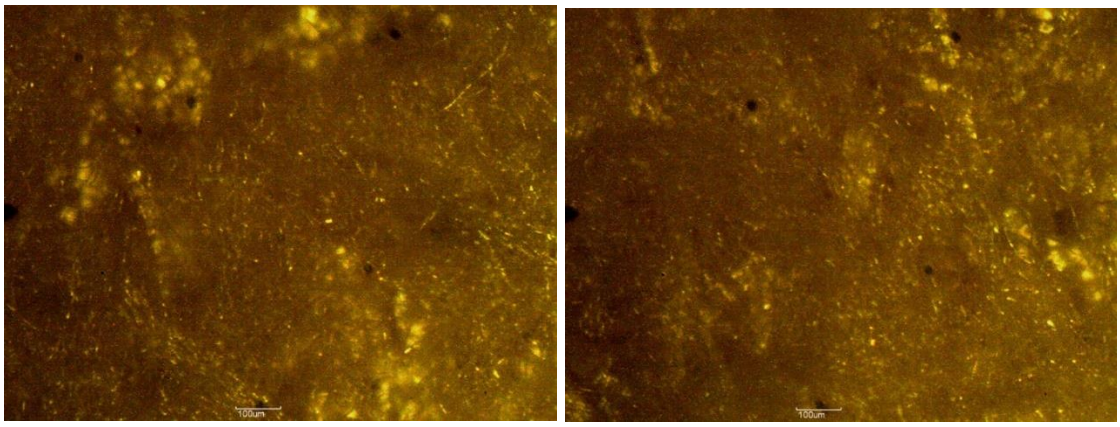

Figure 3.5: 5x magnification of grey PET surface.

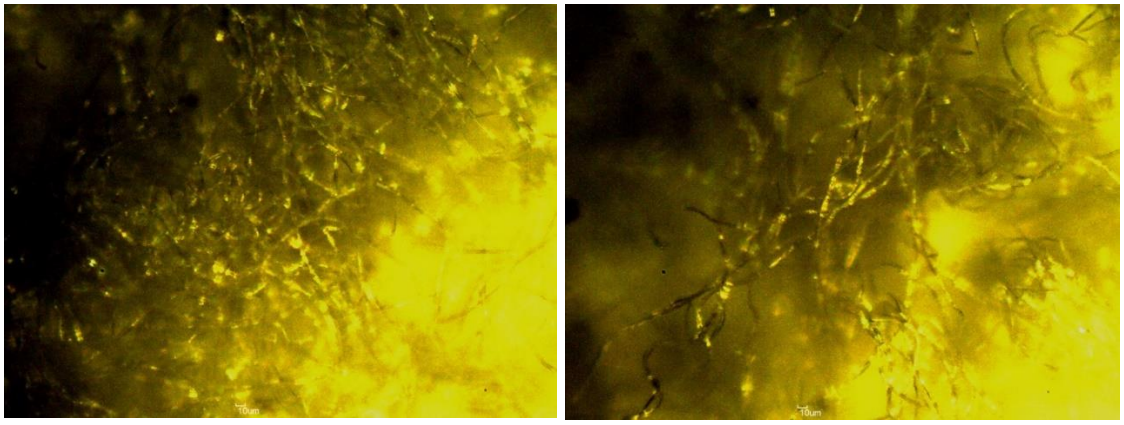

Figure 3.6 10x magnification of grey PET surface.

3.2.6 Microscopy

3.2.6.1 Scanning Electron Microscopy (SEM)

It is evident from the following SEM images that the grey PET is nonwoven. Further imaging reveals bundles of fibers that are randomly oriented.

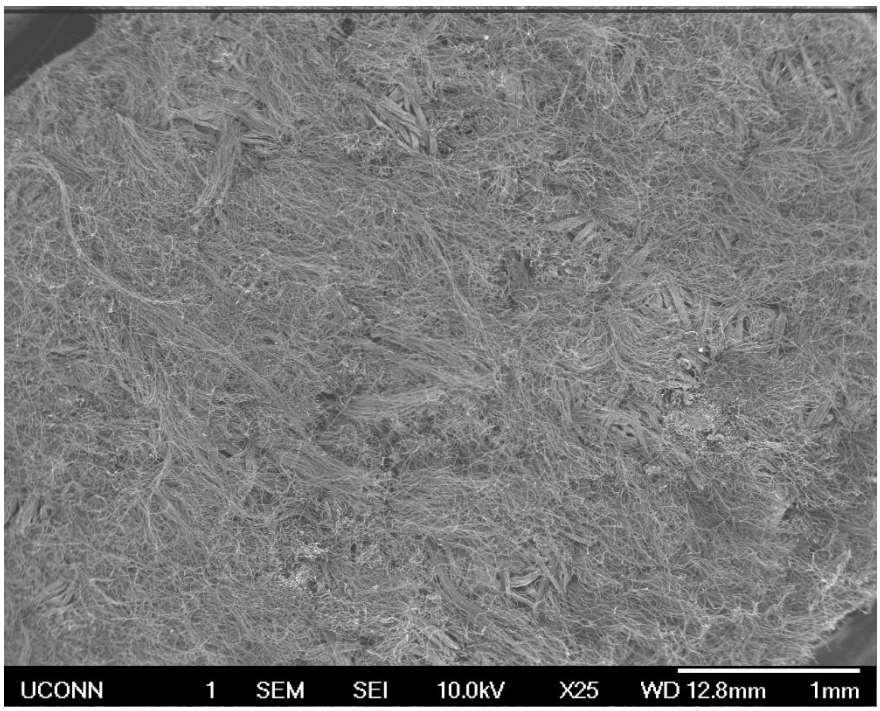

Figure 3.7: SEM X25 magnification of grey PET surface.

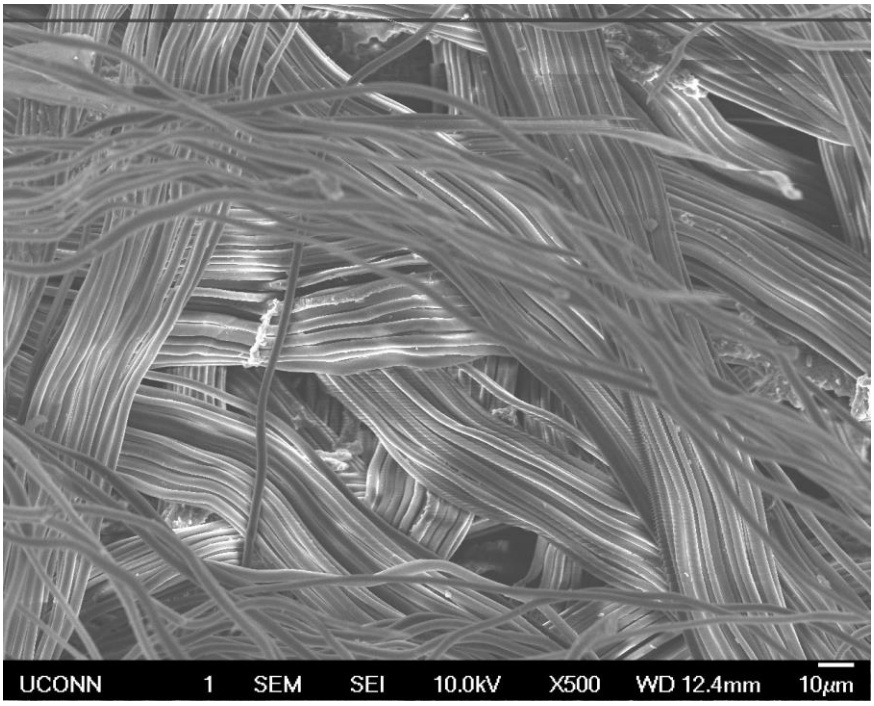

Figure 3.8: SEM X500 magnification of grey PET fiber bundles.

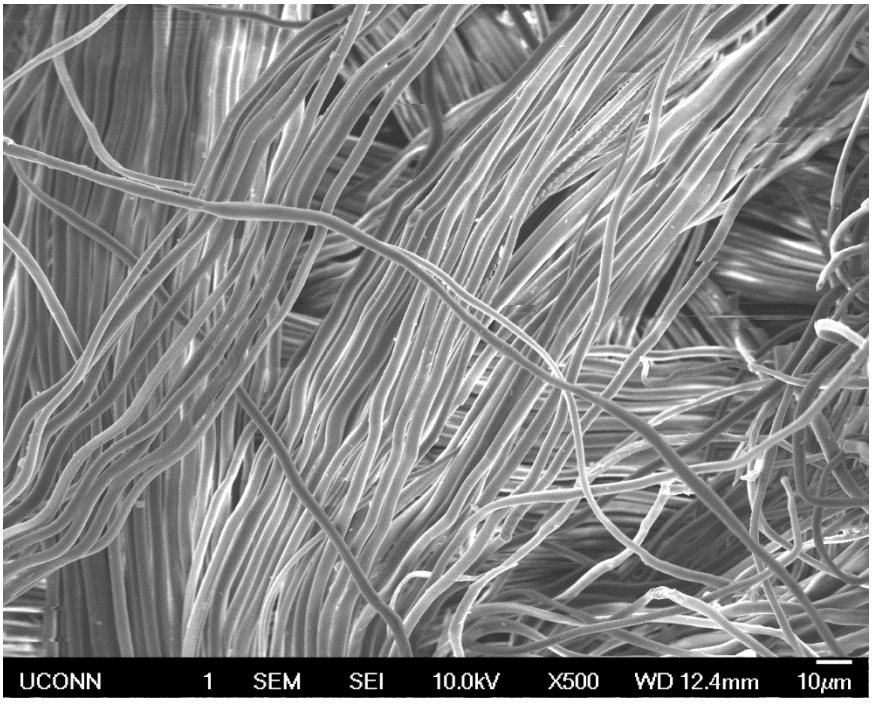

Figure 3.9: SEM X500 magnification of more grey PET fiber bundles.

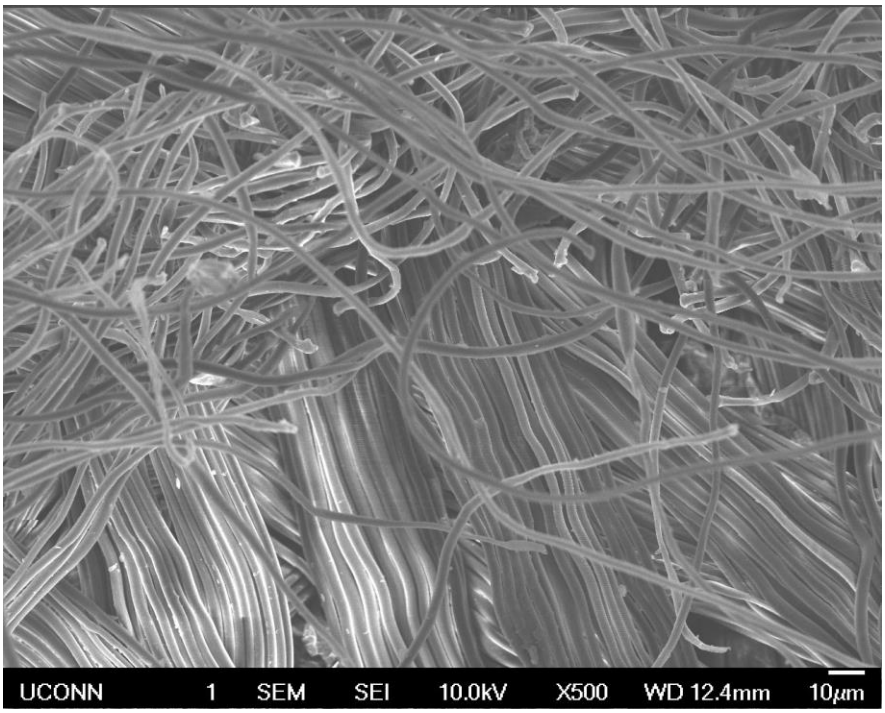

Figure 3.10: SEM X500 magnification of grey PET surface and fiber bundles.

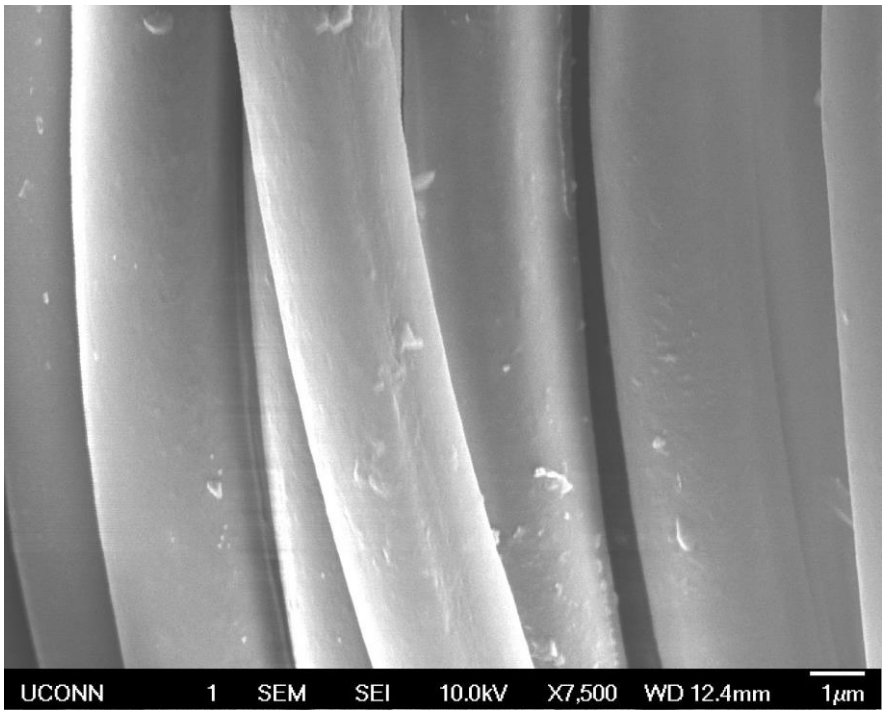

Figure 3.11: SEM X7500 magnification of grey PET fibers.

Energy Dispersive X-Ray Spectroscopy (EDS) was briefly tested on the grey PET. In this technique a point was chosen from the current image while using SEM and an elemental analysis was performed at that point. The results showed silicon in addition to the expected elements.

3.2.6.2 Transmission Electron Microscopy (TEM)

TEM imaging was performed on the grey PET when silicon was discovered by EDS. Figure 3.12 depicts a cross section of a PET fiber, where the dark spots are silica particles within the fiber. The average fiber diameter was 3 μm and the average silica particle size was 86 nm +/- 33 nm.

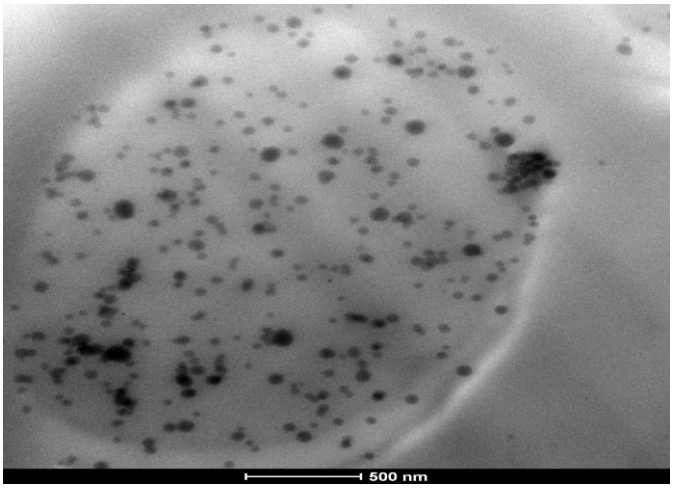

Figure 3.12: TEM fiber cross section of PET.[3]

The silica particles were added to the fabric as a de-lustering agent.

3.2.7 Mechanical Data

A sample press was used to prepare uniformly sized dog-bone-shaped pieces of grey PET.

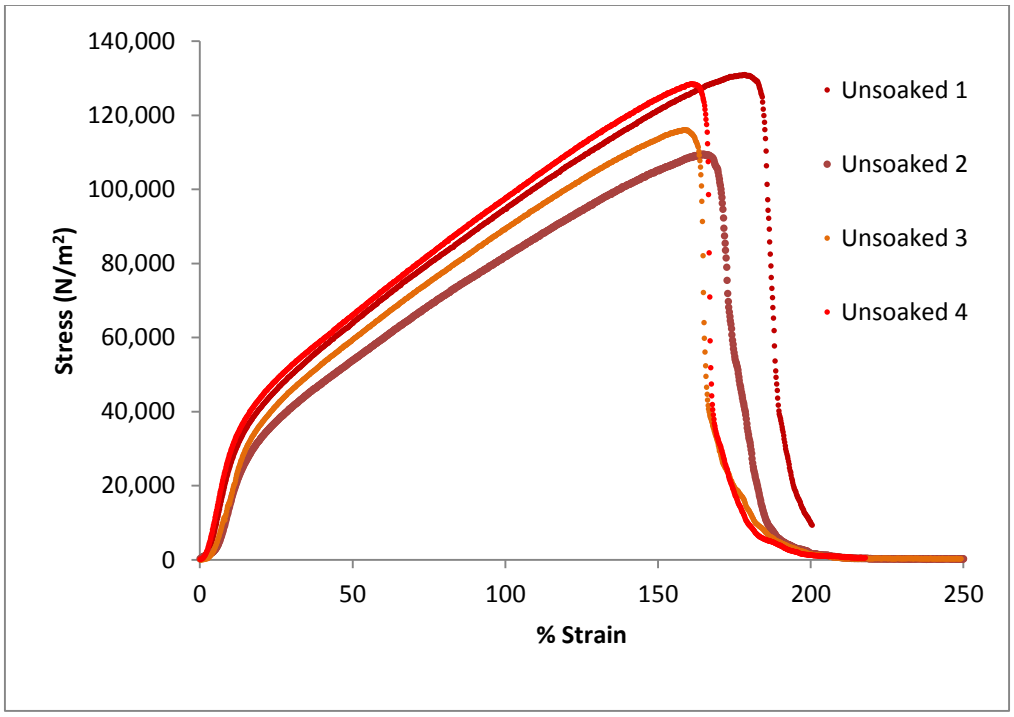

Figure 3.13: Stress/strain curves for the grey synthetic leather.

Sample	Young's Modulus (N/m^2)	Tensile Strength (N/m^2)	Elongation-to-break (%)
Unsoaked 1	3,720	130,000	178
Unsoaked 2	2,903	109,000	164
Unsoaked 3	2,899	116,000	159
Unsoaked 4	3,986	128,000	161
Average	**3,377**	**121,000**	**166**

Table 3.3: Mechanical data for grey PET.

3.2.8 BET

Brunauer-Emmett-Teller (BET) analysis measure nitrogen adsorption as a function of relative pressure. A 5 Point BET Analysis yielded the following results:

- Specific Surface Area: 1.957536 m^2/g
- Sample Size: 0.5072 g
- Surface Area: 0.992862 m^2/g
- Slope: 1515.462646
- Intercept: 263.568329
- Correlation coefficient, r: 0.878315

The BET results were poor because the correlation should be close to 1 and the intercept should be close to zero.

3.3 White PET (Synthetic Leather)

Besides the difference in color (Figure 3.14), the grey and white leathers differed greatly in wetting capability.

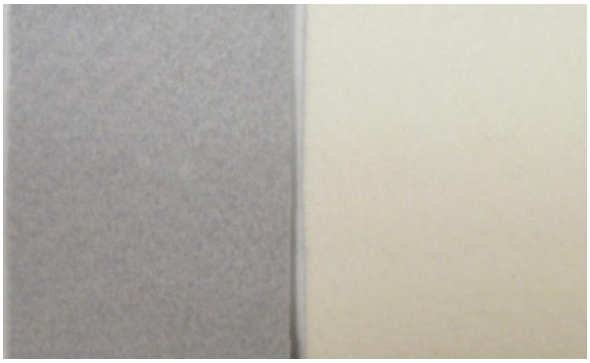

Figure 3.14: Visual comparison of grey (left) and white (right) synthetic leather

Leather	Thickness (mm)
Grey	0.75
White	1.30

Table 3.4: Leather thickness comparison.

The white PET was used as a comparison for the grey PET because of the lack of silica nanoparticles in the fibers.

3.3.1 ATR FTIR

The white synthetic leather matched the same commercial PET as the grey (Figure 3.1).

3.3.2 Thermal Analysis

3.3.2.1 TGA

TGA was run on the grey and white synthetic leathers and yielded 3% weight loss at temperatures of 313°C and 265°C respectively. The samples were run in oxygen and ramped at 10°C/min up to 600°C.

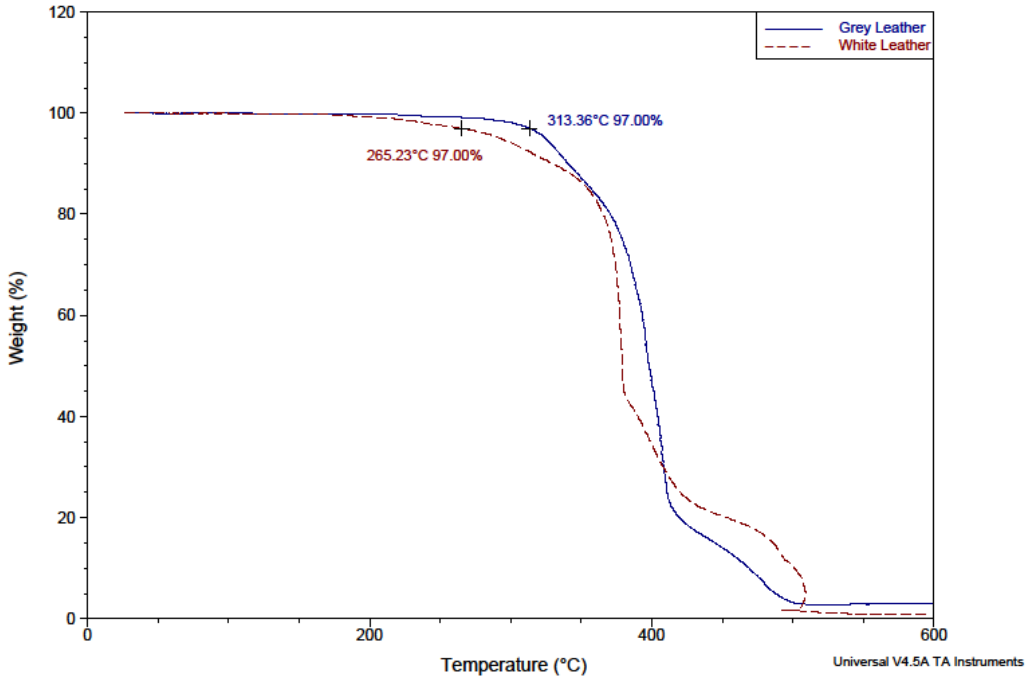

Figure 3.15: Degradation temperature and curve comparison of grey and white unfinished synthetic leathers.

3.3.2.2 DSC

DSC was performed on each of the leathers to determine any melting, glass, or crystallization temperatures. The first heating cycle displayed a small endothermic event for each leather that disappeared upon second heating indicating stresses in the material due to processing (Figure 3.16).

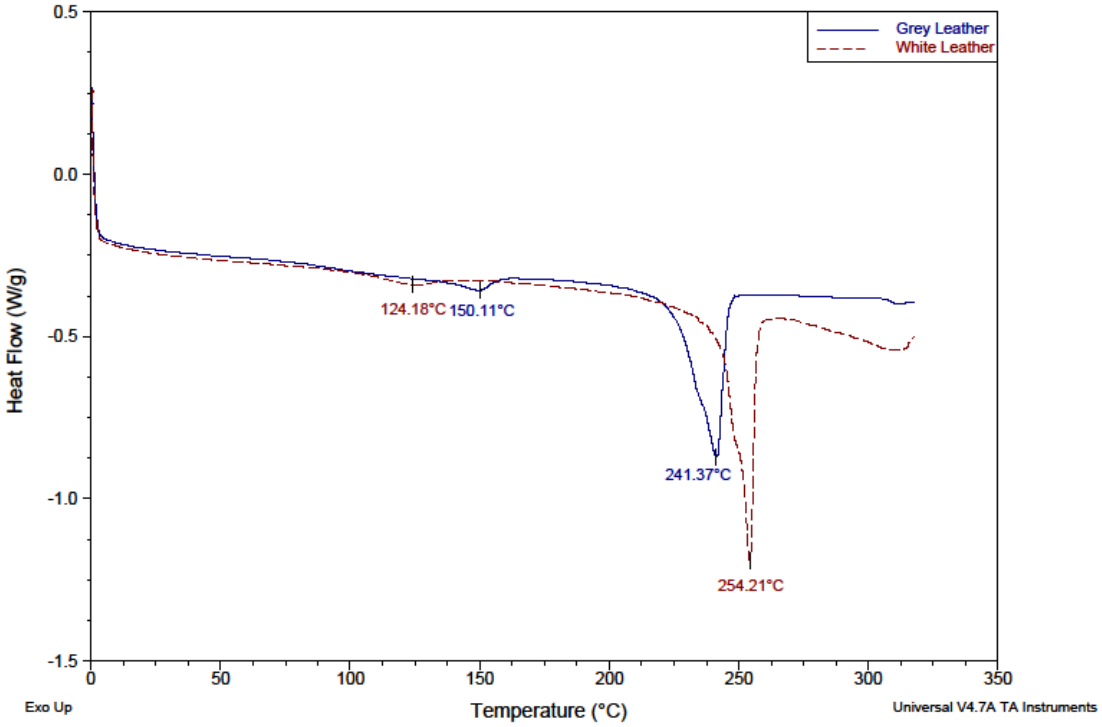

Figure 3.16: DSC first heating trace comparing the grey and white unfinished synthetic leathers.

The second heating cycle yielded melting temperatures of 238°C for the grey leather and 246°C for the white leather (Figure 3.17).

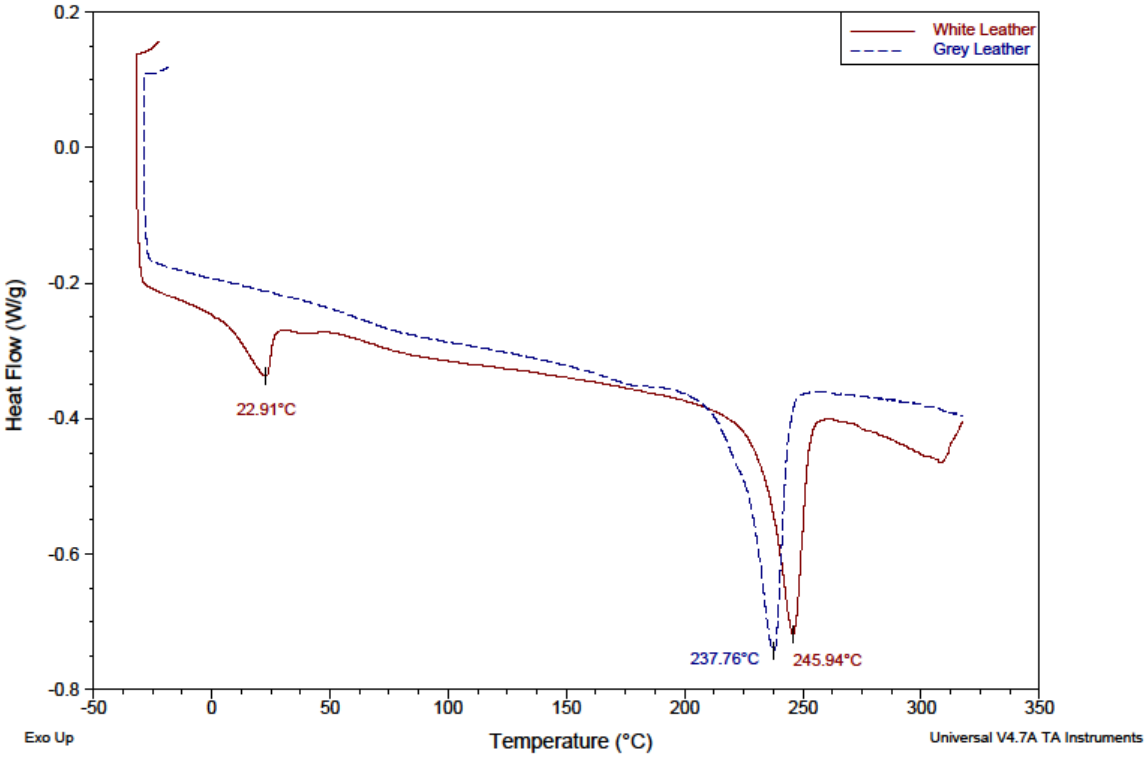

Figure 3.17: DSC second heating trace comparing the grey and white unfinished synthetic leathers.

The white leather displayed another endothermic event near room temperature that could be from additives in the material.

3.3.3 SEM

The white PET is very similar to the grey PET in that the fabric is nonwoven. From the following images, the random orientation of the fibers can be seen. Compared to the grey PET, the white PET has fewer bundles of fibers, the fibers

appear less smooth and not as uniform in diameter across the fiber length, and there are more PET particles in the fabric that are not in fiber form.

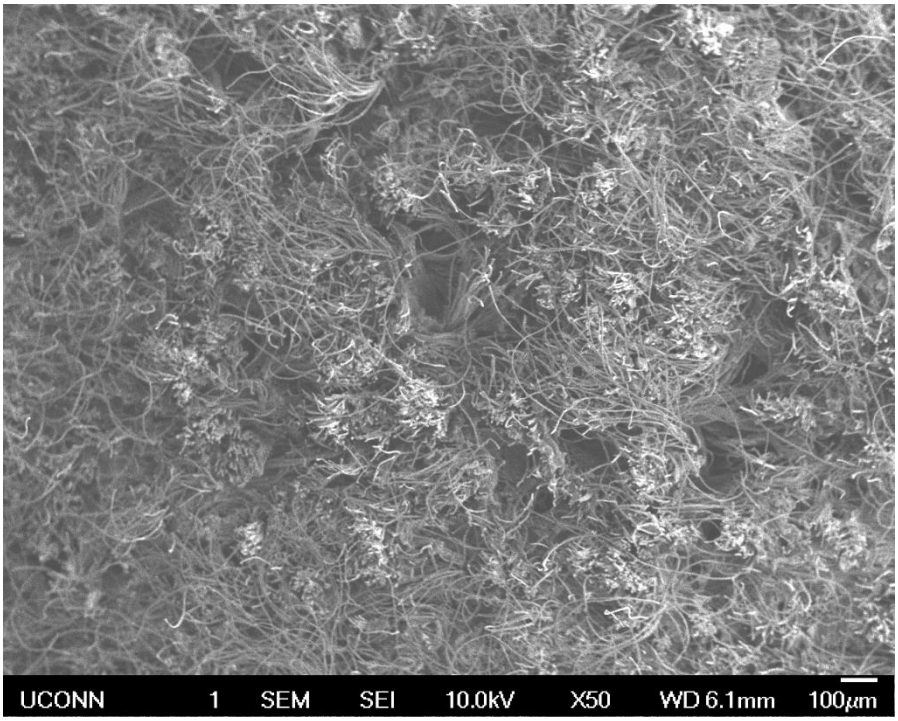

Figure 3.18: SEM X50 magnification of white PET surface.

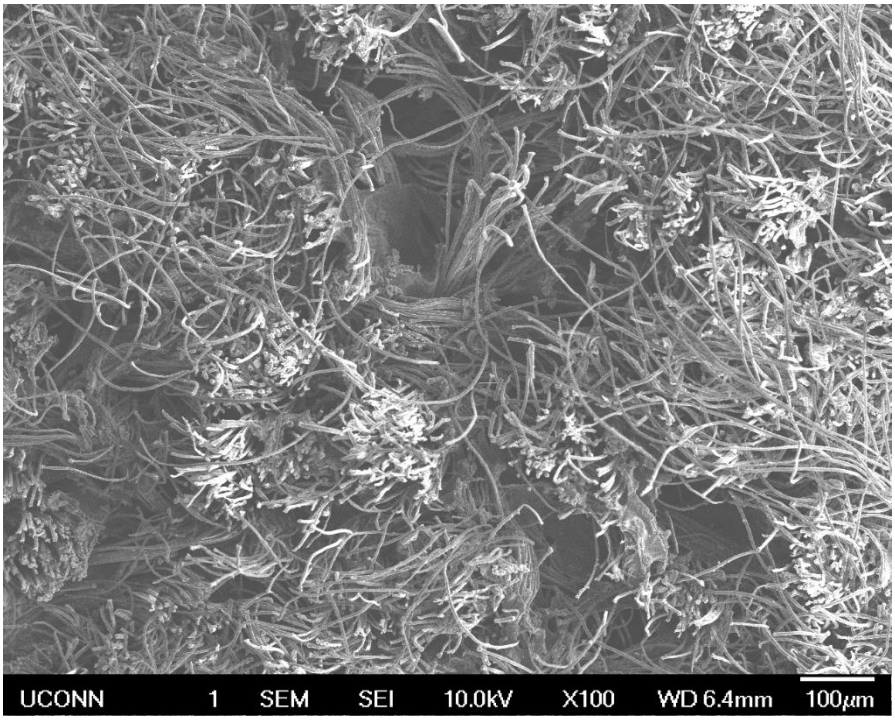

Figure 3.19: SEM X100 magnification of white PET surface.

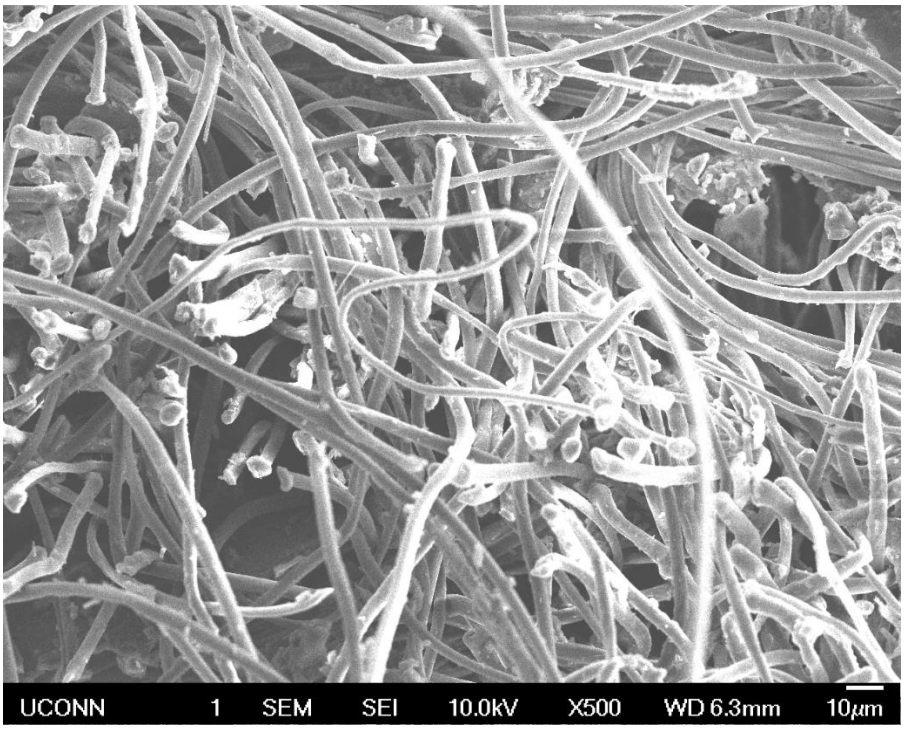

Figure 3.20: SEM X500 magnification of white PET random fiber orientation.

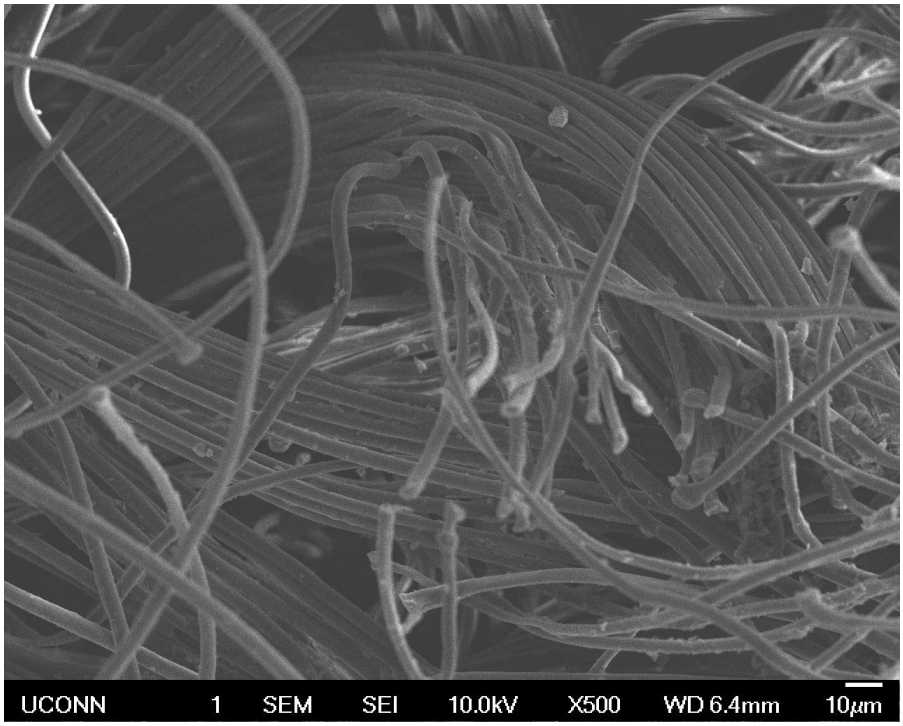

Figure 3.21: SEM X500 magnification of white PET fiber bundles.

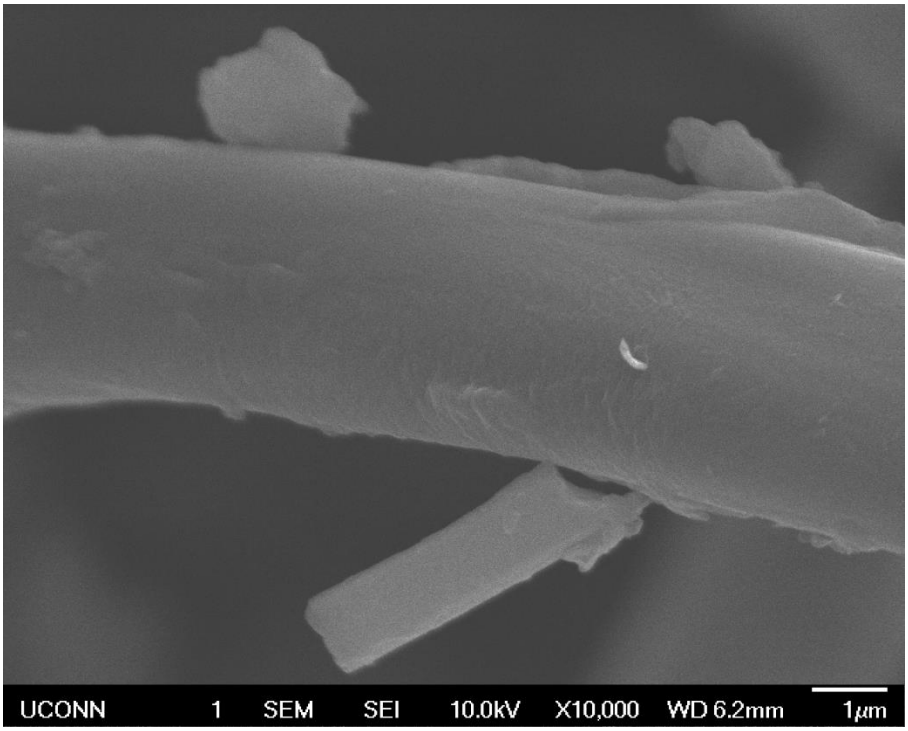

Figure 3.22: SEM X10,000 magnification of white PET fiber.

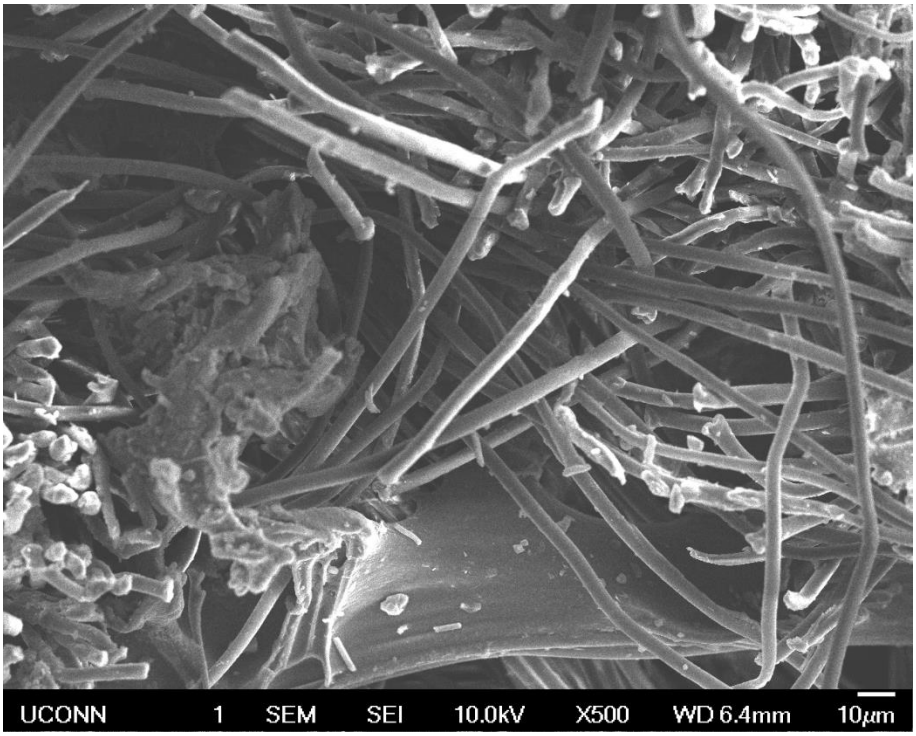

Figure 3.23: SEM X500 magnification of PET particles.

The non-fiber regions were tested using EDS and no unusual elements were found.

3.4 Nylon (White Mesh)

The Nylon fabric is a thin white mesh with a very obvious stamping pattern across both the front and back sides and a thickness of 0.65 mm.

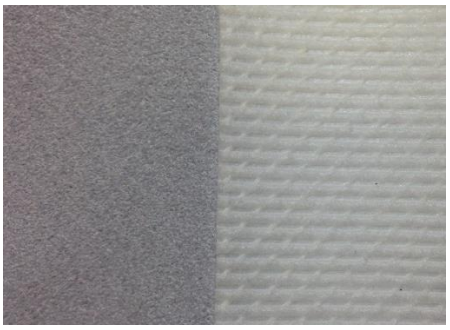

Figure 3.24: Visual comparison of grey PET and Nylon (white mesh).

3.4.1 ATR FTIR Characterization

The white mesh matched both Nylon 6 and Nylon 6,6 in the commercial database, as it could not distinguish between the two.

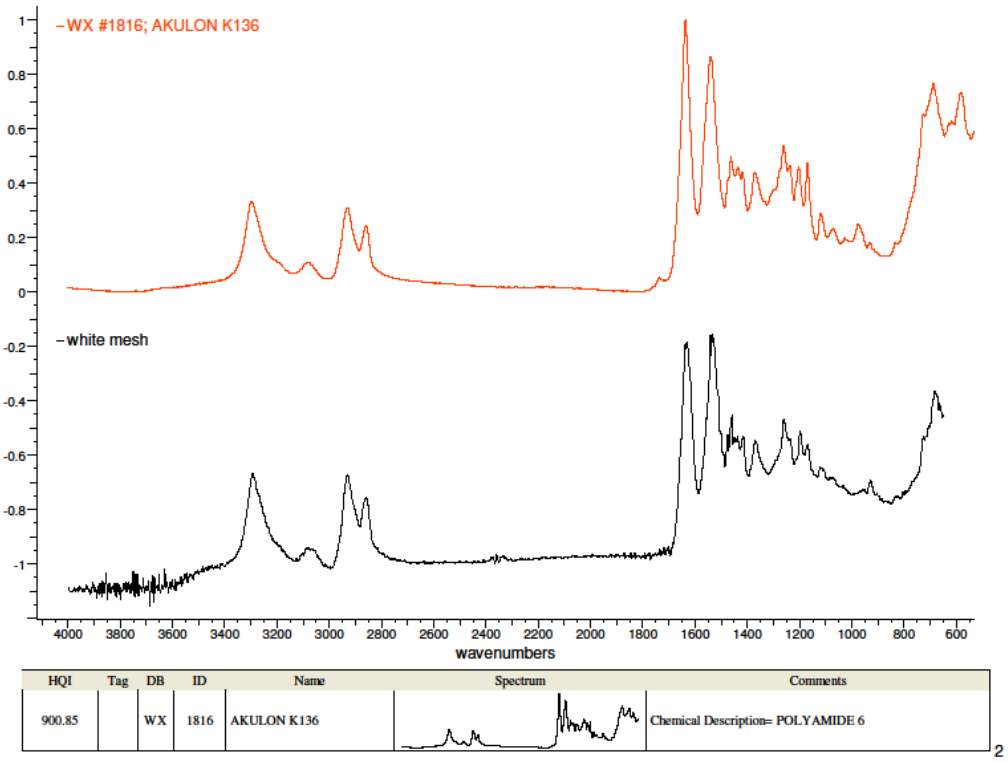

Figure 3.25: ATR FTIR comparison of the white mesh and commercial Nylon.

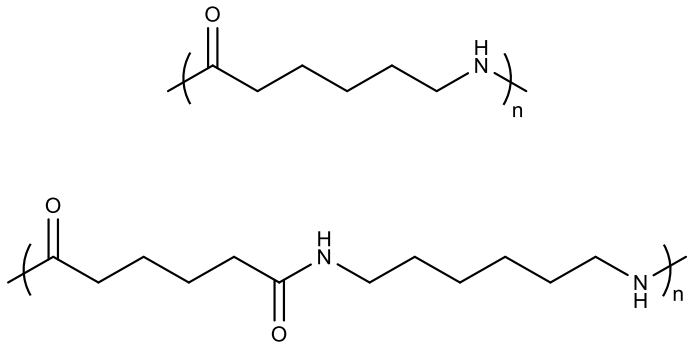

Figure 3.26: Nylon 6 (top) and Nylon 6,6 (bottom)

3.4.2 Thermal Analysis

3.4.2.1 TGA

The Nylon mesh loses some weight right to begin with due to leftover monomer in the fabric (see section 3.4.3). The 3% degradation temperature after being normalized for monomer loss is at 361°C.

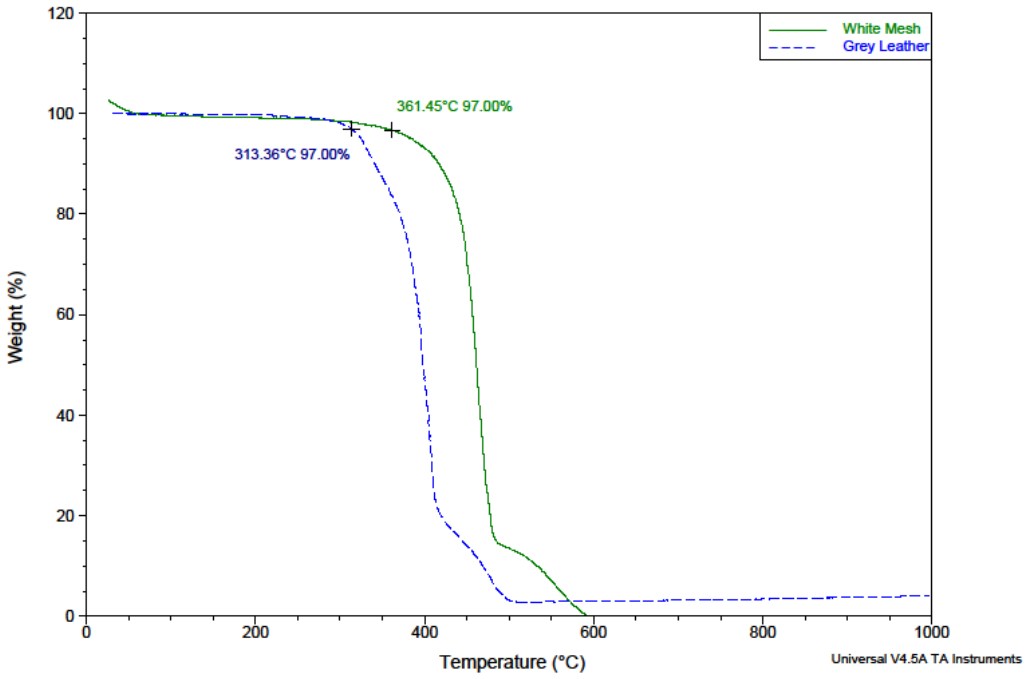

Figure 3.27: Degradation of Nylon versus PET.

3.4.2.2 DSC

DSC was run at 10°C/min. The first heating cycle displays two very sharp melting transitions, one of which disappears on the second heating cycle.

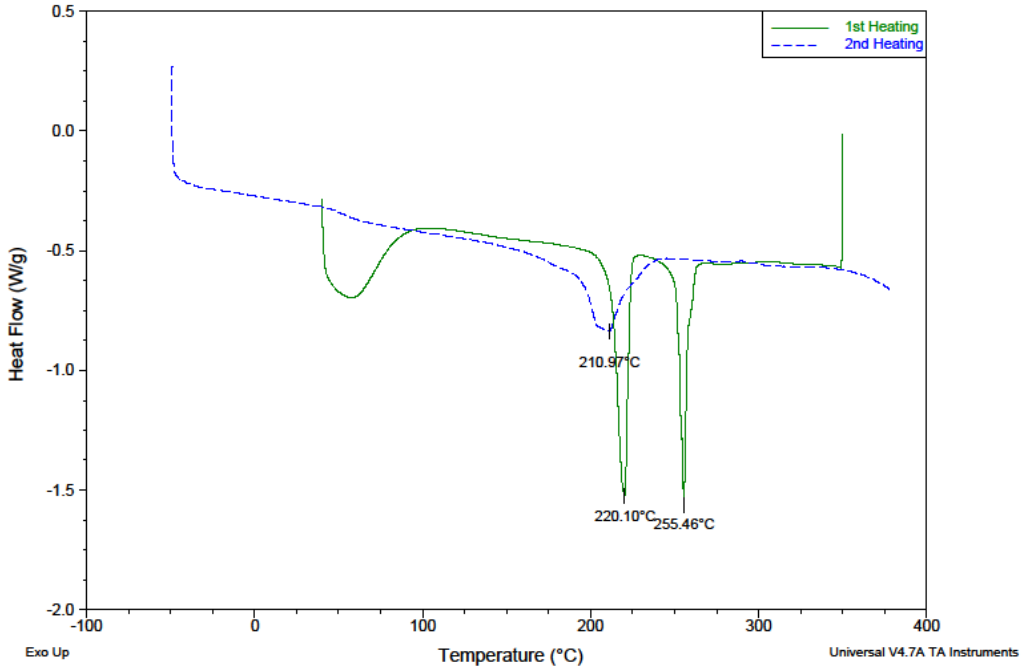

Figure 3.28: First and second heating cycles for Nylon mesh.

From the second heating scan, the glass transition temperature was determined to be 51°C and the melting transition temperature was 210°C.

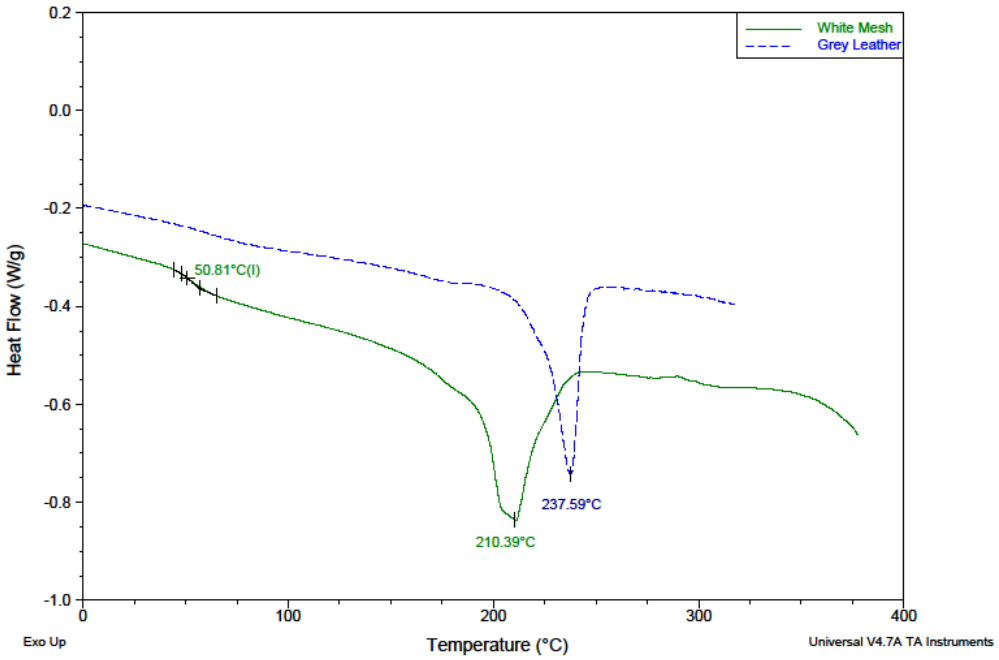

Figure 3.29: Comparison of thermal transitions of Nylon and PET.

The melting and boiling points of possible compounds in the fabric are shown in Table 3.5. Nylon 6 is made from the ring opening polymerization of caprolactam. Nylon 6,6 is made from a condensation reaction between hexamethylenediamine and adipic acid. The white mesh was most likely Nylon 6 from matching the melting points, however GC-MS was used to confirm by looking for leftover monomer.

Compound	Melting Point (°C)	Boiling Point (°C)
Nylon 6	220	N/A
Nylon 6,6	269	N/A
Caprolactam	69	271
Hexamethylenediamine	40	205
Adipic Acid	152	337

Table 3.5: Thermal properties of possible compounds in the Nylon mesh.

3.4.3 GC-MS

The thermal results did not clearly show whether the fabric was Nylon 6 or Nylon 6,6, so GC-MS was used to see if any leftover monomers were present. The GC-MS results revealed that there was caprolactam in the Nylon fabric, which is the monomer used in the ring opening polymerization for Nylon 6.

File :C:\MSDCHEM\1\DATA\Snapshot\Snapshot\WMK_1.D
Operator :
Acquired : 20 Jan 2013 23:21 using AcqMethod 130C SPLITLESS 2MIN.M
Instrument : 7890GCMS
Sample Name: White mesh 130C injection
Misc Info :
Vial Number: 1

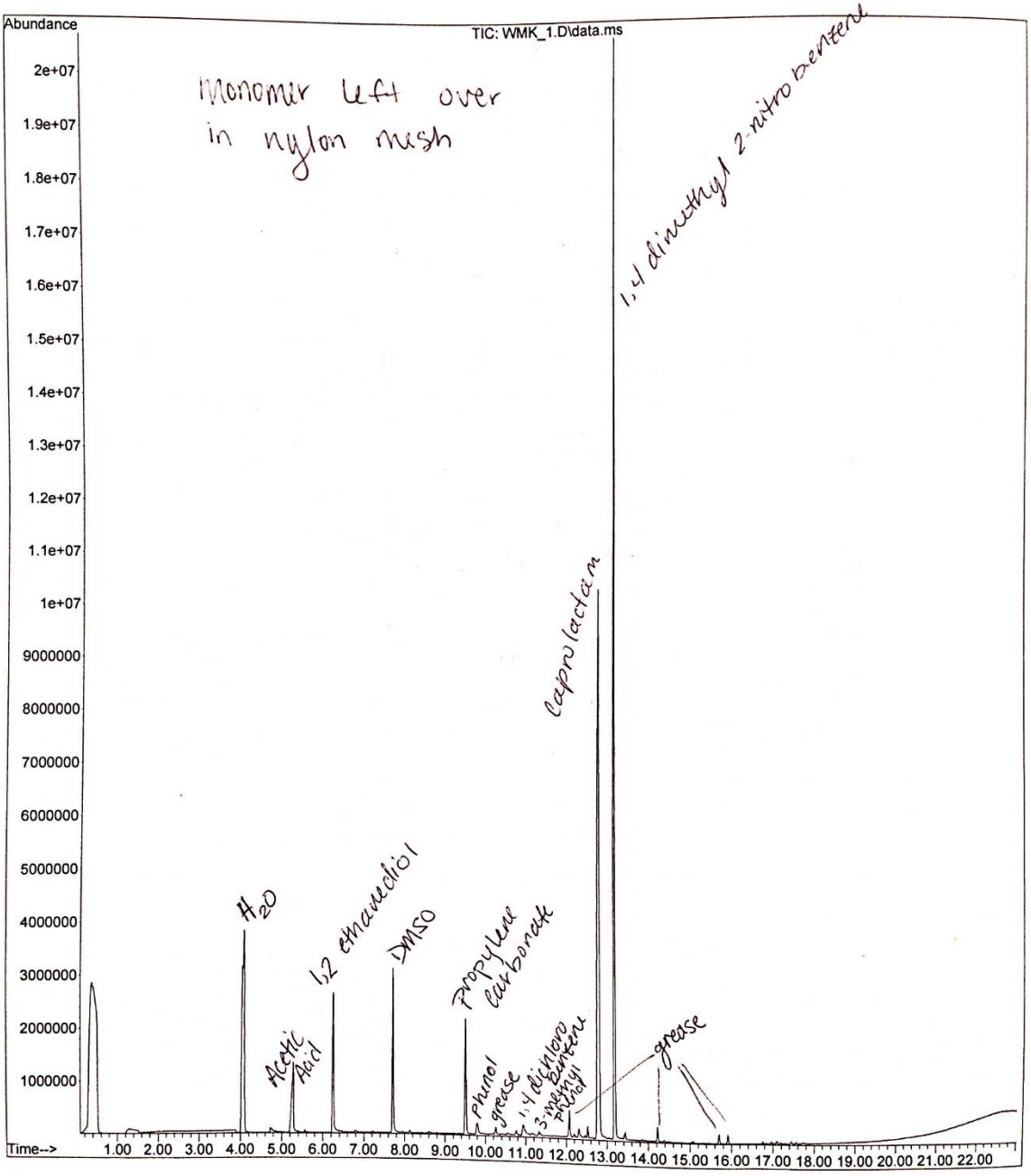

Figure 3.30: GC-MS results for Nylon mesh.

3.4.4 SEM

The Nylon fabric has a melt stamped pattern across the surface (Figure 3.31).

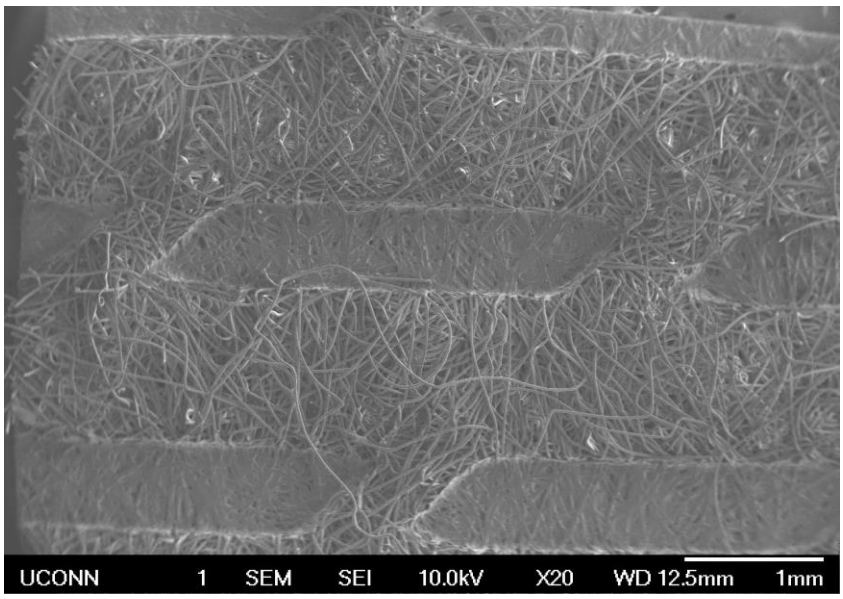

Figure 3.31: SEM X20 magnification of Nylon fabric.

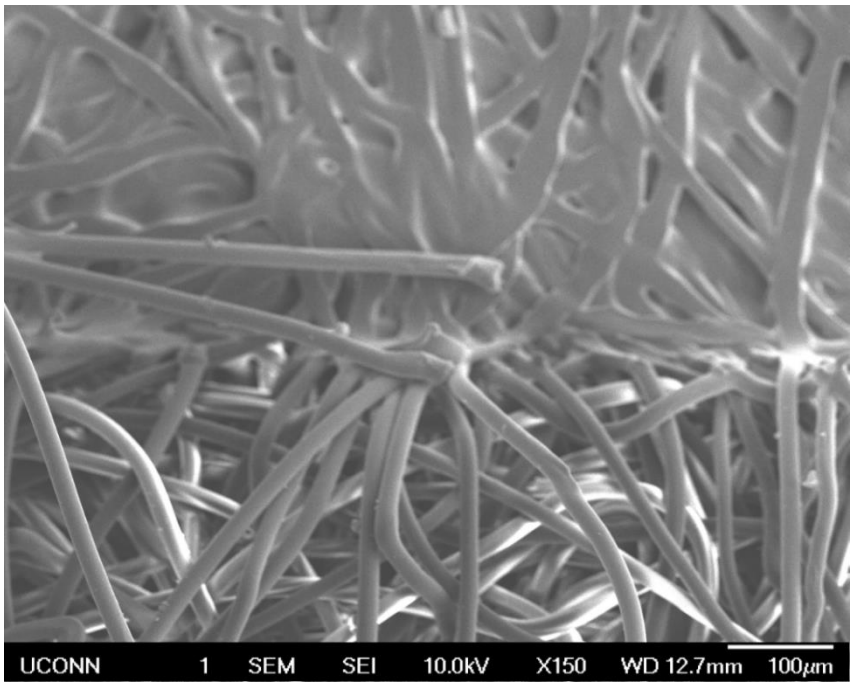

Figure 3.32: SEM X150 magnification of Nylon stamped region border.

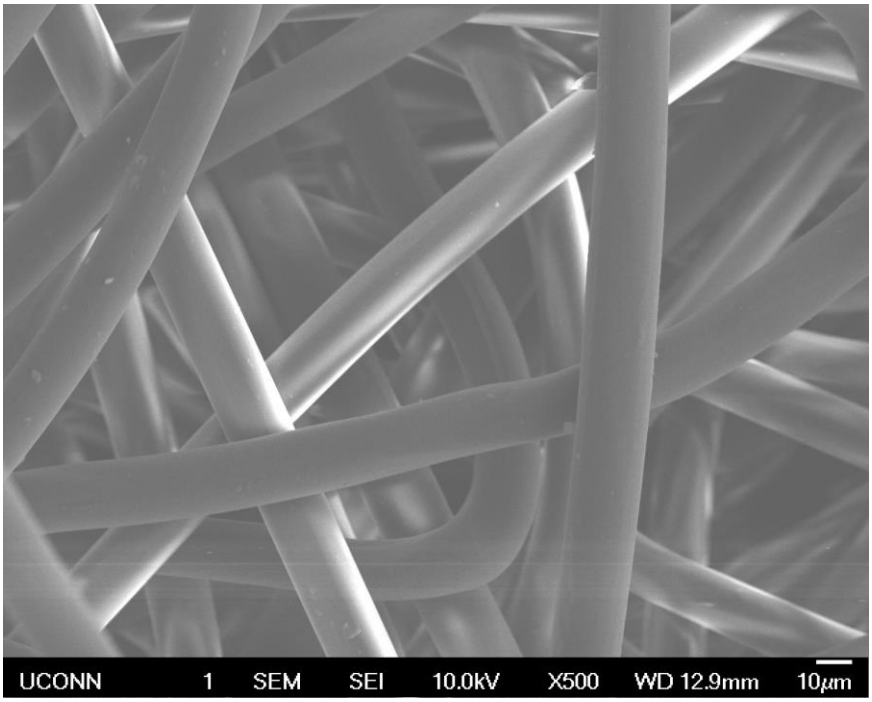

Figure 3.33: SEM X500 magnification of Nylon fibers.

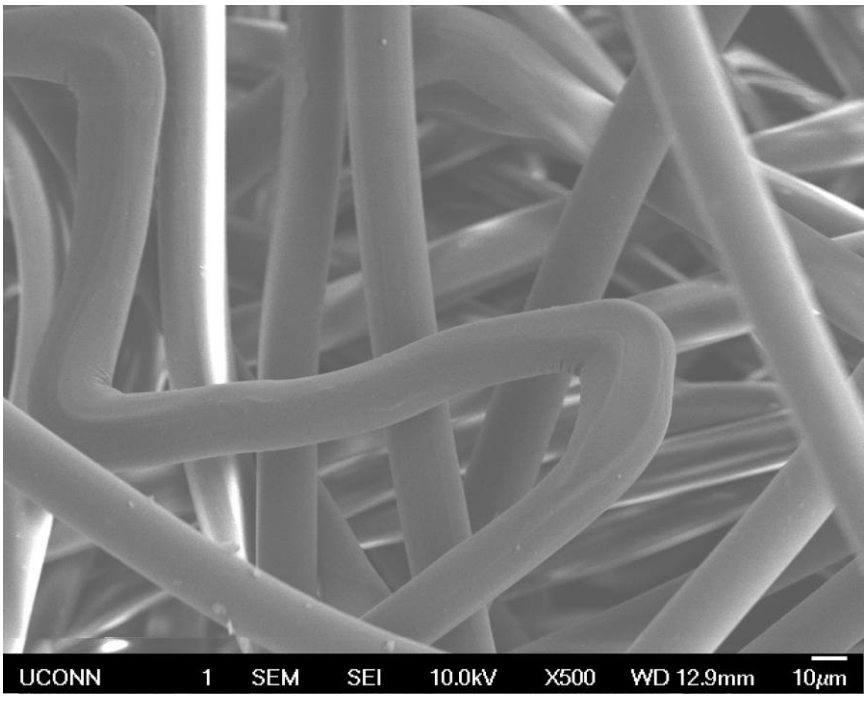

Figure 3.34: SEM X500 magnification of Nylon fibers.

3.5 Spandex

3.5.1 Characterization

The Lycra spandex was donated by Lubrizol and has been used previously in our group.[4,5] This fabric was 50% Nylon and had a thread count of 5882 and a denier of 70. Lycra is a polyester-polyurethane copolymer made from solution dry spinning. A glycol is reacted with a diisocyanate, typically in a 1:2 ratio. Next, the mixture is reacted with an equal amount of diamine. The solution is then diluted with a solvent such as DMAc to produce a spinning solution which can be pumped through a spinneret, forming liquid polymer strands. These strands are heated in the presence of nitrogen and solvent gas, causing the liquid polymer to react and form solid strands. The strands are then bundled together to produce a fiber of the desired thickness. A finishing agent such as magnesium stearate is used to prevent the fibers from sticking together. The Lycra spandex is shown in Figure 3.35 is a woven fabric with the fibers on the back running perpendicular to the fibers on the front, allowing for 4-directional stretching.

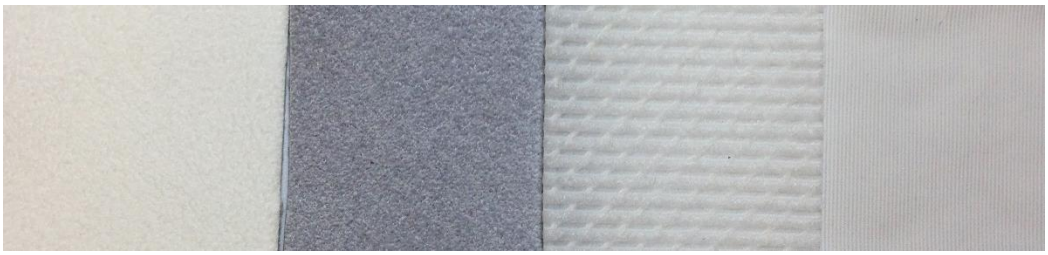

Figure 3.35: Visual comparison of fabrics from left to right: white PET, grey PET, Nylon 6, Lycra spandex.

The spandex has a 3% weight loss degradation temperature of 294°C (Figure 3.36) and a melting temperature of 255°C (Figure 3.37).

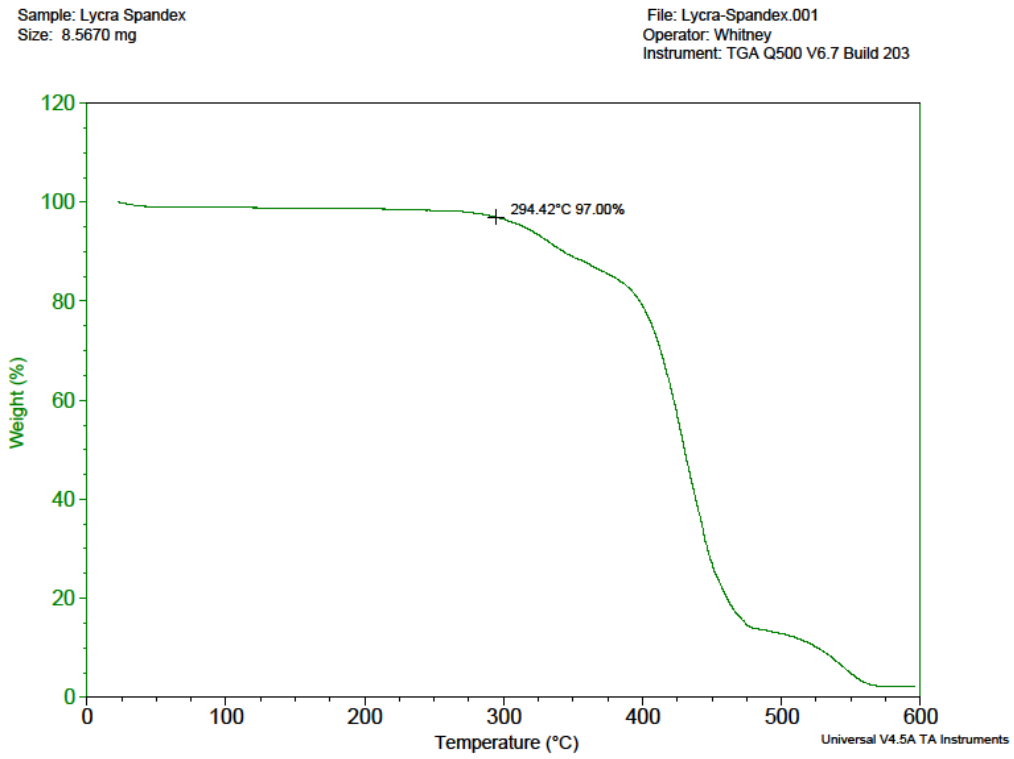

Figure 3.36: Degradation of Lycra spandex.

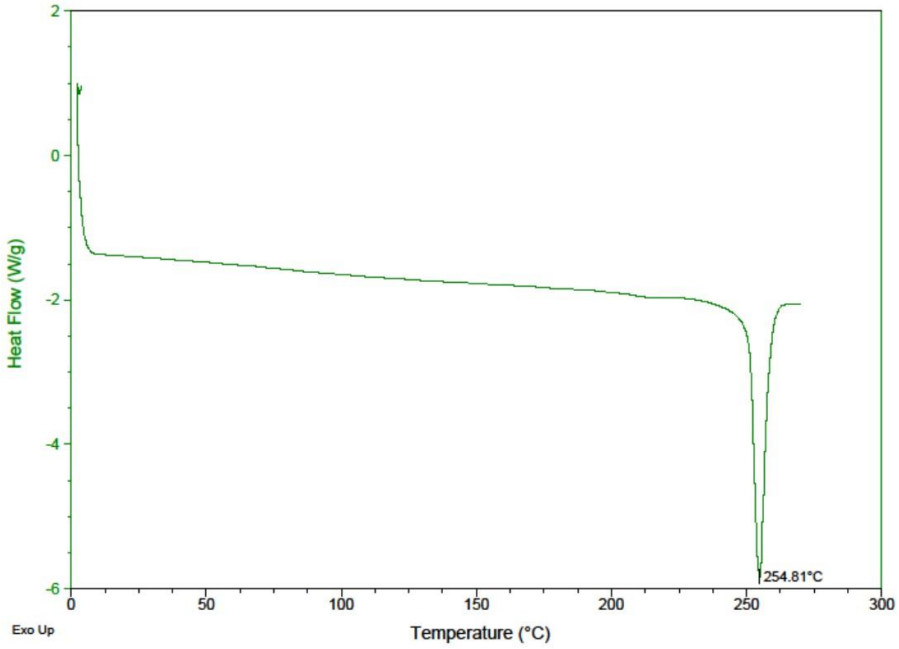

Figure 3.37: Melting temperature of Lycra spandex.

3.6 Black PET

3.6.1 Characterization

Our group received two black PET fabrics, which were confirmed to be PET with ATR IR. One of these fabrics was visually very similar to the grey PET and has a thickness of 1.10 mm, but no further testing has been performed. The fabric in this section appears like the grey PET on one side, but the other side has been melted. This fabric was 0.75 mm in thickness. The black fabrics were not used much because the PEDOT:PSS loading could not be seen and electrochromic polymers would not show up.

The half-melted black PET had a 3% weight loss degradation temperature of 291°C, as compared to 313°C for the grey PET.

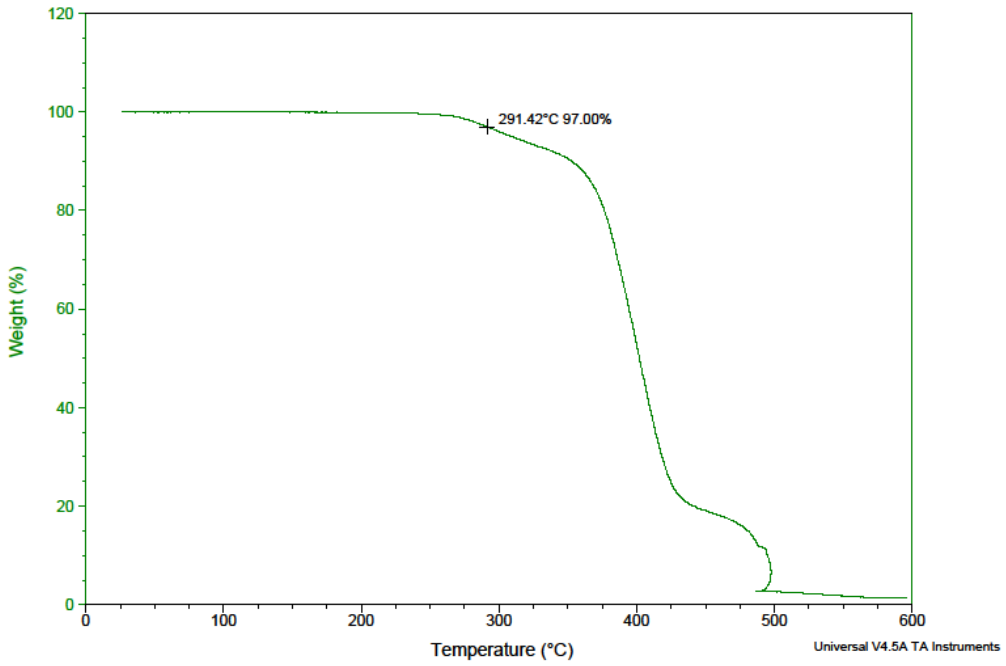

Figure 3.38: Degradation of half-melted black PET.

3.6.2 SEM

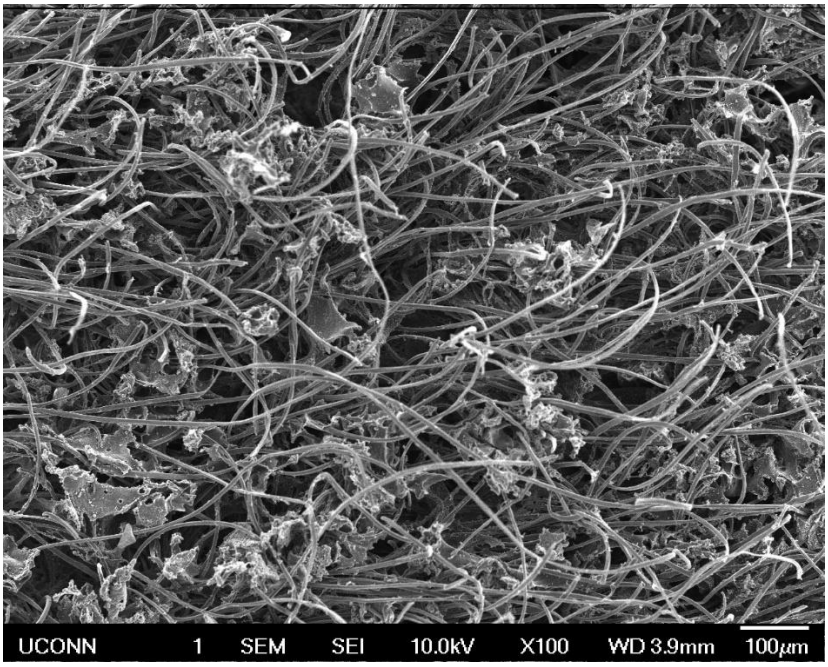

Figure 3.39: SEM X100 magnification of half-melted Black PET, fuzzy side.

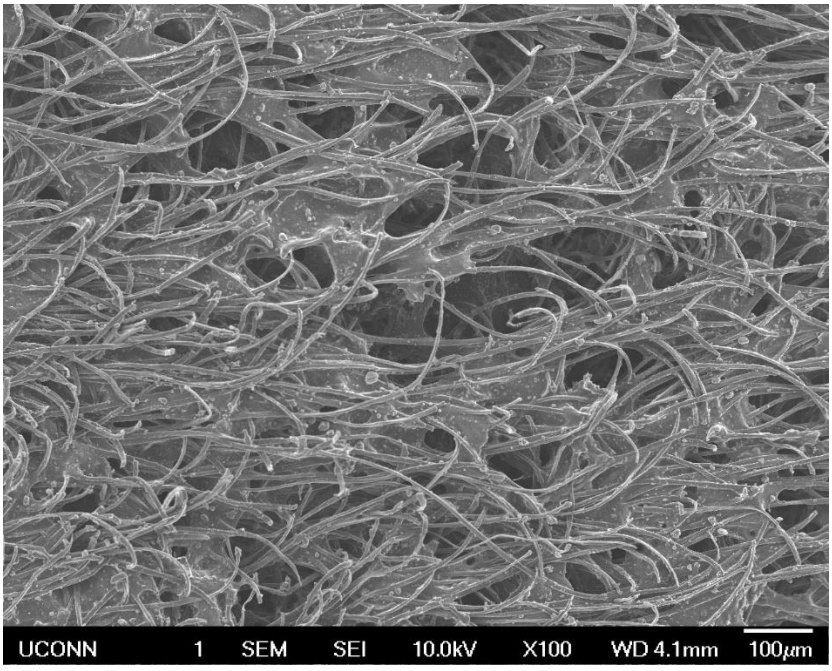

Figure 3.40: SEM X100 magnification of half-melted Black PET, melt side.

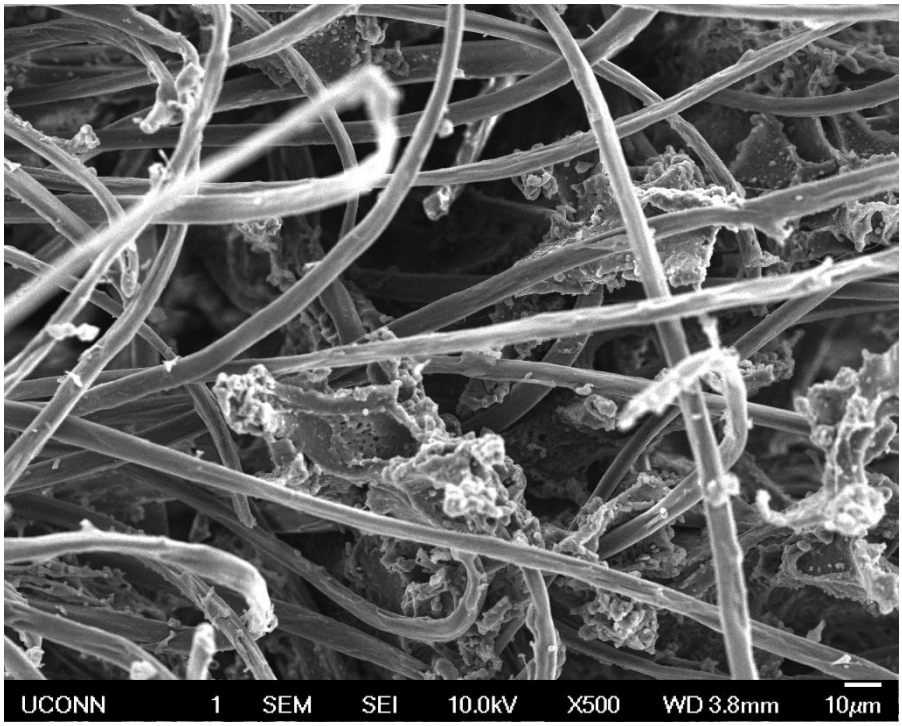

Figure 3.41: SEM X500 magnification of half-melted Black PET, fuzzy side.

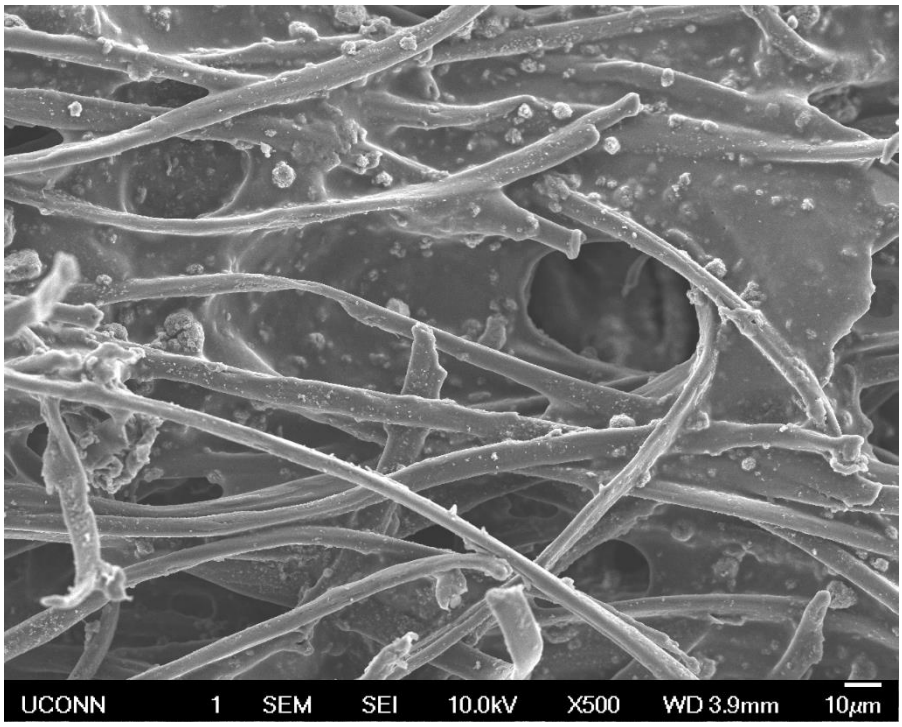

Figure 3.42: SEM X500 magnification of half-melted Black PET, melt side.

3.7 References

[1] Perkin Elmer; www.perkinelmer.com; FT-IR Spectroscopy Attenuated Total Reflectance (ATR)

[2] Samperi, F.; et. al. *Polymer Degradation and Stability*. 2004, 83, 3-10.

[3] Image courtesy of Jose Santana

[4] Invernale, M.A.; Ding, Y.; Sotzing, G.A.; *ACS Appl. Mater. Interfaces* 2010, 2, 296-300

[5] Ding, Yujie; Thesis Ch. 7, 2011

Chapter 4: Preparing and Characterizing Conductive Fabric

4.1 Introduction

4.1.1 PEDOT:PSS

CleviosPH1000, a highly conductive form of Poly(3,4-ethylenedioxythiophene)-poly(styrenesulfonate) (PEDOT:PSS) was used for most of this work. The manufacturer (Heraeus) lists the solid content at between 1 and 1.3% and the conductivity at 850 S/cm after the addition of dimethyl sulfoxide (DMSO).[1]

A TGA was run on the CleviosPH1000 dispersion to determine the weight once all the water had been evaporated. The sample was ramped at 10°C/min to 100°C and held isothermal for 20 minutes. The remaining matter after being held isothermally was 1.389%.

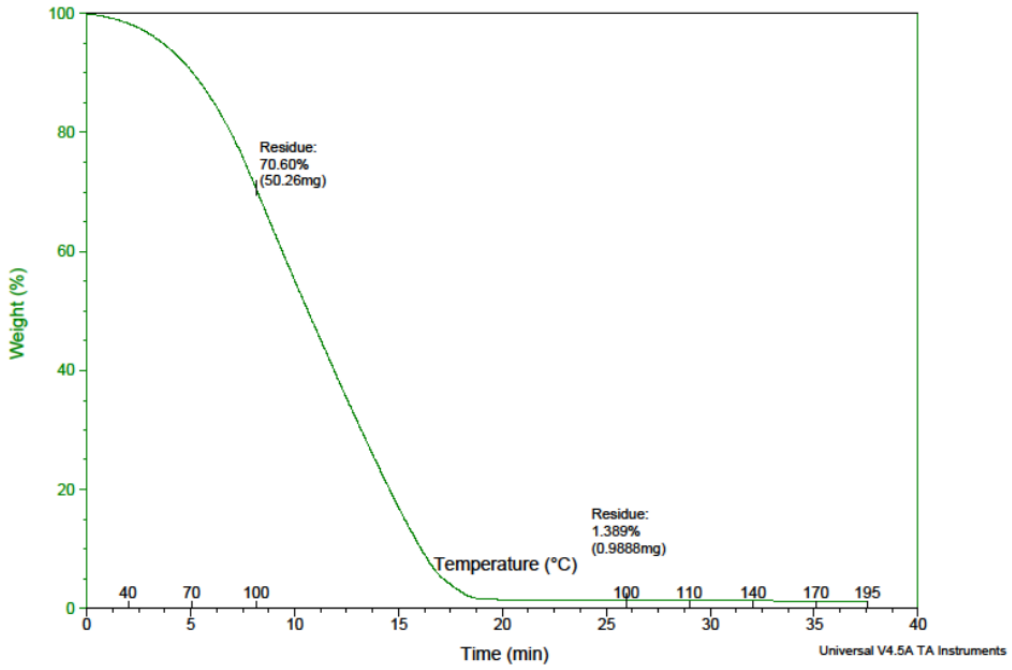

Figure 4.1: Solid content in CleviosPH1000.

4.1.2 Weight Percent

In order to quantify the amount of conductive material (doped PEDOT:PSS) in each fabric sample, a weight percent calculation was used. The fabric samples were weighed before treatment and again after drying and the weight percent was calculated according to Equation 4.1.

$$\frac{Weight_{Final} - Weight_{Initial}}{Weight_{Final}} x100 = Weight\ \%\ of\ Conductive\ Material \quad \text{Equation 4.1}$$

4.1.3 Resistance Measurements

Resistance was measured using a sample holder with two steel electrodes placed ¾" apart. The resistance was measured using a Keithley Integra Series 2700 Multimeter. Later in this work, sheet resistance was measured using the 4-line setup described in Section 2.2.8.

4.2 Grey PET

4.2.1 Wicking Behavior

The grey PET readily absorbs the PEDOT:PSS. Four drops of PEDOT:PSS (two on each side) were added to each fabric piece (Figure 4.2). After drying, the two point resistance, as measured with gold tabs, was about 20 Ω.

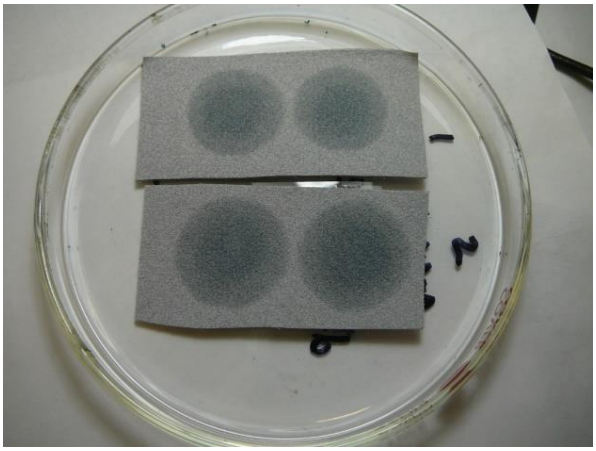

Figure 4.2: Droplet diffusion in grey PET.

The CleviosPH1000 brand of PEDOT:PSS was doped with 5 wt. % DMSO and drop coated onto the grey fabric until completely saturated. The grey fabric was allowed to sit for 30 minutes and then dried at 90 °C for 1.5 hours. The finished fabric was less than 2 % by weight conductive material and the resistance as measured with gold tabs was 6 Ω & 8 Ω.

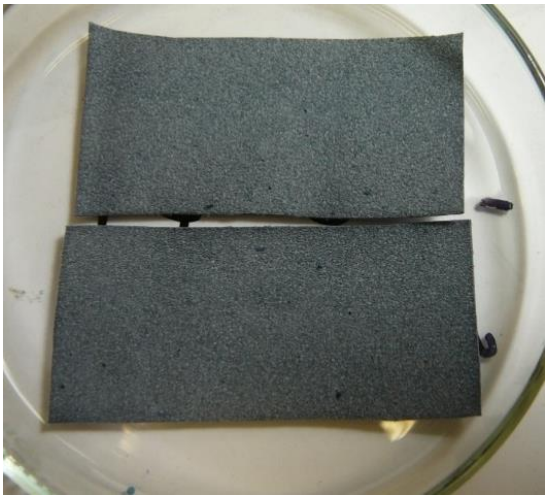

Figure 4.3: Treated grey PET.

Additional PEDOT:PSS lowers the resistance (Table 4.1). A sample was saturated with 5% DMSO doped CleviosPH1000, allowed to sit for 30 minutes, then dried at 90°C for 1.5 hours. The resistance was measured with gold tabs.

Treatment	Weight of PEDOT:PSS (%)	Resistance (Ω)
1st Soaking	2.1	8
2nd Soaking	4.4	4
3rd Soaking	6.4	2

Table 4.1: Increasing PEDOT:PSS concentration decreases resistance.

After these initial observations, a sample holder was fashioned for uniform pressure and distance between fabric samples.

4.2.2 Characterization of Treated PET

4.2.2.1 TGA

There was very little difference in the decomposition curve between the treated (soaked leather) and untreated (unsoaked leather) grey PET.

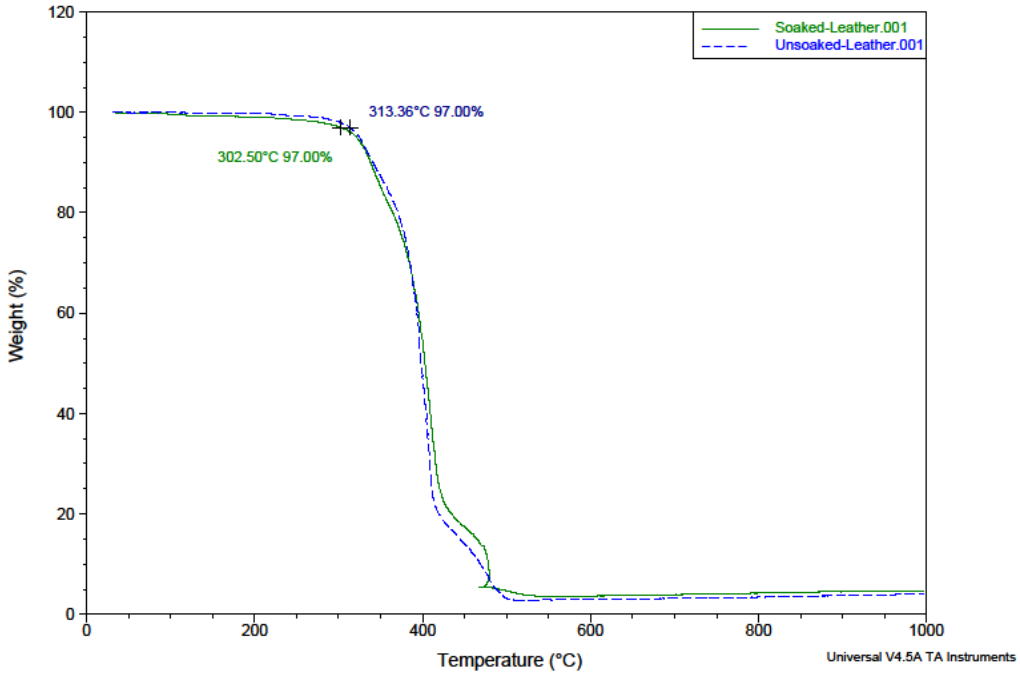

Figure 4.4: Decomposition curve for treated and untreated grey PET.

Samples were also treated with solutions of 5% DMSO in water and 100% DMSO (Figure 4.5) to observe the solubility of PET in DMSO. The untreated PET degraded at 313°C, the 5% DMSO PET degraded at 308°C, and the 100% DMSO PET degraded at 227°C.

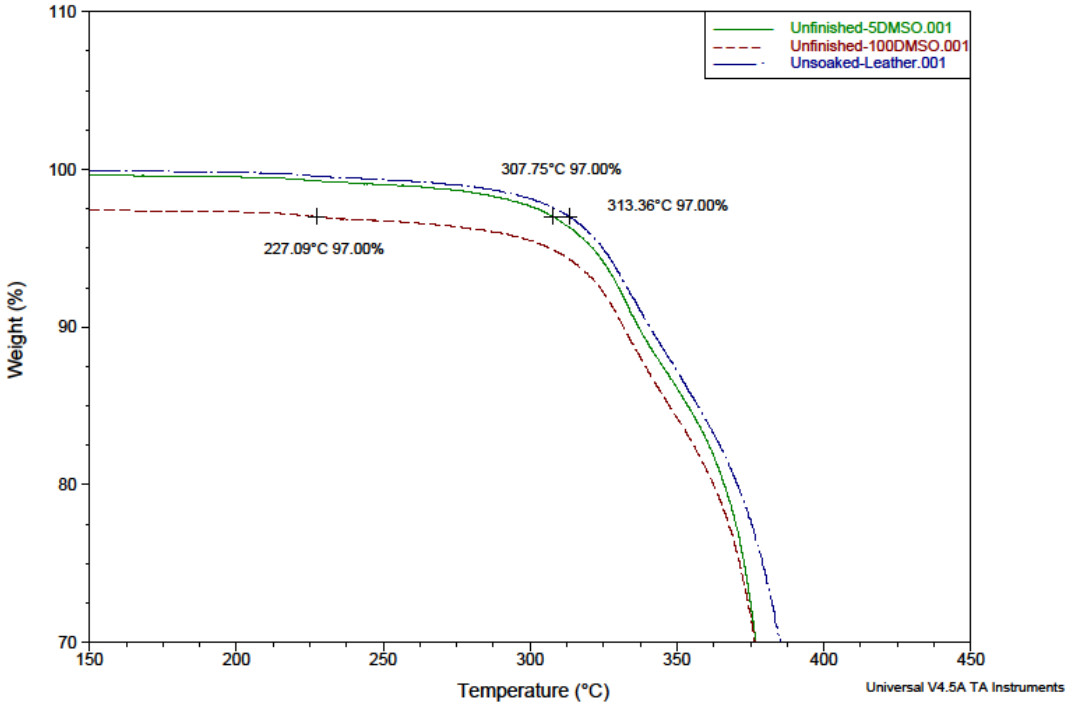

Figure 4.5: Grey PET degradation after soaking in DMSO.

4.2.2.2 DSC

The addition of DMSO doped PEDOT:PSS did not change the thermal properties of the grey PET.

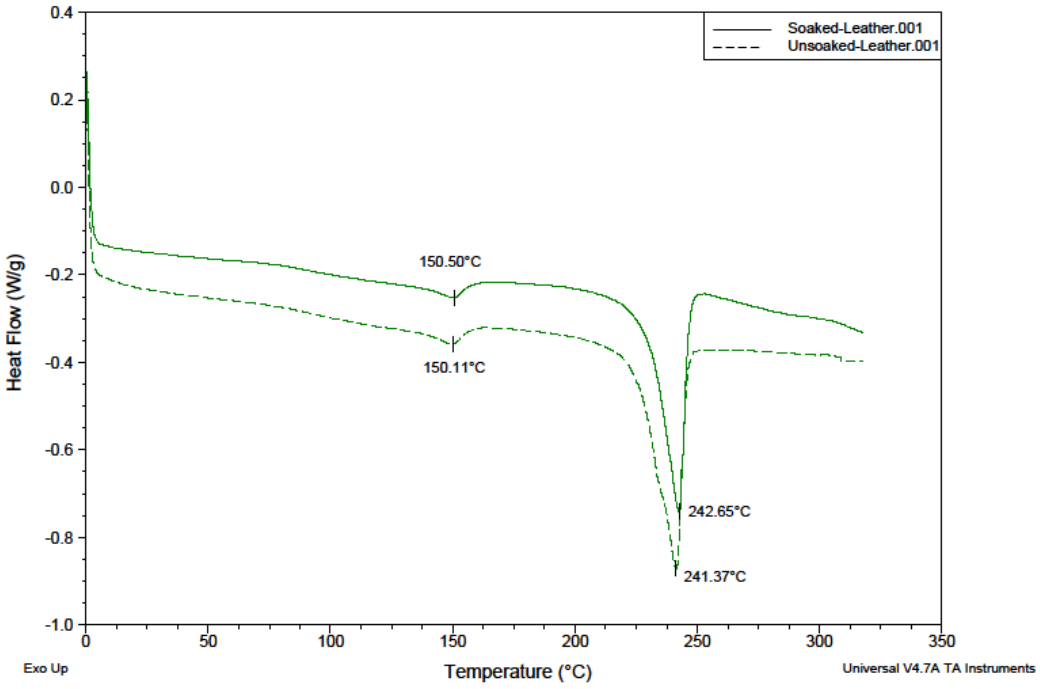

Figure 4.6: First heating cycle of treated and untreated grey PET.

4.2.2.3 GC-MS

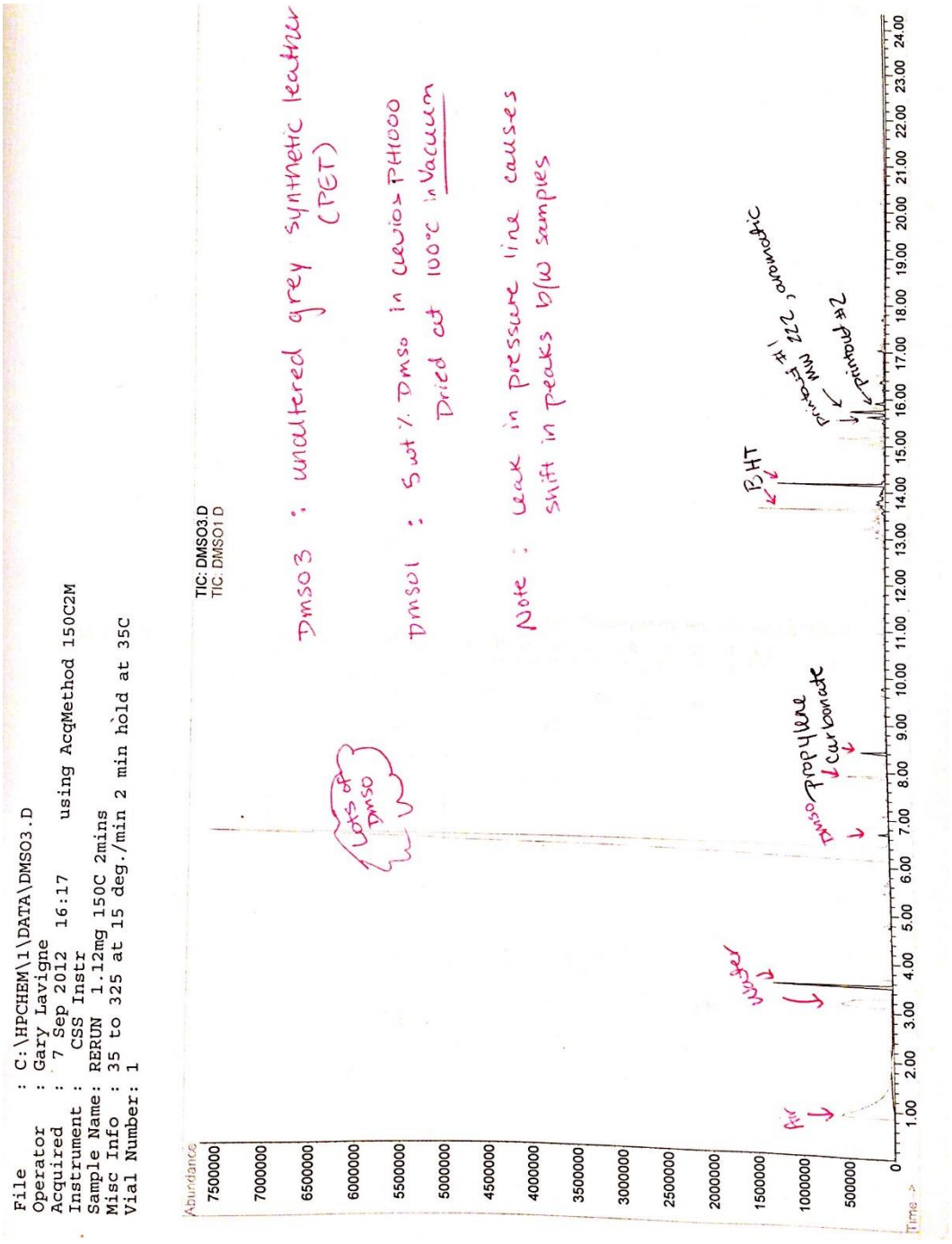

Figure 4.7: GC-MS comparison of untreated fabric (dark trace, DMSO3) vs treated fabric (light trace, DMSO1).

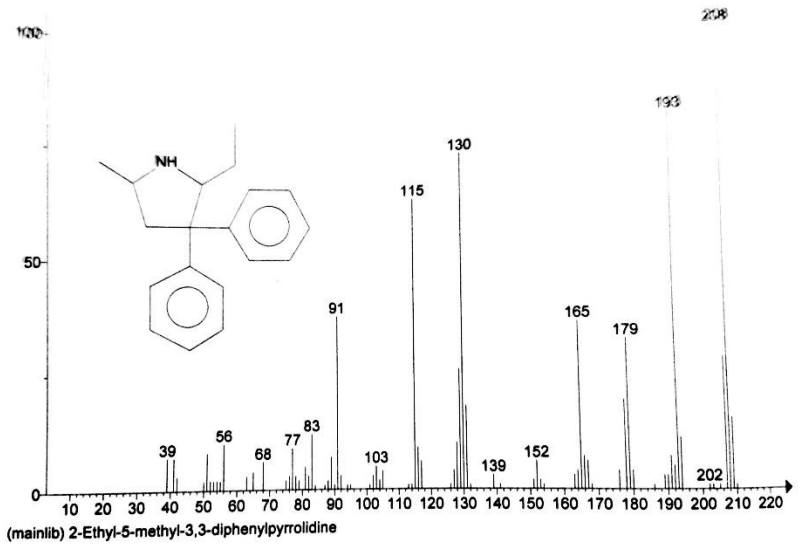

Figure 4.8: Aromatic compound in grey PET (labeled printout1)

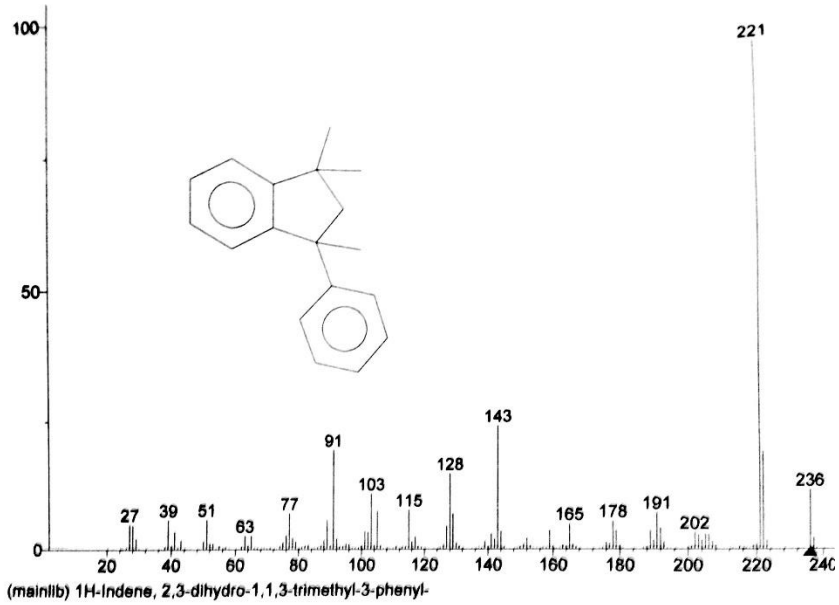

Figure 4.9: Aromatic compound in grey PET (labeled printout2)

4.2.2.4 Mechanical Properties

Stress/Strain curves were obtained for treated grey PET and compared to the untreated PET. A sample press was used to cut uniformly sized dogbone shaped samples. The bottom four curves (shown in red) are the unaltered grey PET. The top three curves (shown in blue) are grey PET that has been saturated with CleviosPH1000 once and dried. The treated samples have a higher Young's modulus and tensile strength.

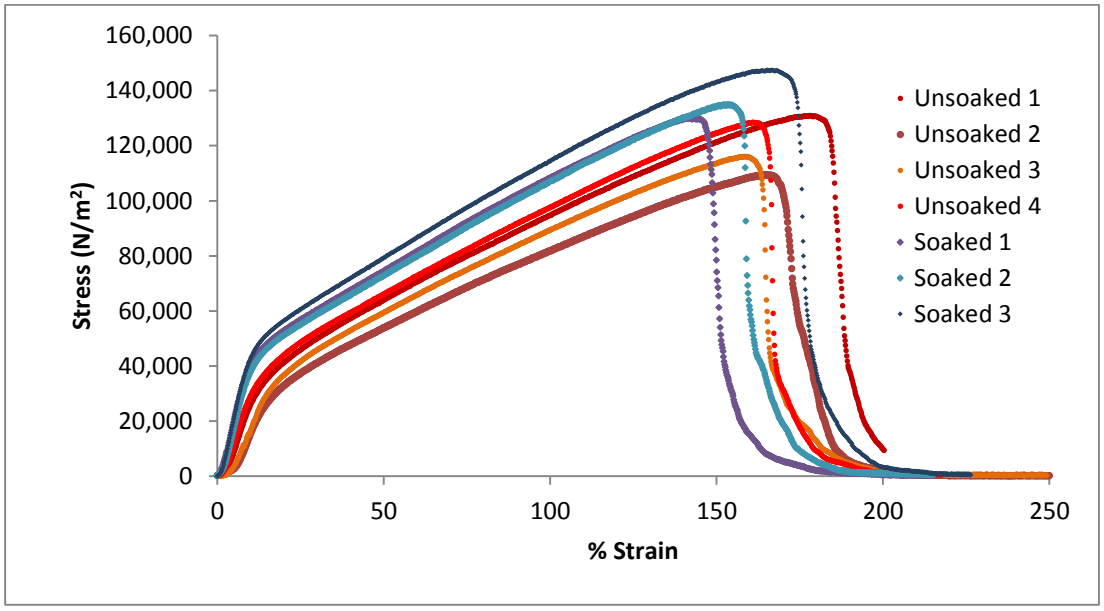

Figure 4.10: Stress/strain curves for treated and untreated grey synthetic leather.

Sample	Young's Modulus (N/m^2)	Tensile Strength (N/m^2)	Elongation-to-break (%)
Unsoaked 1	3,720	130,000	178
Unsoaked 2	2,903	109,000	164
Unsoaked 3	2,899	116,000	159
Unsoaked 4	3,986	128,000	161
Average Unsoaked	**3,377**	**121,000**	**166**
Soaked 1	5,519	130,000	141
Soaked 2	4,936	135,000	154
Soaked 3	5,362	147,000	166
Average Soaked	**5,272**	**137,000**	**154**

Table 4.2: Mechanical results for treated and untreated grey PET.

4.2.2.5 BET

BET was unable to produce a measurement due to the decreased surface area of the treated grey PET.

4.2.2.6 Optical Microscopy

Grey PET samples that have been soaked once with DMSO doped PEDOT:PSS solution were observed with a microscope. The optical microscopy images of the

treated PET looked identical to the untreated. The dark spots in the 5X magnification image are from the microscope lens.

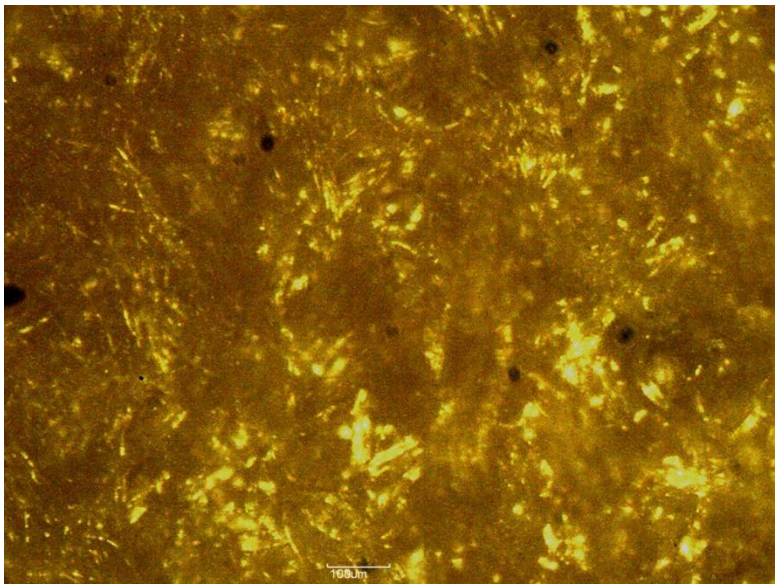

Figure 4.11: 5X magnification of treated grey PET.

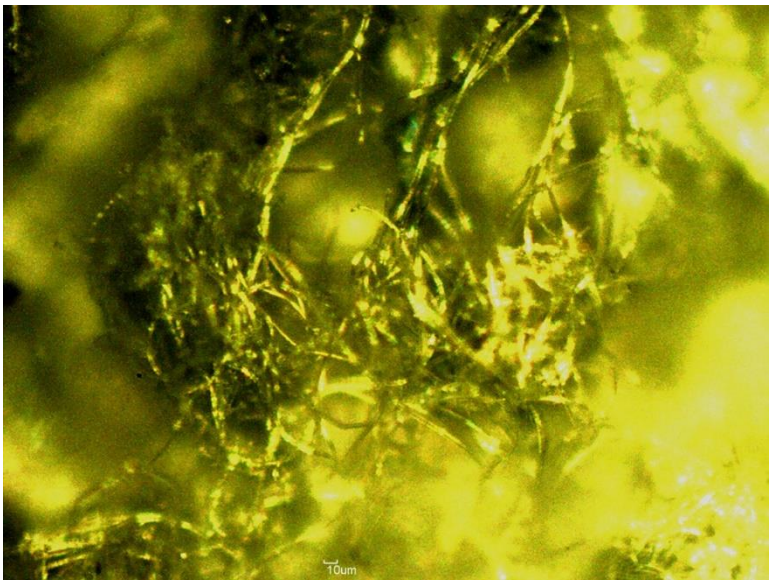

Figure 4.12: 10X magnification of treated grey PET.

4.2.2.7 SEM

Scanning electron microscopy (SEM) images display the increasing amount of film formation on the PET fibers as the concentration of PEDOT:PSS in the fabric increases.

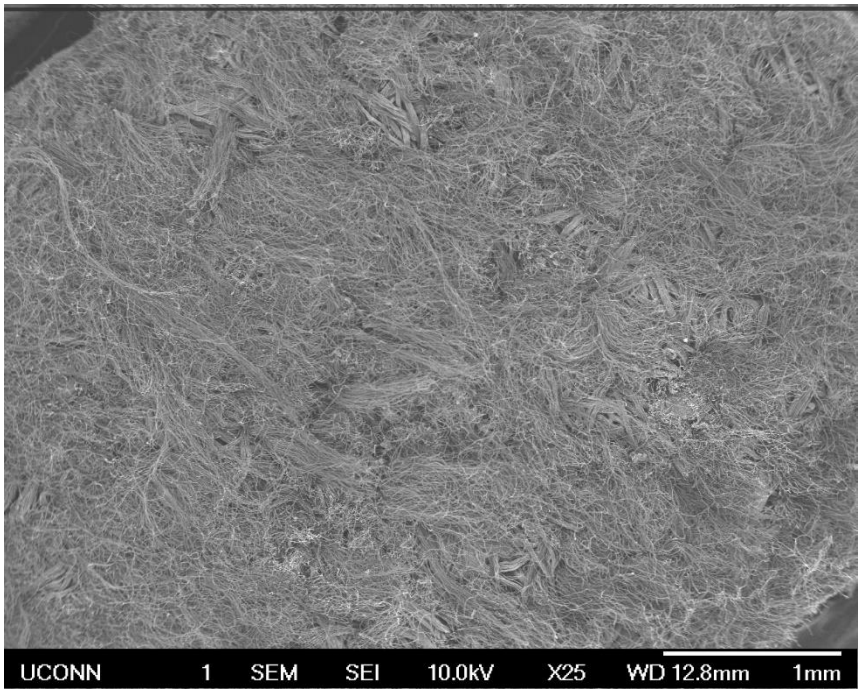

Figure 4.13: X25 image of untreated grey PET.

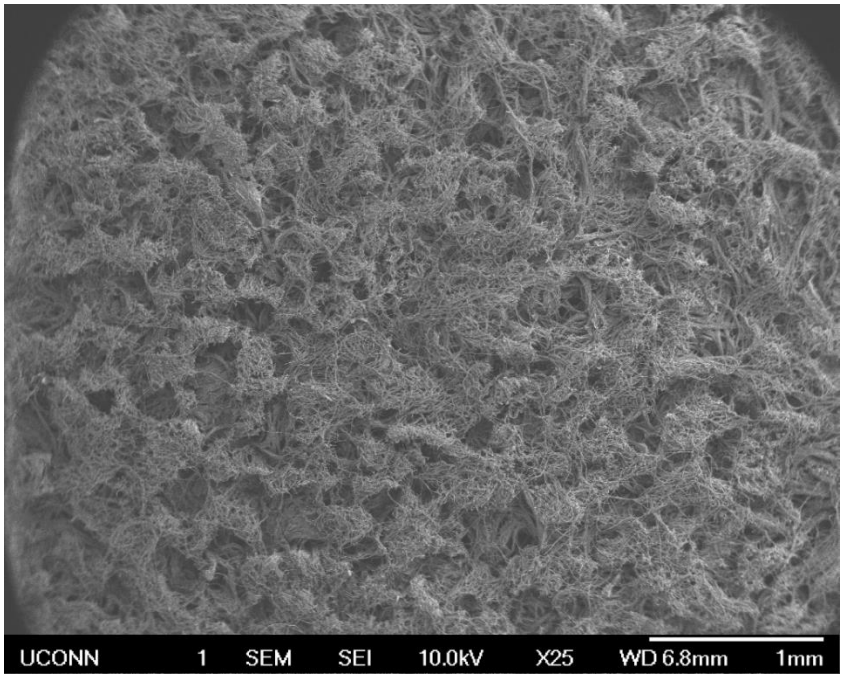

Figure 4.14: X25 image of 1 wt. % treated grey PET.

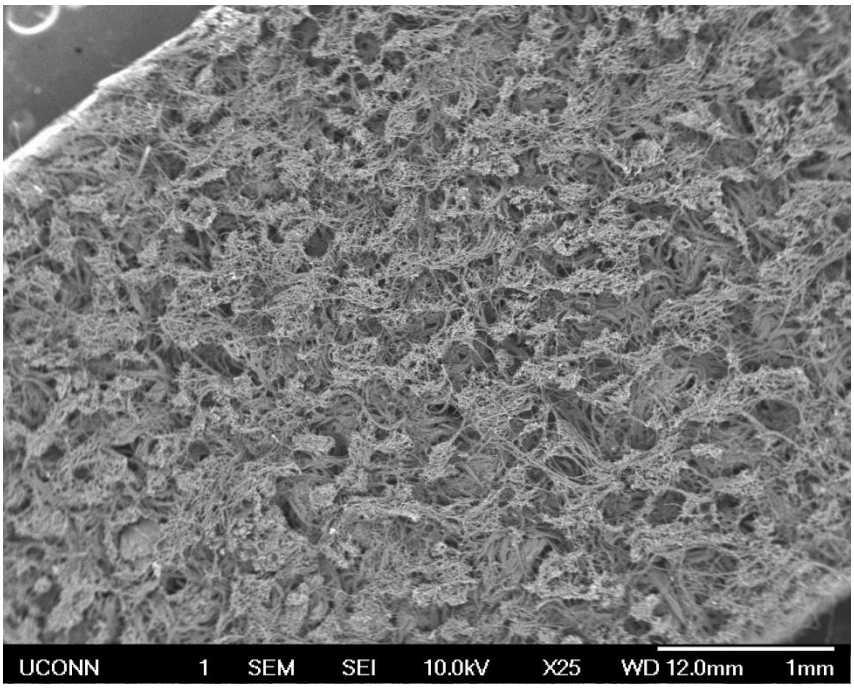

Figure 4.15: X25 image of 2 wt. % treated grey PET.

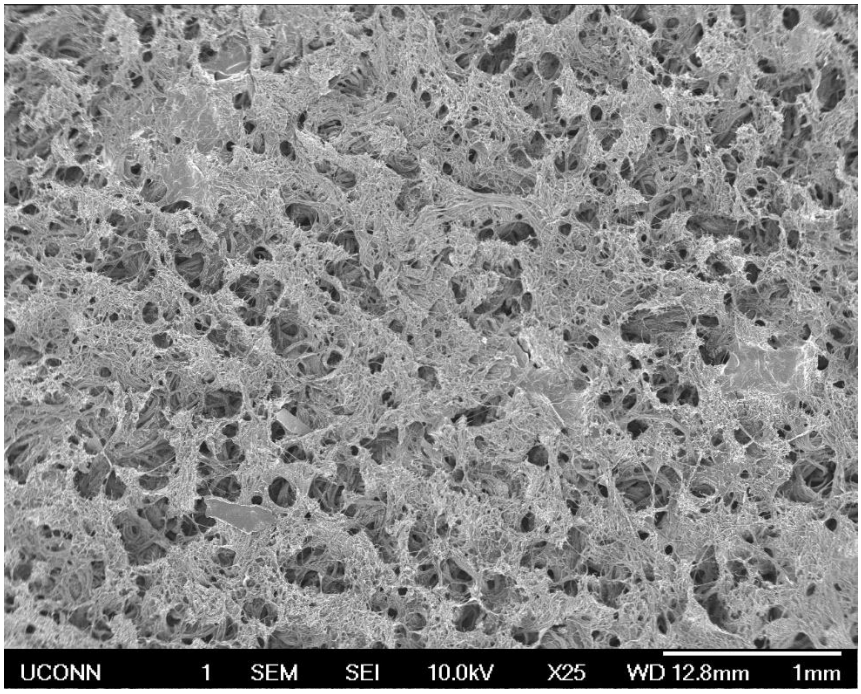

Figure 4.16: X25 image of 4 wt. % treated grey PET.

SEM was also used to observe the type of film formation. Film doesn't just coat each individual fiber, it also spreads out between fibers and bundles.

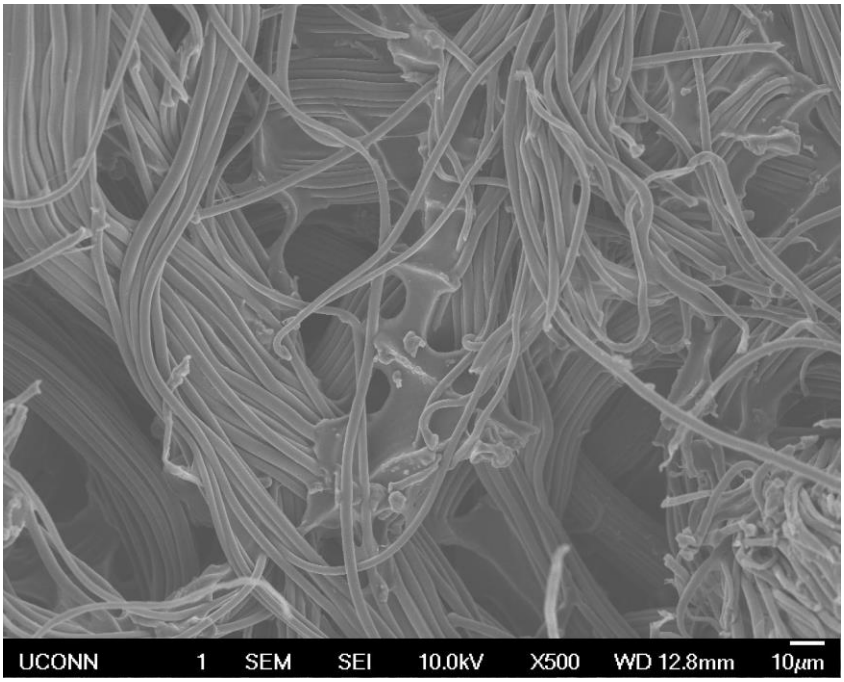

Figure 4.17: X500 image of 2 wt. % treated grey PET.

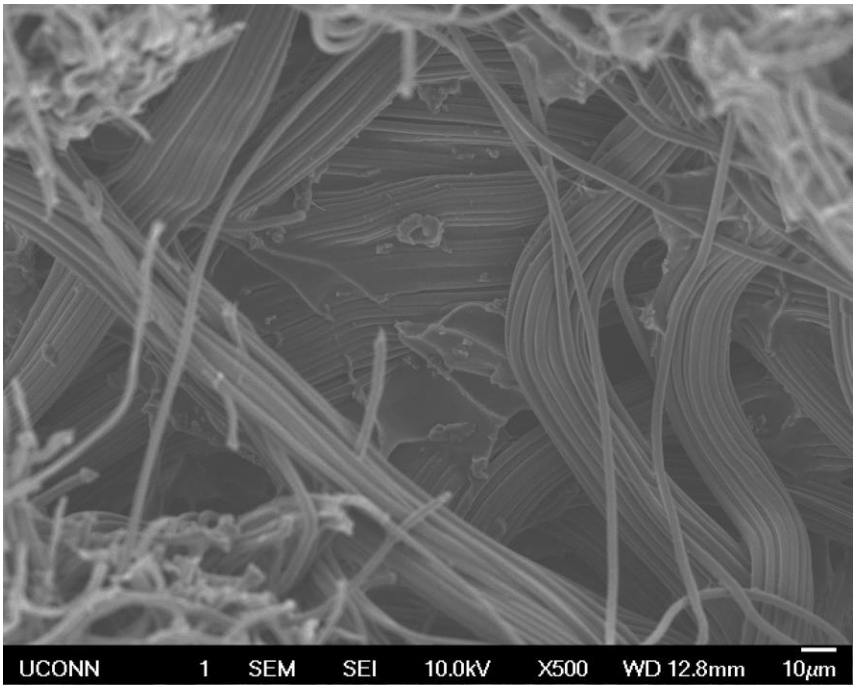

Figure 4.18: X500 image of 2 wt. % treated grey PET.

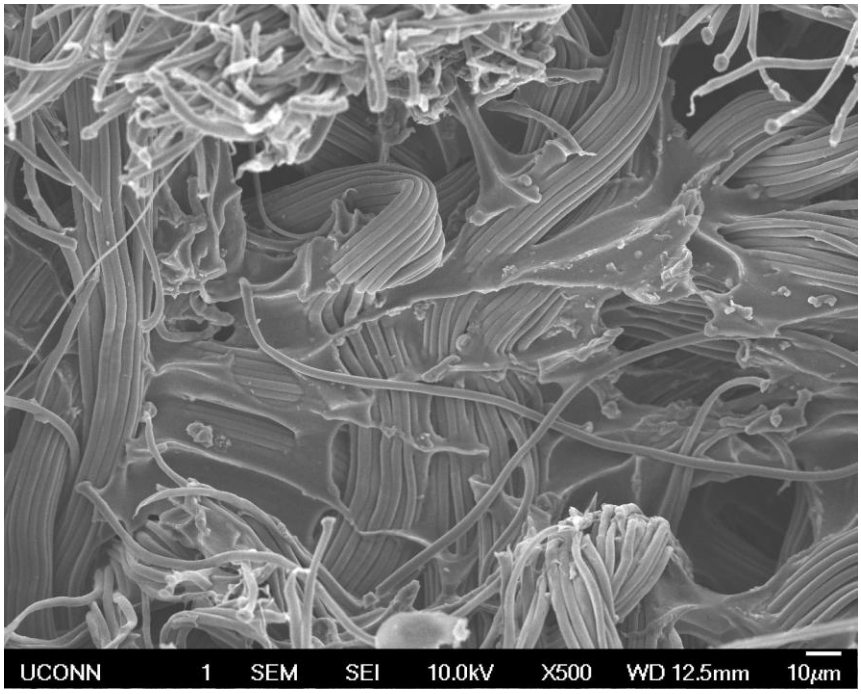

Figure 4.19: X500 image of 2 wt. % treated grey PET.

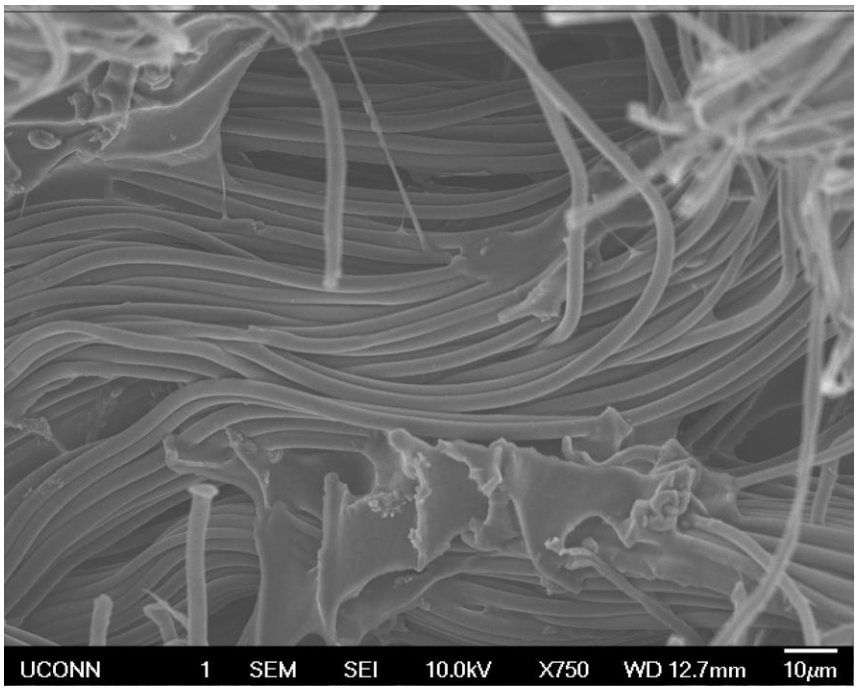

Figure 4.20: X750 image of 2 wt. % treated grey PET.

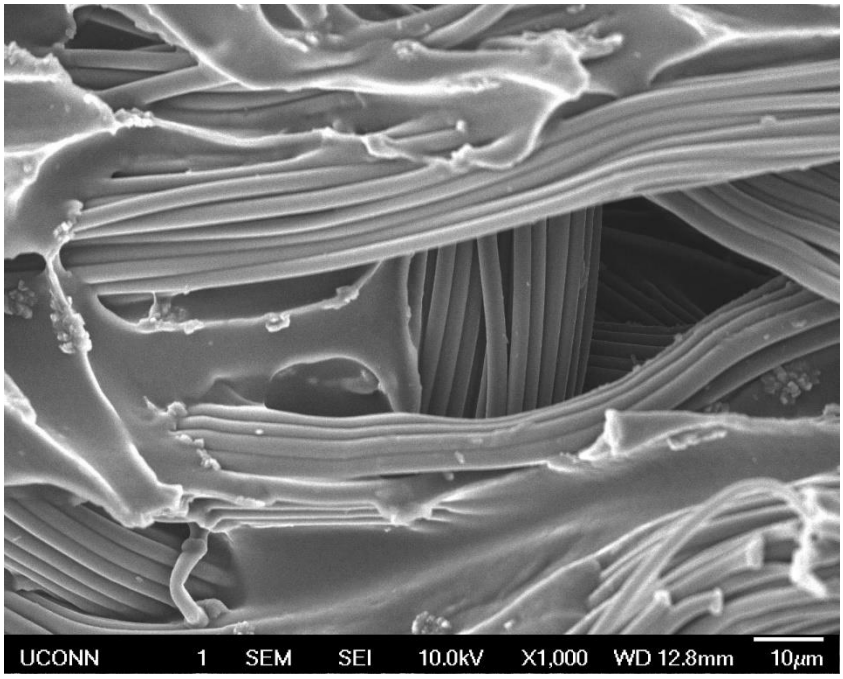

Figure 4.21: X1000 image of 2 wt. % treated grey PET.

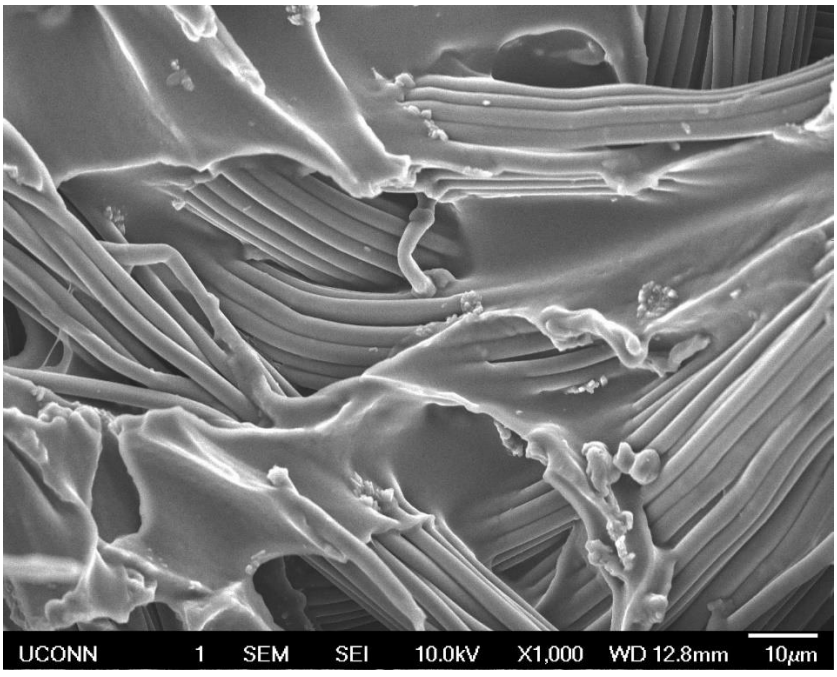

Figure 4.22: X1000 image of 2 wt. % treated grey PET.

Film sections were much more prevalent as the concentration of PEDOT:PSS increased.

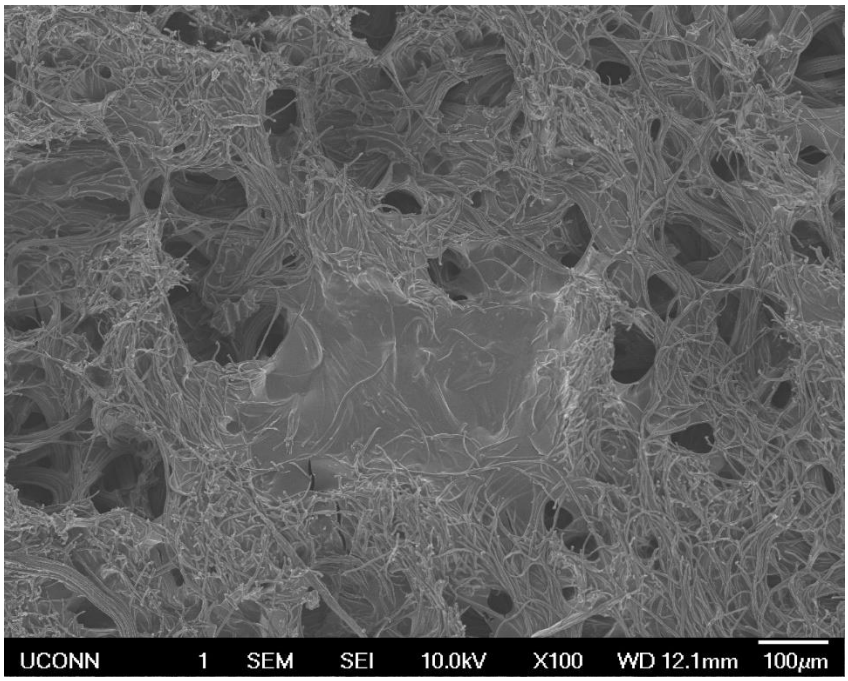

Figure 4.23: X100 image of 4 wt. % treated grey PET.

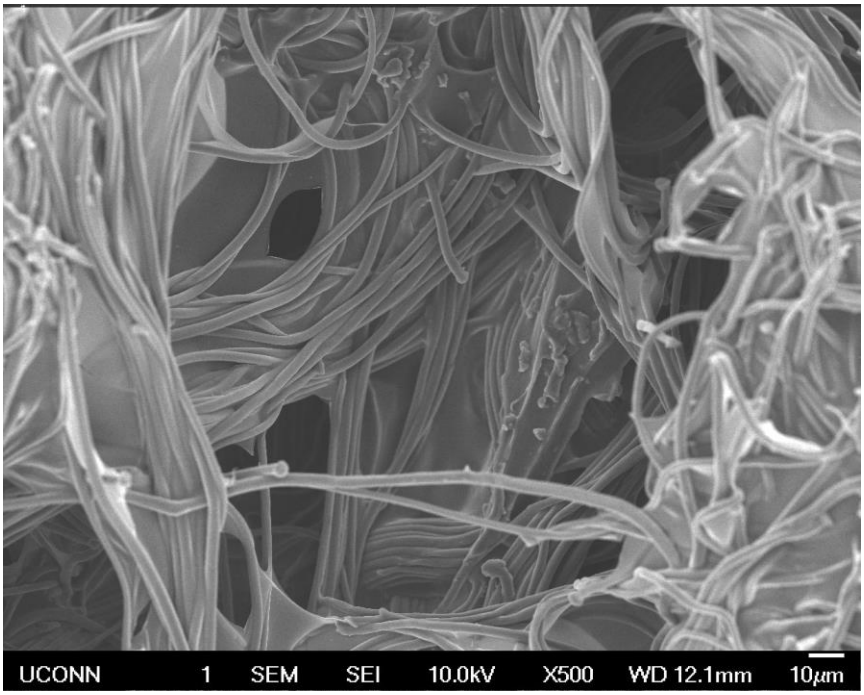

Figure 4.24: X500 image of 4 wt. % treated grey PET.

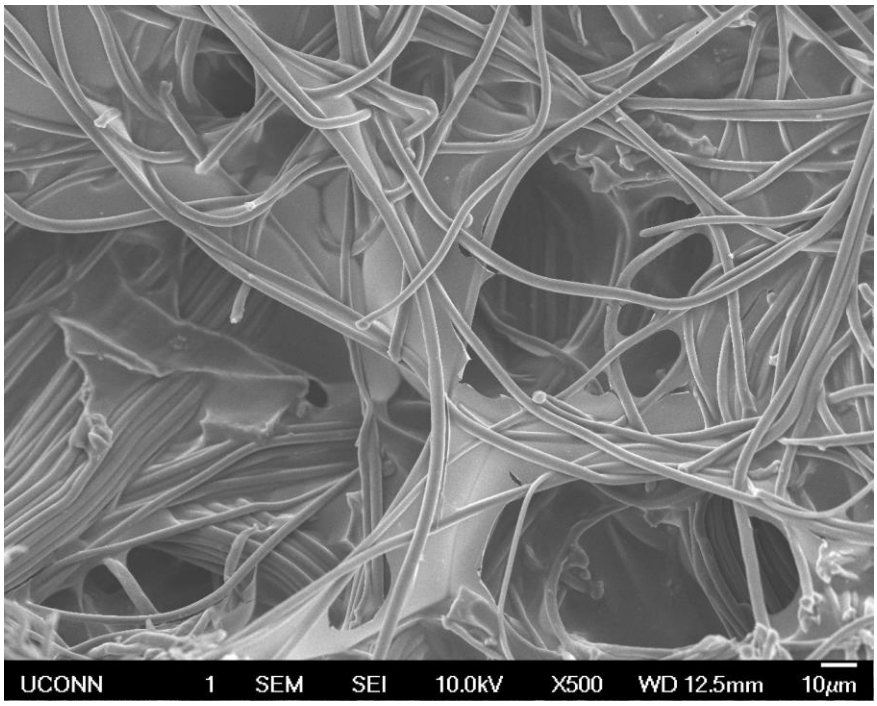

Figure 4.25: X500 image of 4 wt. % treated grey PET.

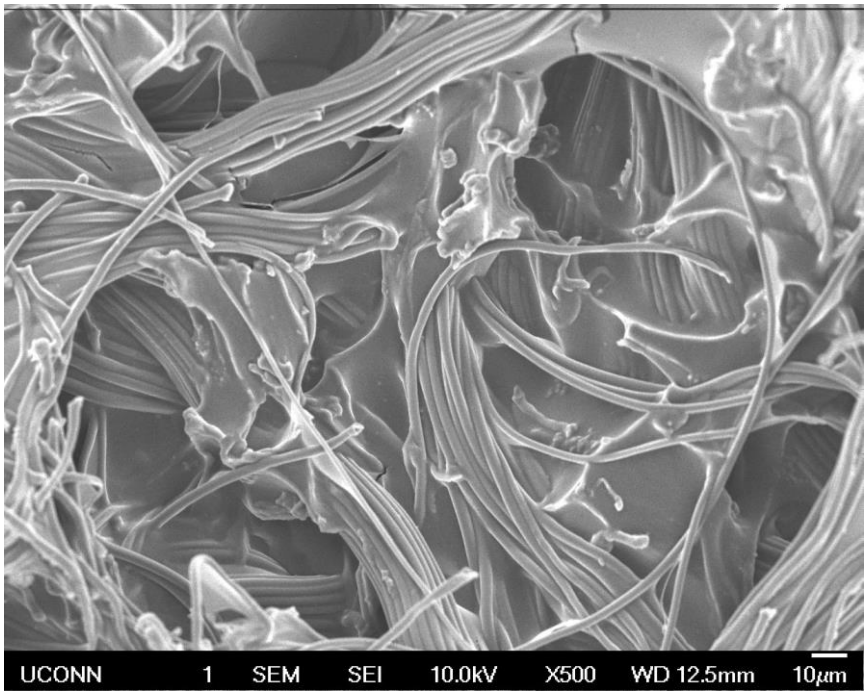

Figure 4.26: X500 image of 4 wt. % treated grey PET.

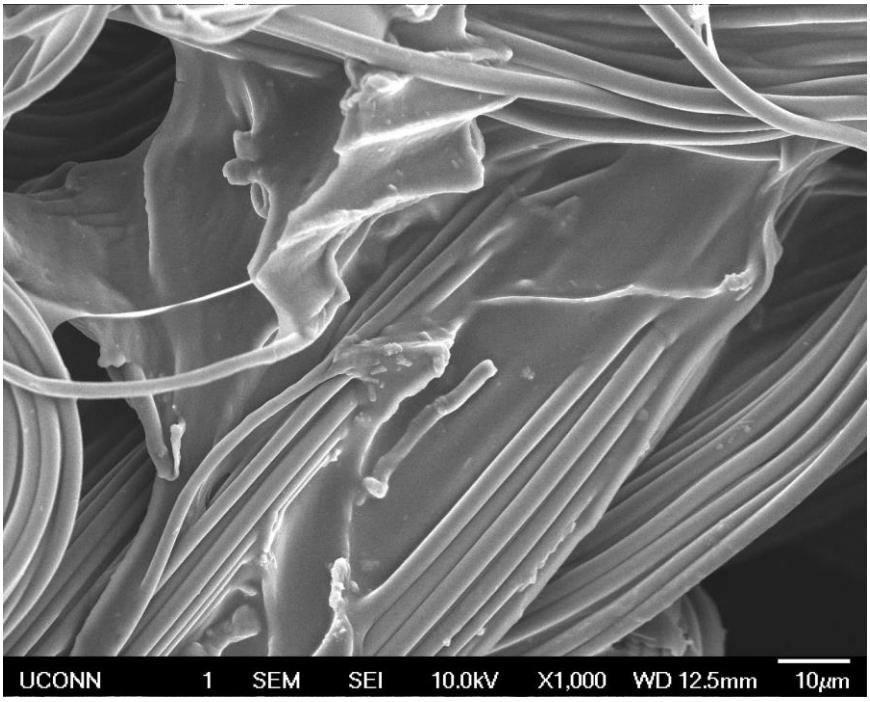

Figure 4.27: X1000 image of 4 wt. % treated grey PET.

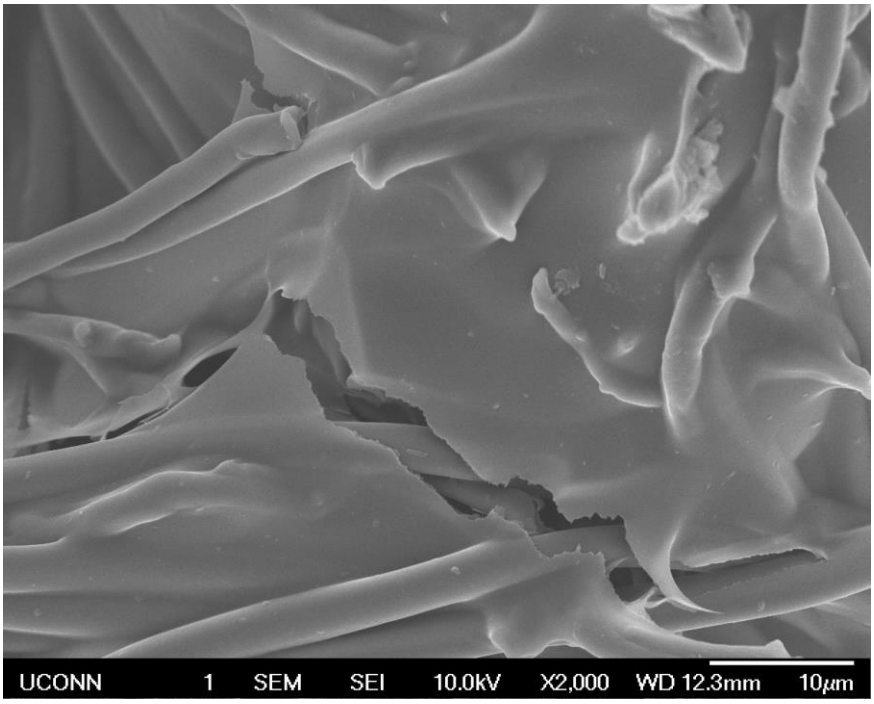

Figure 4.28: X2000 image of 4 wt. % treated grey PET.

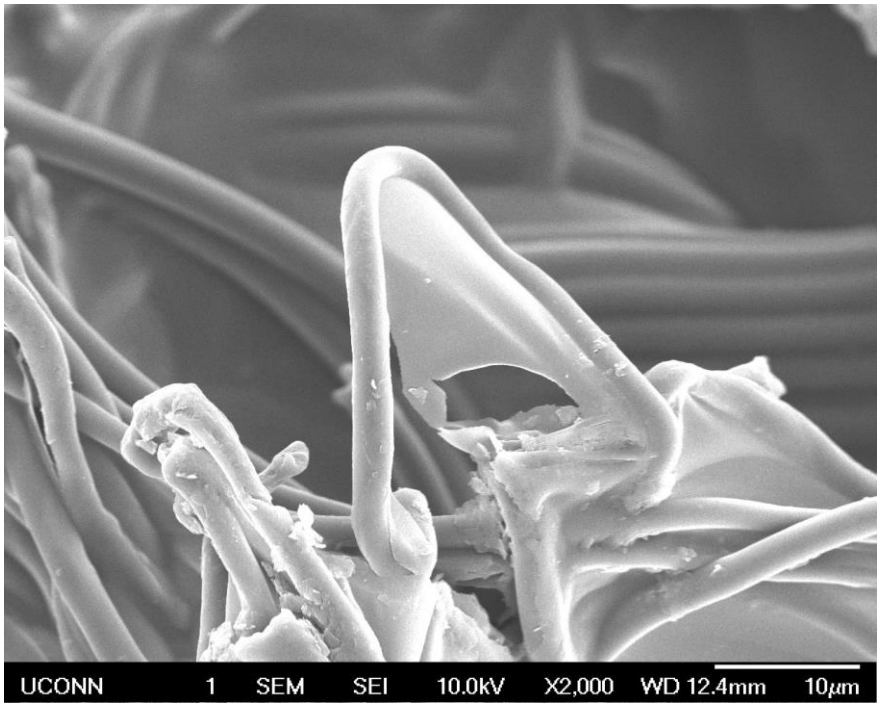

Figure 4.29: X2000 image of 4 wt. % treated grey PET.

With even more PEDOT:PSS, film is common between loose fibers.

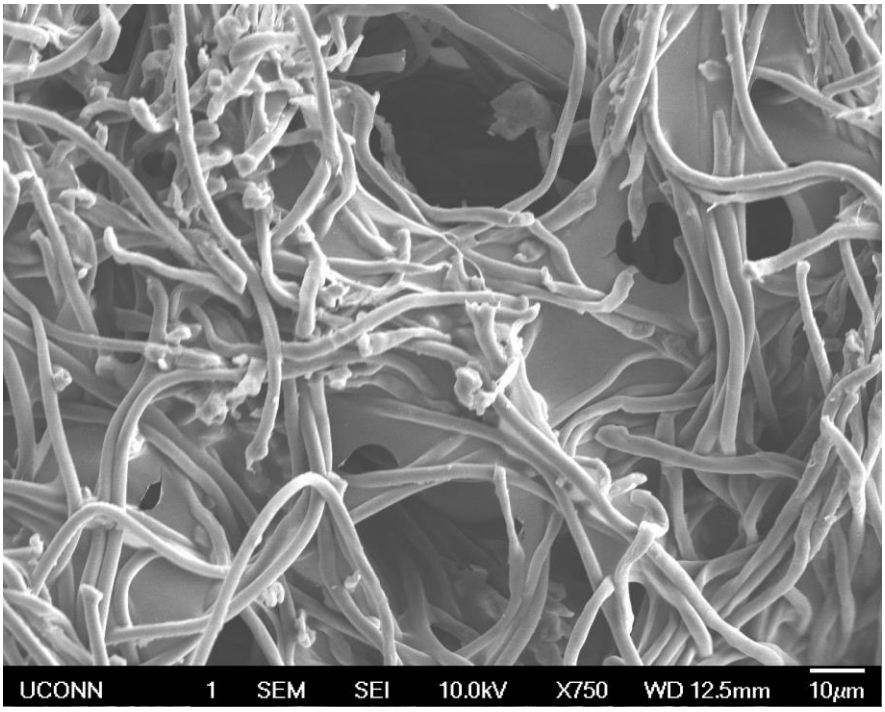

Figure 4.30: X750 image of 6 wt. % treated grey PET.

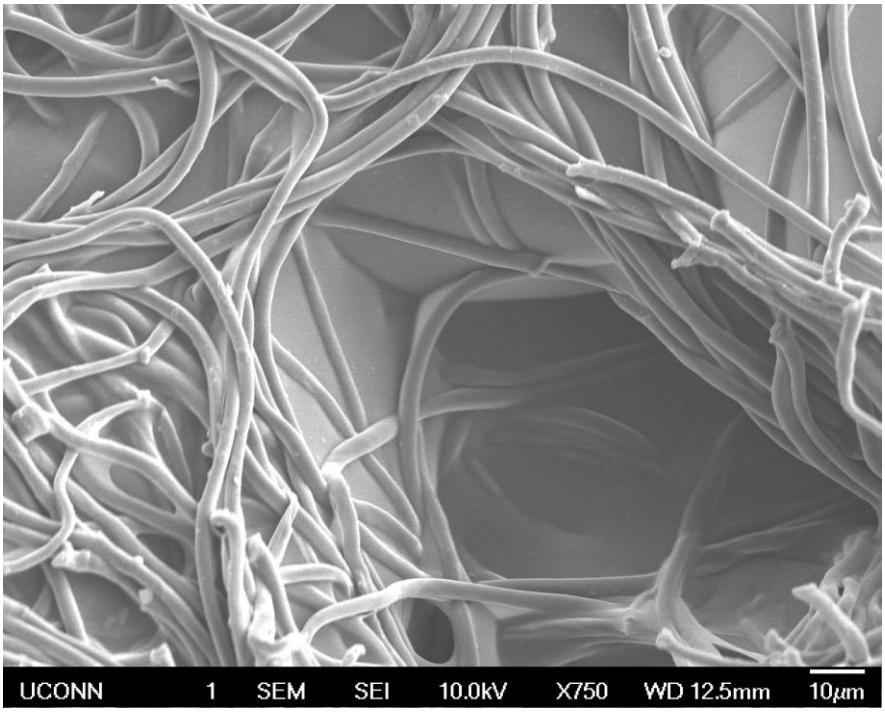

Figure 4.31: X750 image of 6 wt. % treated grey PET.

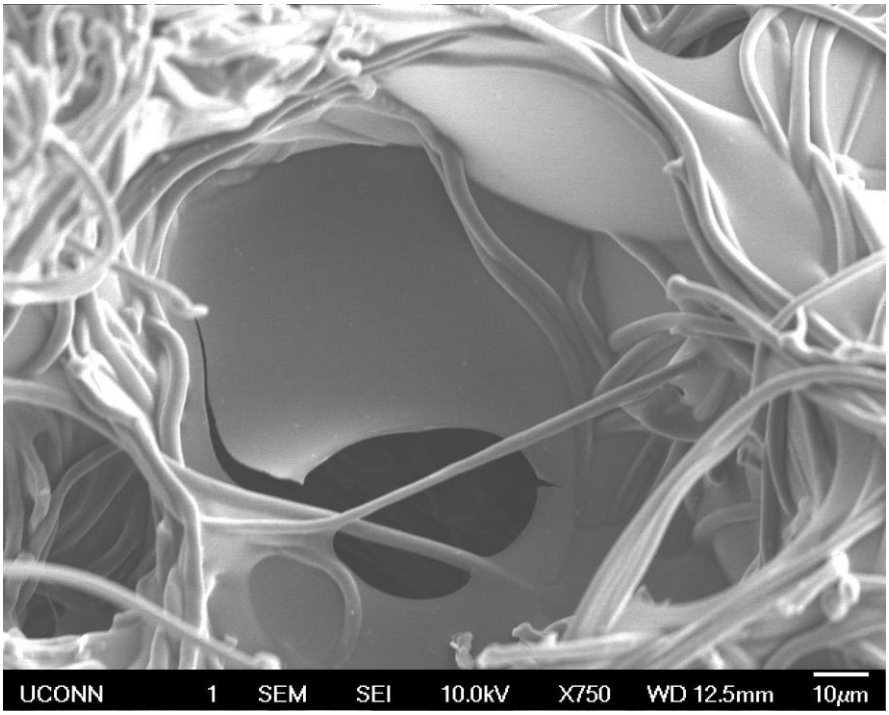

Figure 4.32: X750 image of 6 wt. % treated grey PET.

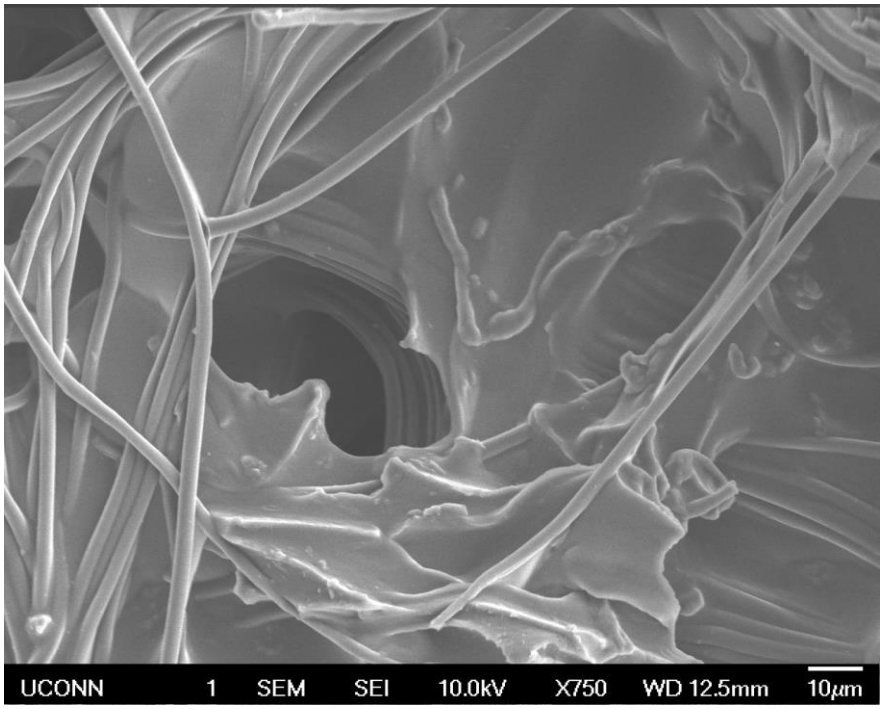

Figure 4.33: X750 image of 6 wt. % treated grey PET.

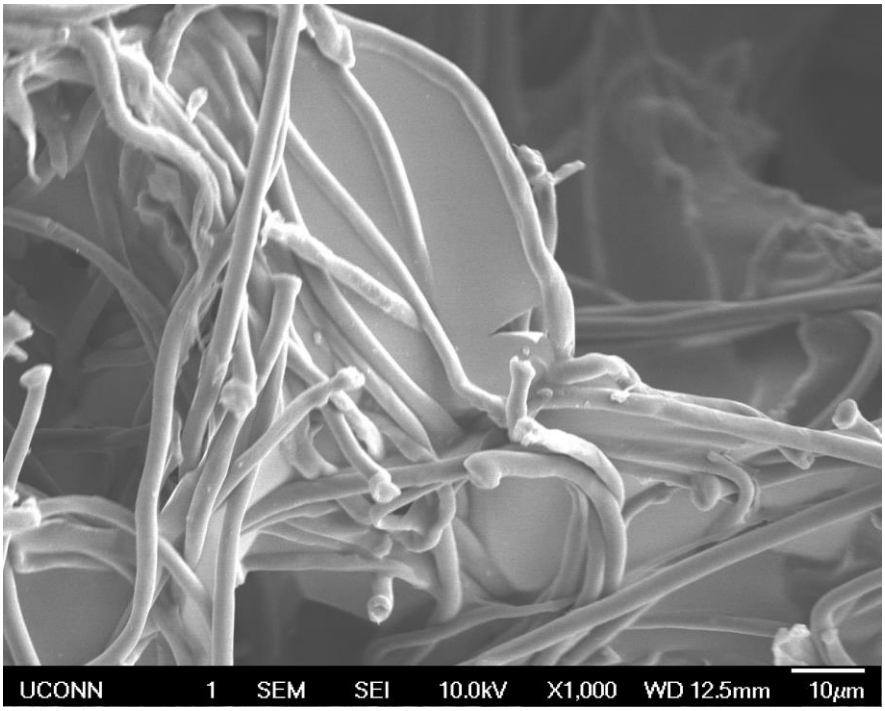

Figure 4.34: X1000 image of 6 wt. % treated grey PET.

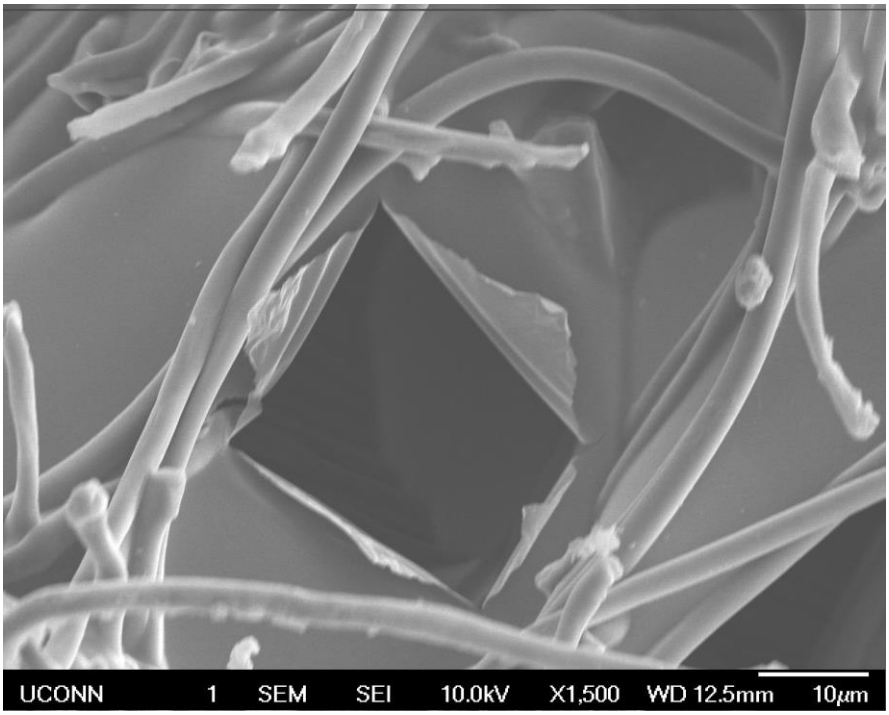

Figure 4.35: X1500 image of 6 wt. % treated grey PET.

4.2.3 Optimal Drying Conditions

Initial studies proved that soaking the PET fabric with PEDOT:PSS doped with 5 wt% DMSO (as recommended by Heraeus for their Clevios PH1000) and drying the fabric yielded samples with low resistance. However, since there are no standards for drying methods with fabric, a study was prepared for determining the optimal drying procedure for the PET synthetic leather.

In order to dry thin PEDOT:PSS films, the films are usually baked at elevated temperatures, under infrared, radiation, or by applying a vacuum. Sometimes a combination of these techniques is applied. However, thin films (with a thickness on the order of microns) are often dry within seconds, and the fabric is much thicker.

For this experiment, the temperature was varied for 1 hour of drying time. Samples were tested using both vacuum and no vacuum (Figure 4.36). Early results using one soak (1000 mg of solution) resulted in a fabric with a concentration of about 2 wt. % PEDOT:PSS. In order to achieve a lower weight percent, the solutions were diluted with deionized water. Fabric samples with a weight percent higher than 3 still had water present in the fabric and therefore would require a longer drying time. For studies in which multiple soakings of the fabric were required (in order to reach high concentration of PEDOT:PSS), a drying time of longer than 1 hour largely impacted the sample preparation total time.

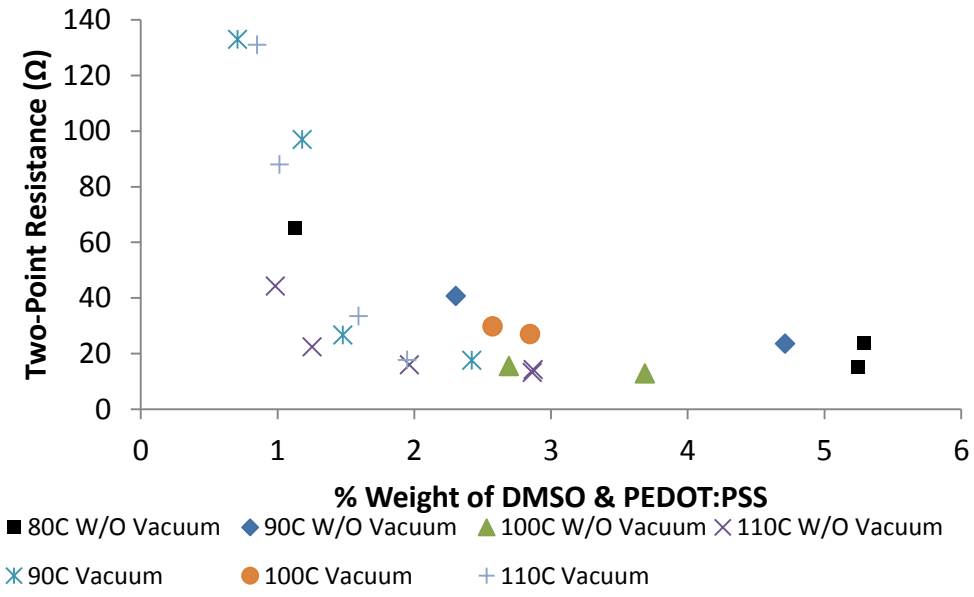

Figure 4.36: Ideal drying temperature determination for PET synthetic leather and DMSO doped PEDOT:PSS.

The samples that were dried in a vacuum lost PEDOT:PSS, so it was apparent that a regular oven was the best way to dry the fabric samples. From the results, 110°C displayed the most promising (lowest resistance) values for each weight percent and 100°C was the second most promising. Temperatures lower than 80°C were not explored because removing water at such low temperatures would take much more time. Temperatures above 110°C were not used because while the PEDOT:PSS is stable at 100°C for many hours, the PET fabric undergoes an endothermic transition at 150C. PEDOT:PSS is stable up until about 200°C. Between 100°C and 200°C, the weight loss is determined by evaporation of remaining water. Above 250°C, fragments due to oxidation are detected.[2]

A drying time study was performed at the most promising temperature (110°C) and 1 hour was the best drying time (Figure 4.37). Above 1 hour did not decrease the resistance.

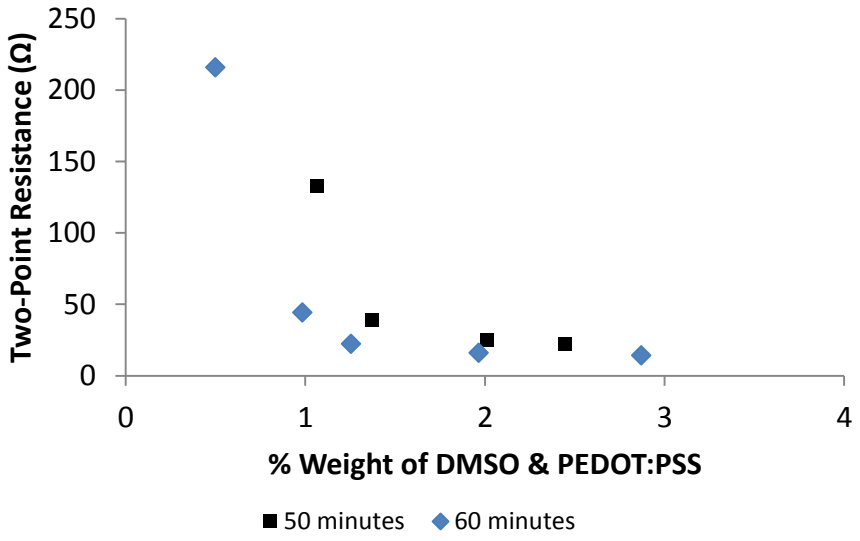

Figure 4.37: Drying time at 110°C for grey PET.

4.2.4 Varying Secondary Dopant

As reported by Heraeus, the conductivity of CleviosPH1000 can be up to 1000 S/cm when doped with 5 weight % ethylene glycol (EG) or dimethyl sulfoxide (DMSO). The solutions were wicked into the grey PET and dried at 110°C for 1 hour. From the results in Figure 4.38, the DMSO doped fabric samples had slightly lower resistance.

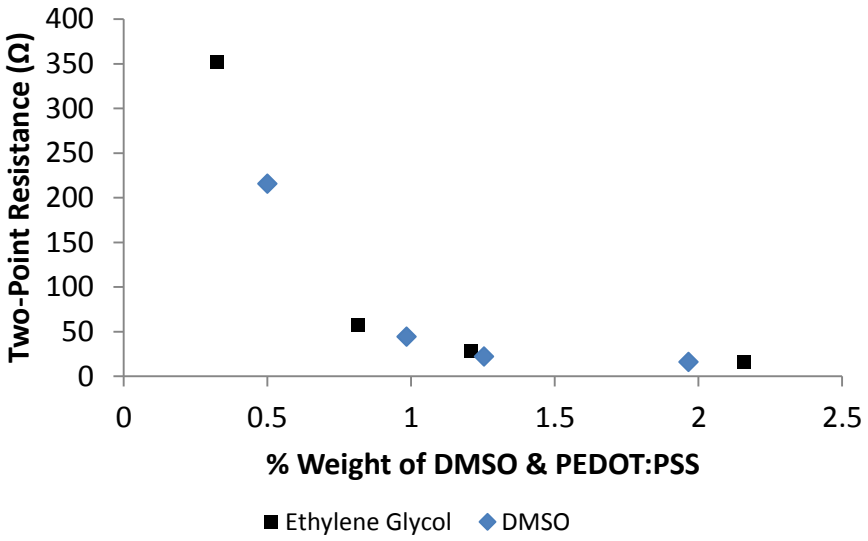

Figure 4.38: PEDOT:PSS doped with 5% EG or DMSO.

The concentration of EG and DMSO were also varied. The results clearly show that DMSO produces a fabric with a lower sheet resistance and that increasing the amount of DMSO also decreases the sheet resistance. However, there is a large error margin that could be improved by more iterations.

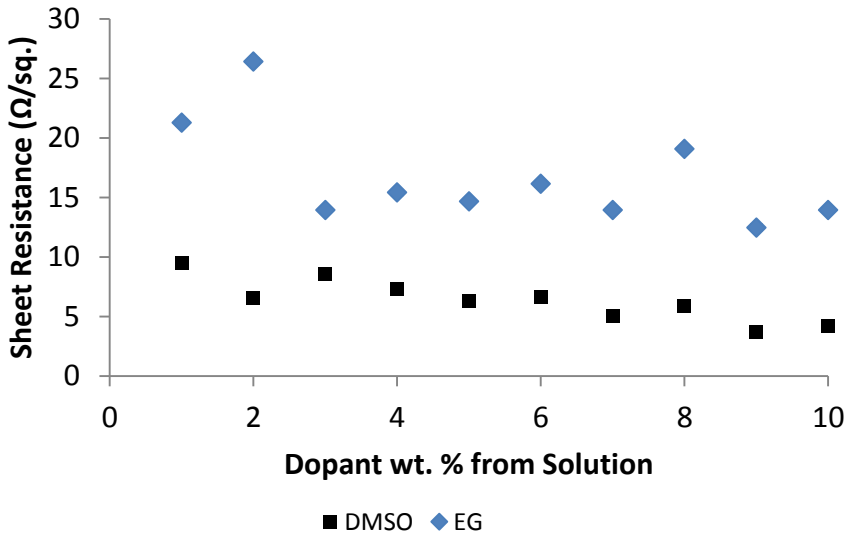

Figure 4.39: Varying concentration of secondary dopant.

4.2.5: PEDOT:PSS Saturation in PET

Increasing the concentration of PEDOT:PSS in the grey PET leads to lower resistance (Figure 4.40). Concentrations lower than 2 wt% were achieved by diluting the doped PEDOT:PSS solution with deionized water and concentrations above 2 wt% were achieved by multiple soakings. The resistance measurement was a 2-point surface resistance that was converted to sheet resistance using the sample dimensions.

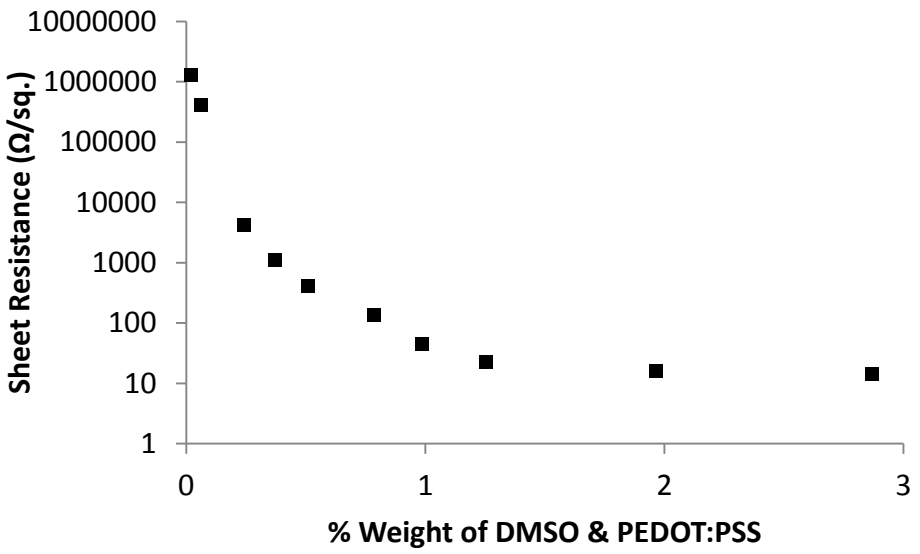

Figure 4.40: Trend for decreasing resistance with increasing concentration of PEDOT:PSS in the PET fabric.

The difference in sheet resistance from the 2-point and the 4-line measurements is shown in Figure 41. The 2-point measurement does not account for contact resistance and is therefore slightly higher.

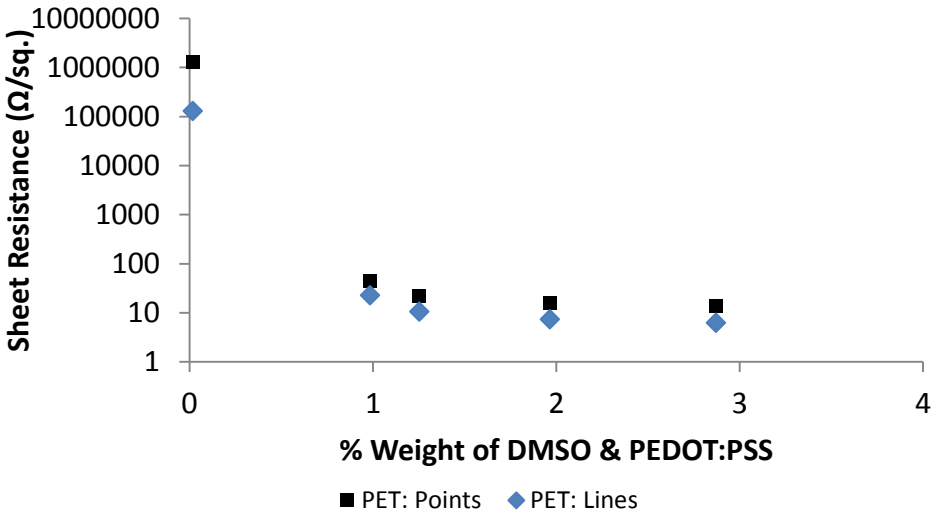

Figure 4.41: 2-point vs. 4-line sheet resistance.

Based on the trends in Figures 4.40 and 4.41, it can be concluded that the fabric reaches a saturation point in resistance at just above 1 wt. % of PEDOT:PSS and DMSO.

4.2.5.1 SEM at Saturation

With the addition of 1% by weight PEDOT:PSS to the grey PET, the surface of the fabric appears blue and is vastly different in SEM images. Film formation of the PEDOT:PSS can already be easily found at this concentration.

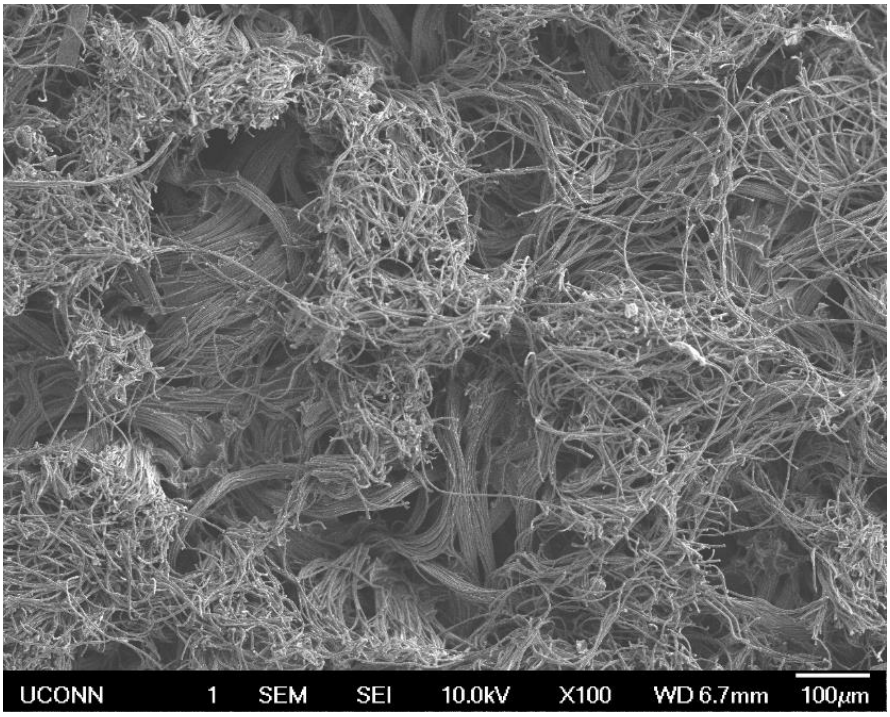

Figure 4.42: X100 magnification SEM image at saturation of grey PET.

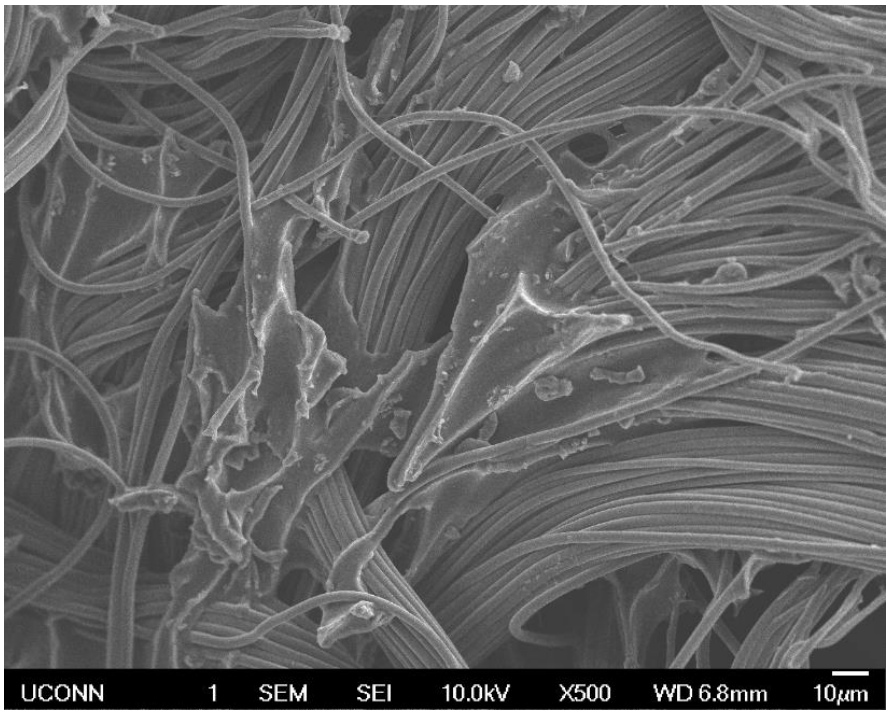

Figure 4.43: X500 magnification SEM image at saturation of grey PET.

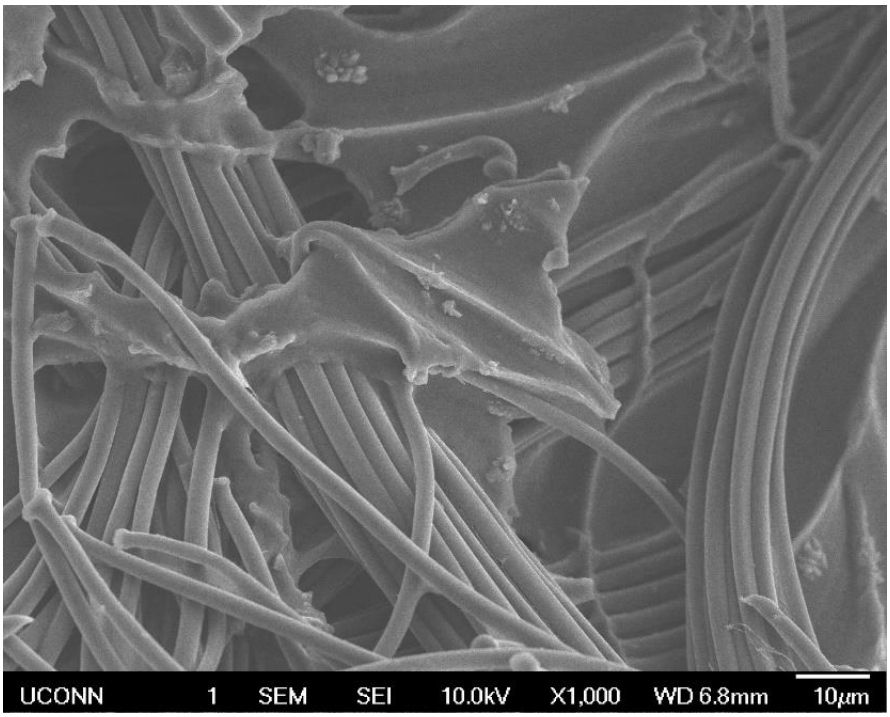

Figure 4.44: X1000 magnification SEM image at saturation of grey PET.

4.2.6 Scalability

Larger pieces of soaked PET had consistent resistance measurements across the entire sample.

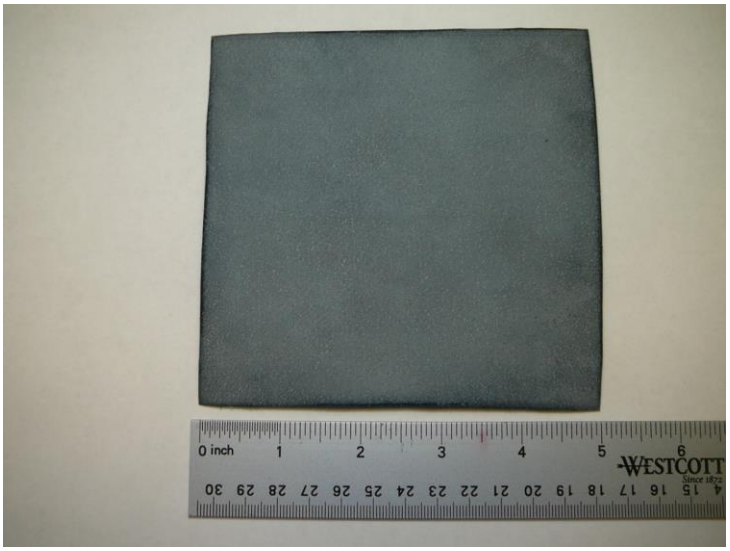

Figure 4.45: 5” piece of treated grey PET.

4.2.7 Washing Machine Test

Various fabrics were washed in cold water for 25 minutes (bright clothes cycle) and dried on regular for 30 minutes (no low heat option). Grey PET samples soaked once and twice with PEDOT:PSS lost less than 1% by weight.

Description	Pre-weight (mg)	After weight (mg)	weight loss (%)
1 Soak Grey PET	2327.7	2310.4	0.74
2 Soaks Grey PET	2686.4	2664	0.83
Green poly/cotton Blend with Steel	179.9	178.4	0.83
Silver plated Nylon	217	217	0
Steel Mesh	32.5	32.5	0
Graphene on Grey PET	727.8	689	5.33

Table 4.3: Weight difference in various fabrics after washed and dried.

4.3 White PET

4.3.1 Wicking Behavior

The white PET is resistant to water (Fig. 4.46) probably due to an additive or coating during manufacture.

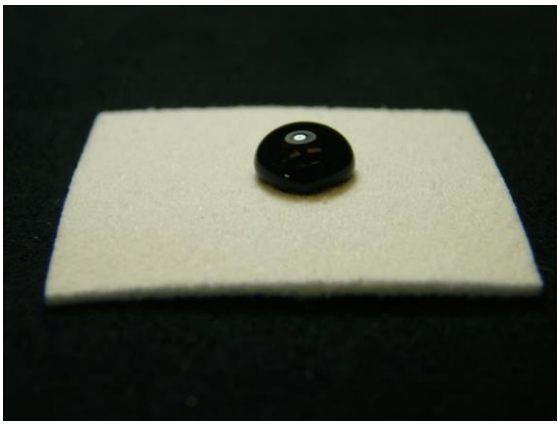

Figure 4.46: Hydrophobic visual for the white PET.

The white PET was soaked for 15 minutes and dried for 1 hour at 110 °C for the images in Figure 4.47. Some PEDOT:PSS does eventually soak into the fabric. As the PEDOT:PSS dries, it creates a non-uniform film on the surface of the fabric.

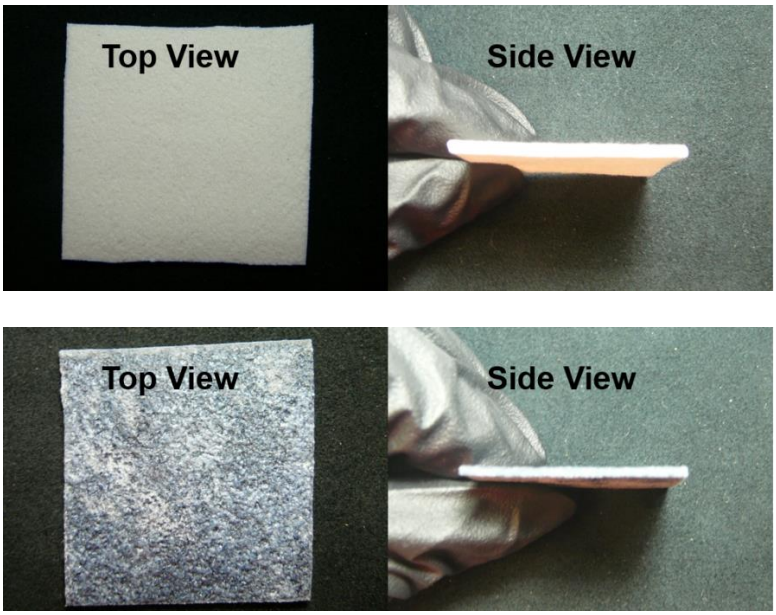

Figure 4.47: Untreated (top) vs. treated (bottom) white PET.

Four drops of PEDOT:PSS (two on each side) were added to each fabric piece (Figure 4.48). The droplet diffusion shows that some of the PEDOT:PSS is absorbed, while some remains on the surface. The resistance on the white leather samples ranges from ~40 Ω in the center to ~140 Ω in the outer ring.

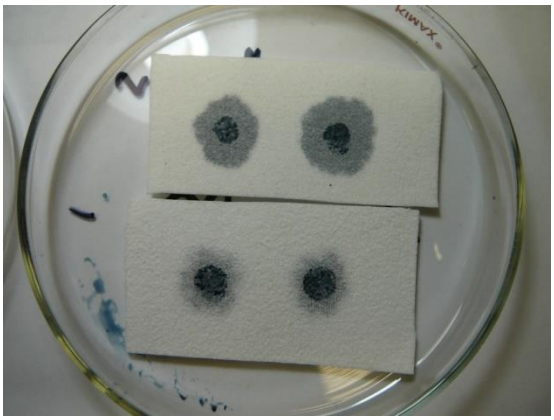

Figure 4.48: Droplet diffusion in white PET.

The white fabric was allowed to soak in a PEDOT:PSS solution doped with 5 wt. % DMSO for 10 minutes. Excess solution was removed and the fabric was allowed to sit for an additional 20 minutes. It was then dried at 90 °C for 1.5 hours. Between 10-12 % by weight conductive material was added and the resistance (measured with gold tabs) was between 5-20 Ω, and depended greatly on location.

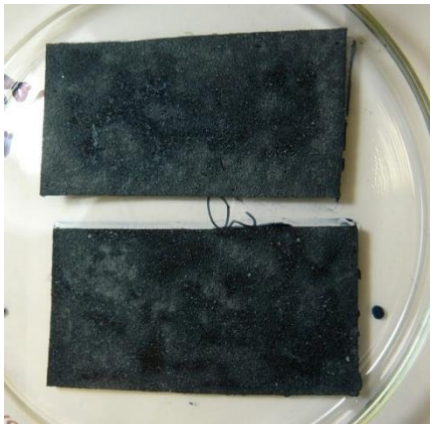

Figure 4.49: Treated white PET.

Whereas the PEDOT:PSS solution diffuses readily into the grey leather, it is obvious from these results that the white leather is resistant to water.

4.3.2 SEM

The white PET PEDOT:PSS film formation is much smoother due to the hydrophobic properties of the fabric. Most of the PEDOT:PSS creates a film layer on the top of the white PET, with cracks in the film likely forming due to flexing of the fabric.

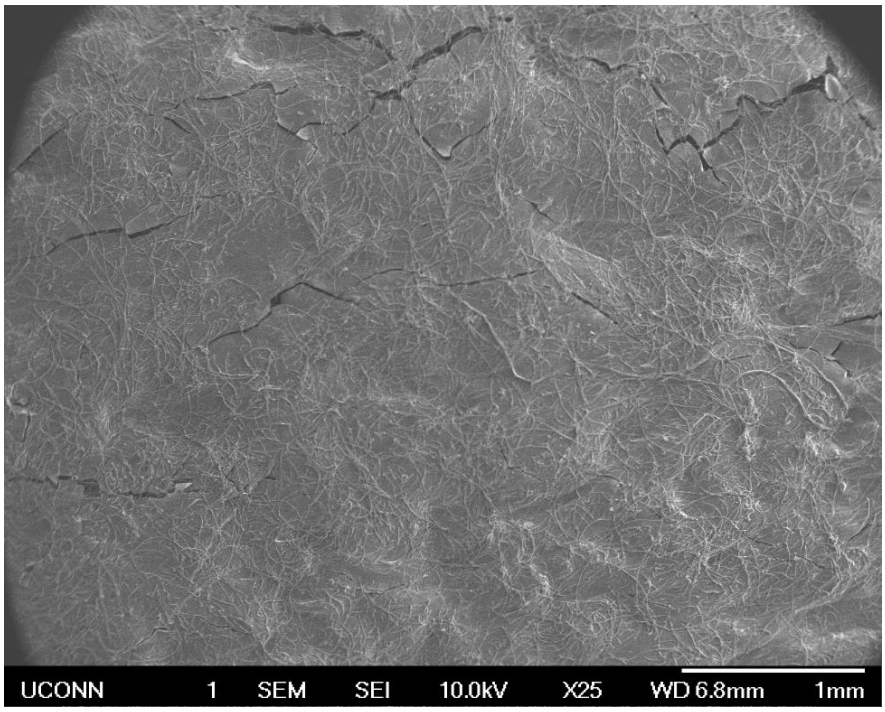

Figure 4.50: X25 magnification SEM image of 6 wt. % white PET.

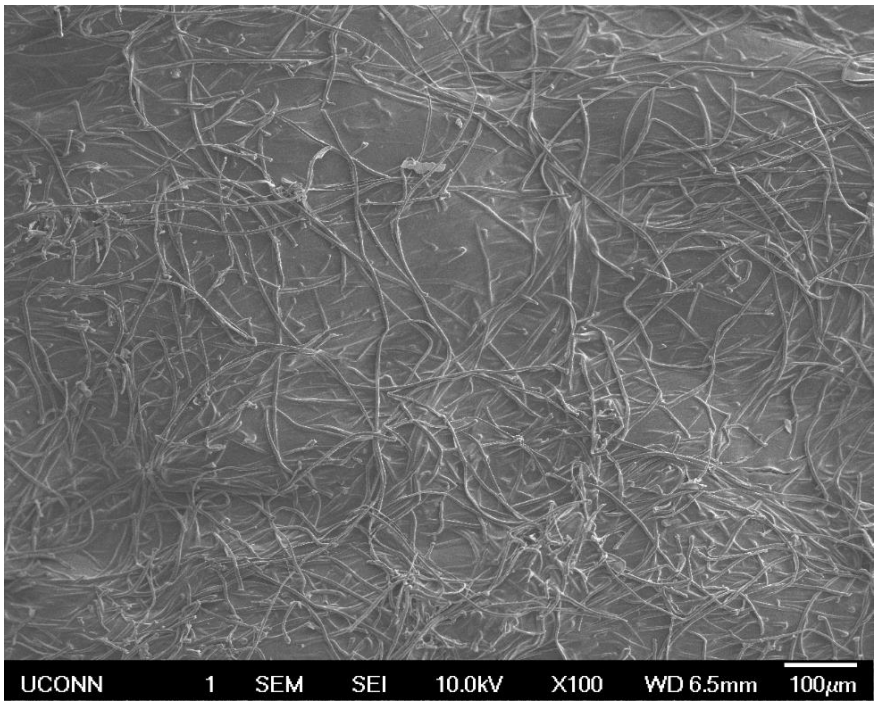

Figure 4.51: X100 magnification SEM image of 6 wt. % white PET.

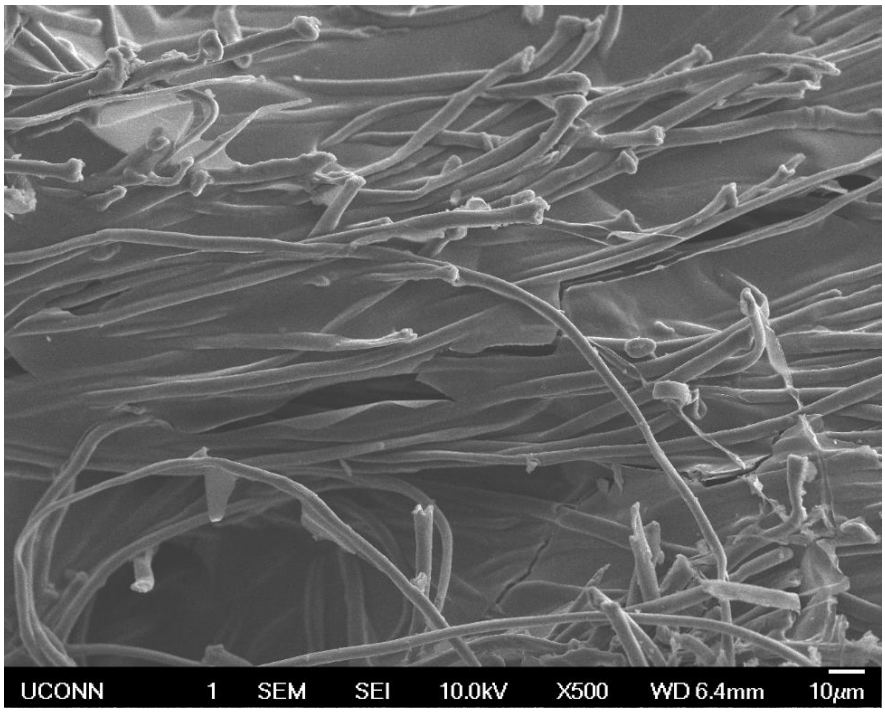

Figure 4.52: X500 magnification SEM image of 6 wt. % white PET.

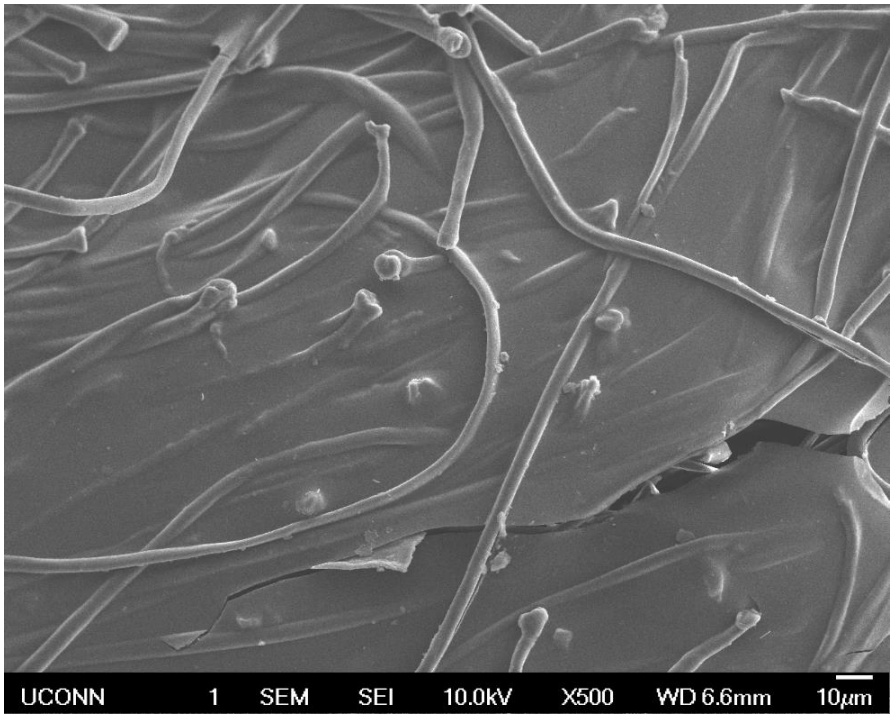

Figure 4.53: X500 magnification SEM image of 6 wt. % white PET.

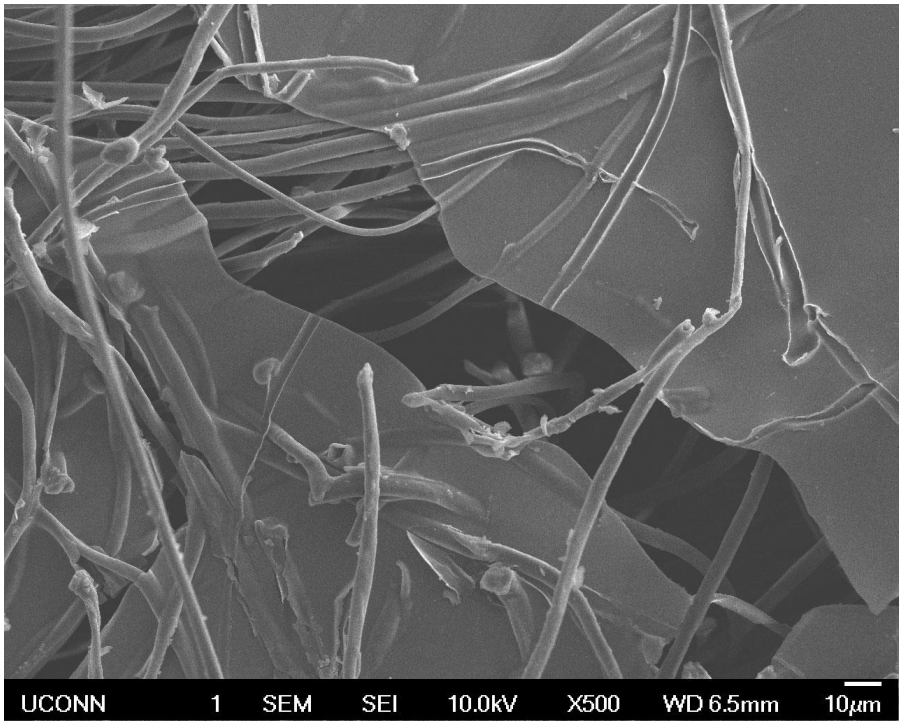

Figure 4.54: X500 magnification SEM image of 6 wt. % white PET.

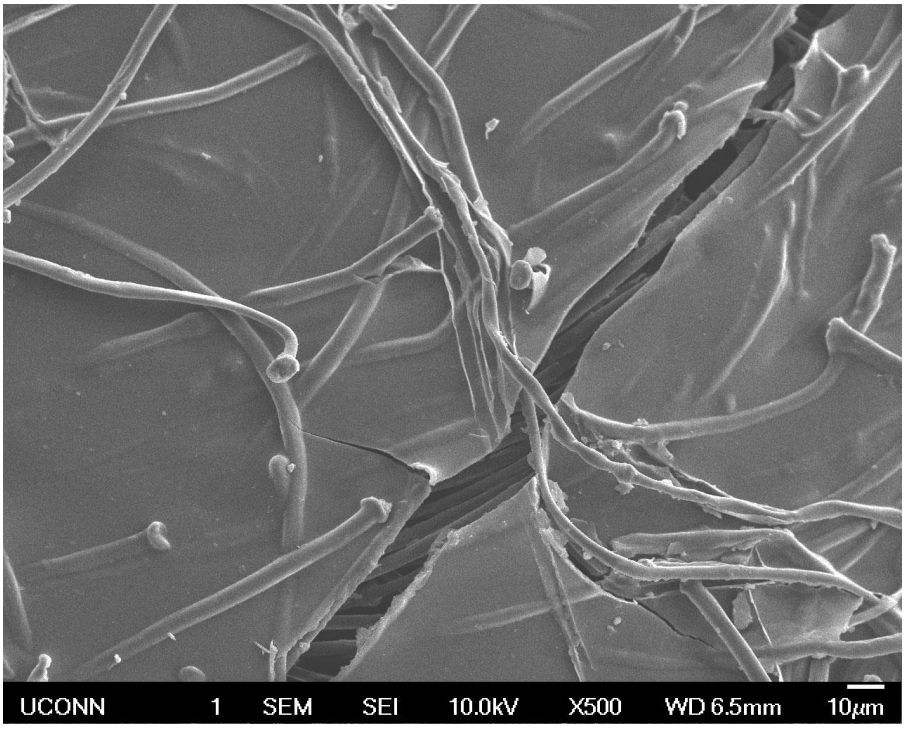

Figure 4.55: X500 magnification SEM image of 6 wt. % white PET.

4.4 Nylon

4.4.1 TGA

A piece of Nylon fabric was soaked with DMSO doped CleviosPH1000 and dried at 110°C for one hour (the procedure used for the grey PET). A TGA was run on the sample, revealing significant change in the degradation temperature. The untreated Nylon had a 3 % weight loss T_d of 357 °C after normalization for monomer loss. The treated Nylon had a 3 % weight loss T_d of 234 °C after normalization (Figure 4.56).

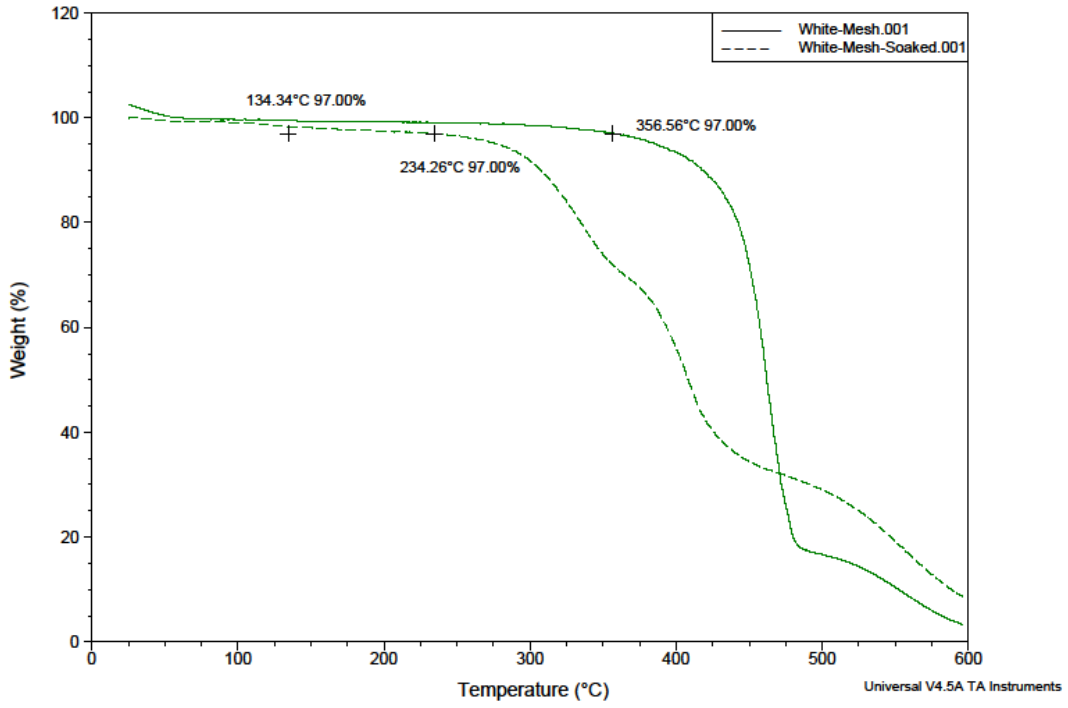

Figure 4.56: Degradation of Nylon after PEDOT:PSS Treatement.

The reason for this extreme change could be hydrolytic degradation from the PEDOT:PSS drying step at 110 °C. To process Nylons, they must have low moisture content to avoid splay or brittleness from degradation. It is generally recommended to dry them in an oven or dehumidifying dryer at low temperatures (~80 °C) for 12 hours.

4.4.2 SEM

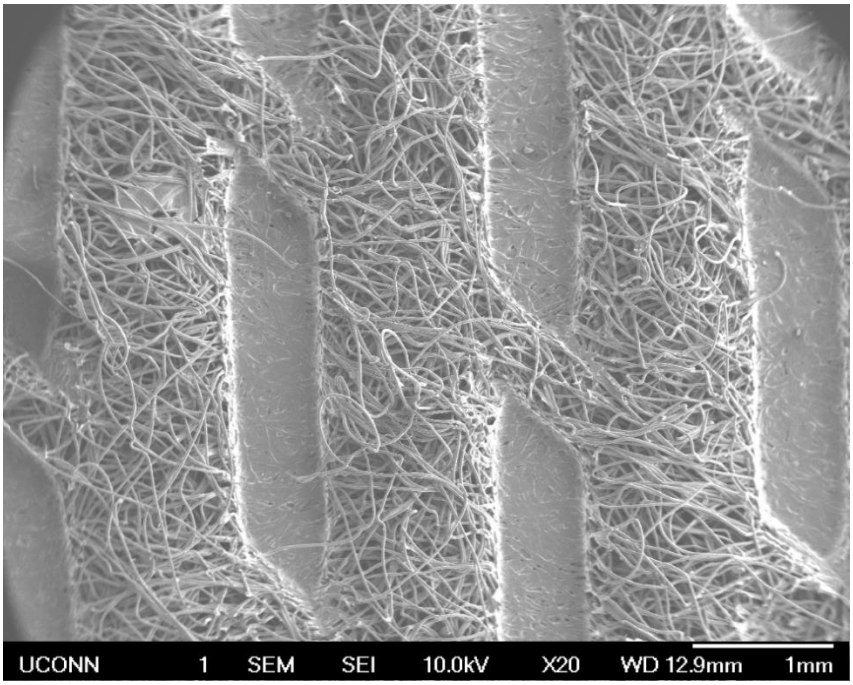

Figure 4.57: X20 SEM image of treated Nylon.

Figure 4.58: X500 SEM image of treated Nylon.

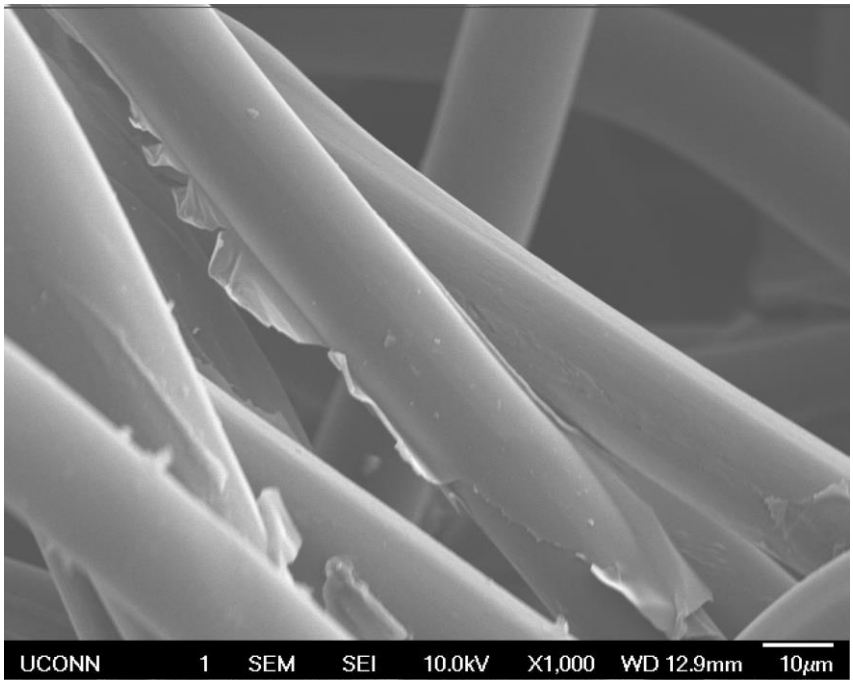

Figure 4.59: X1000 SEM image of treated Nylon.

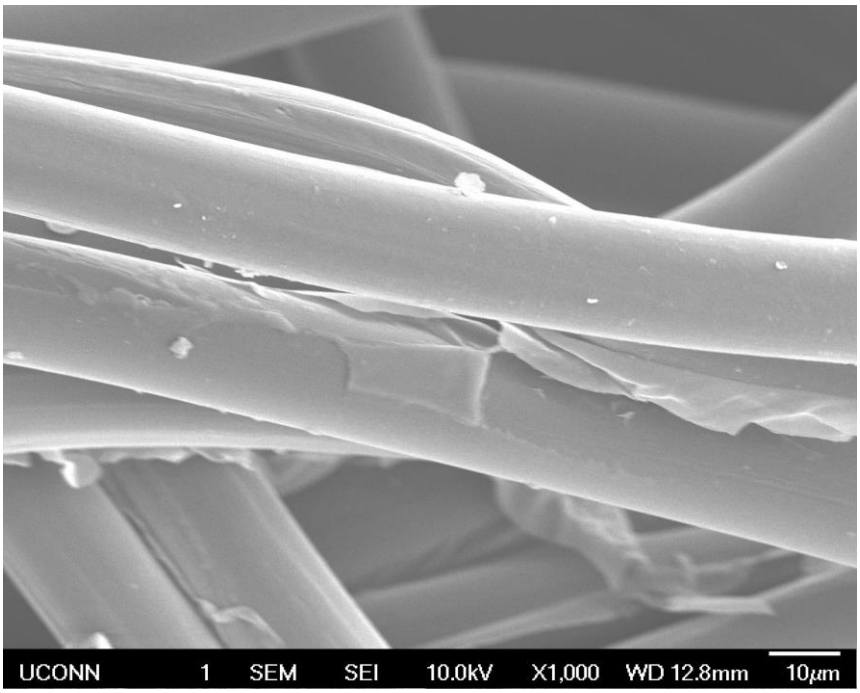

Figure 4.60: X1000 SEM image of treated Nylon.

4.4.3 Nylon PEDOT:PSS Saturation

Obtaining a saturation curve for the Nylon fabric was difficult due to the presence of the monomer, which evaporated upon heating. The treated fabric at low concentrations would end up weighing less after treatment with PEDOT:PSS due to the monomer evaporation. To alleviate this problem, the Nylon fabric in Figure 4.61 was heated at 110°C for an hour, saturated with PEDOT:PSS doped with 5 wt. % DMSO, then heated again at 110°C for an hour. The sheet resistance was measured using the 4-line probe. From the results, the Nylon fabric reaches a saturation point at about 5 wt. % conductive material.

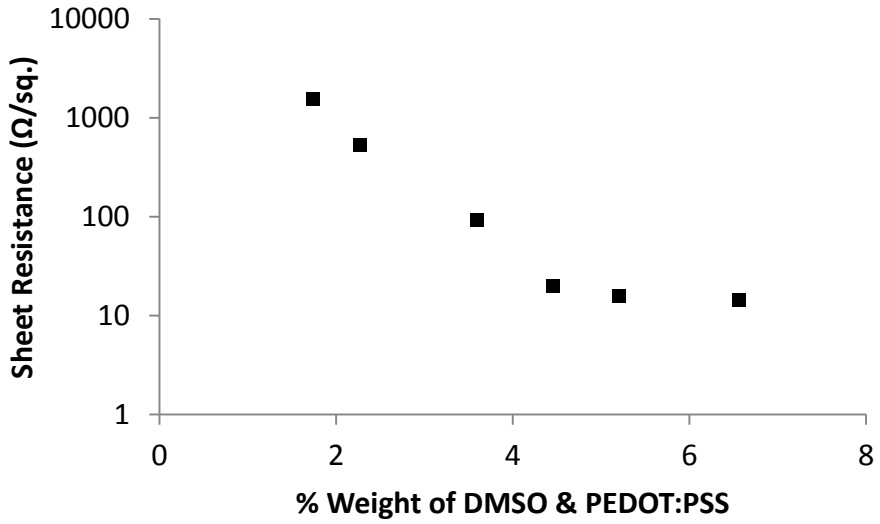

Figure 4.61: Saturation of PEDOT:PSS in Nylon.

Since the Nylon fabric weighed less than the PET, one treatment with doped PEDOT:PSS produced a fabric with approximately 5 wt. % conductive material.

4.5 Spandex

4.5.1 Saturation of PEDOT:PSS in Spandex

To better understand the relationship between conductivity and PEDOT:PSS loading in the fabric, the saturation threshold was first determined. In this study, spandex was treated with PEDOT:PSS solutions comprised of 10, 15, 25, 50, 75, and 100 wt. % PEDOT:PSS in deionized water. In all cases, the solutions were doped with 5 wt. % of dimethylsulfoxide (DMSO) to maximize the conductivity, as per the manufacturer's specifications.[3] These spandex samples were cut to approximately 1" squares and were saturated with the aforementioned conductive solutions via drop casting. They were subsequently allowed to air dry for 12 hours before conductivity measurements were made using the 4-line method. The concentrations of the solutions are described in Table 4.4.

CleviosPH1000 Concentration (wt. %)	Deionized Water Concentration (wt. %)
10	90
15	85
25	75
50	50
75	25
100	0

Table 4.4: Concentration of diluted CleviosPH1000 solutions. All solutions were doped with 5% DMSO after diluting.

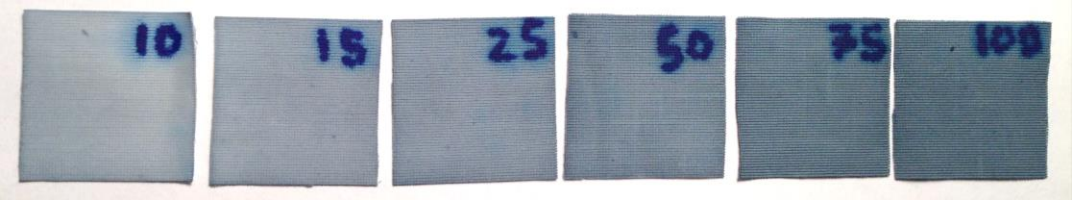

Figure 4.62: Dilutions of CleviosPH1000 on spandex, where the numbers correspond to the CleviosPH1000 concentration listed in Table 4.4.

For making an EFD, there is a trade-off between conductivity and coloring; higher loadings of PEDOT:PSS impart a deeper blue color to the spandex (Figure 4.62), making the electrochromic material more difficult to see. The ideal spandex electrode will be conductive enough to facilitate color change in the electrochromic material, but will be light enough to show an intense electrochromic color change.

The resultant saturation graph shown below (Figure 4.63), demonstrates that sheet resistance saturation is reached with an approximately 50 wt. % solution, with a sheet resistance in the 150 Ω/sq. regime.

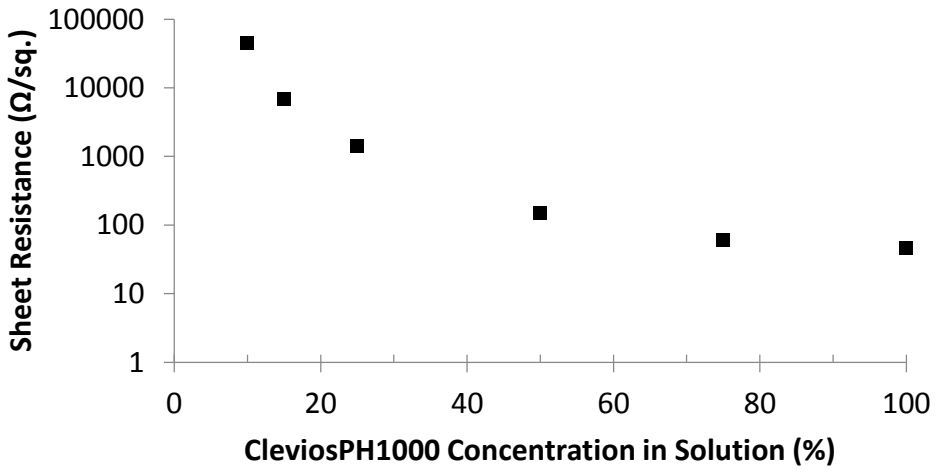

Figure 4.63: Sheet resistance of diluted CleviosPH1000 on spandex.

4.5.2 Conductivity

For the conductivity calculation, the PEDOT:PSS film thickness was determined using scanning electron microscopy (SEM). The resulting thicknesses are displayed in Table 4.5, as well as the weight % of PEDOT:PSS in each fabric after completely drying.

Solution Concentration of CleviosPH1000 (%)	Weight %	Average Film Thickness (μm)
10	1.32	0.100
15	1.64	0.112
25	1.81	0.120
50	2.53	0.127
75	3.55	0.131
100	4.72	0.145

Table 4.5: Solution concentration and corresponding weight % and film thickness of CleviosPH1000 on spandex.

The conductivity at each concentration is graphed in Figure 4.64. The conductivity of the 50% CleviosPH1000 solution sample was 514 S/cm and reached a maximum of 1380 S/cm for just one treatment of doped PEDOT:PSS. Additional soakings would increase the conductivity of the spandex.

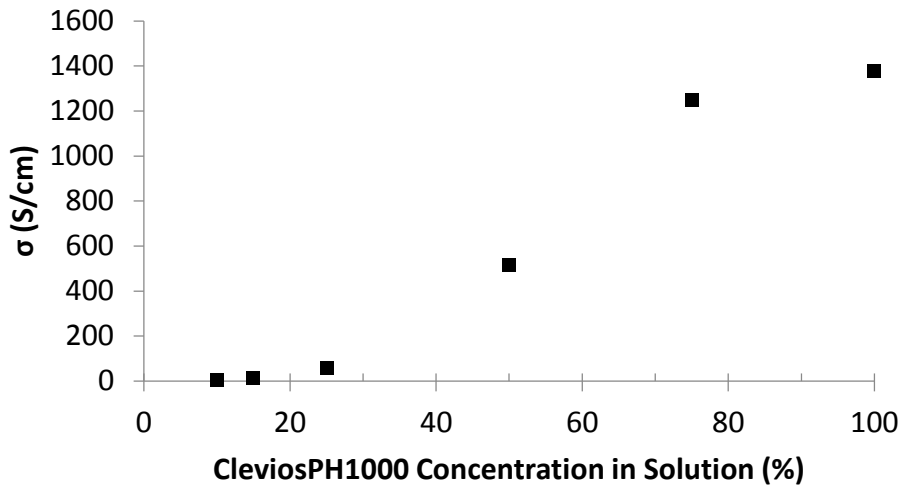

Figure 4.64: Conductivity of diluted CleviosPH1000 on spandex.

The 50% CleviosPH1000/ 50% Water solution imparts a similar depth of color to the spandex as the Orgacon PEDOT:PSS (Figure X). The Orgacon is also a good choice of PEDOT:PSS for EFDs, although most of the electrochromic experiments in this work use a diluted Clevios solution instead.

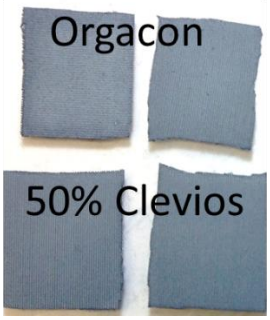

Figure 4.65: Comparison of Orgacon and 50% Clevios colors.

Several images were used at each CleviosPH1000 concentration in order to determine the film thickness of PEDOT:PSS. The images were evaluated with ImageJ software.

4.5.3 SEM

The increasing amount of film across the solution concentration samples isn't very apparent, especially at lower magnification. However, the PEDOT:PSS film tends to peel off the spandex, which allowed for direct measurements of the film thickness from SEM.

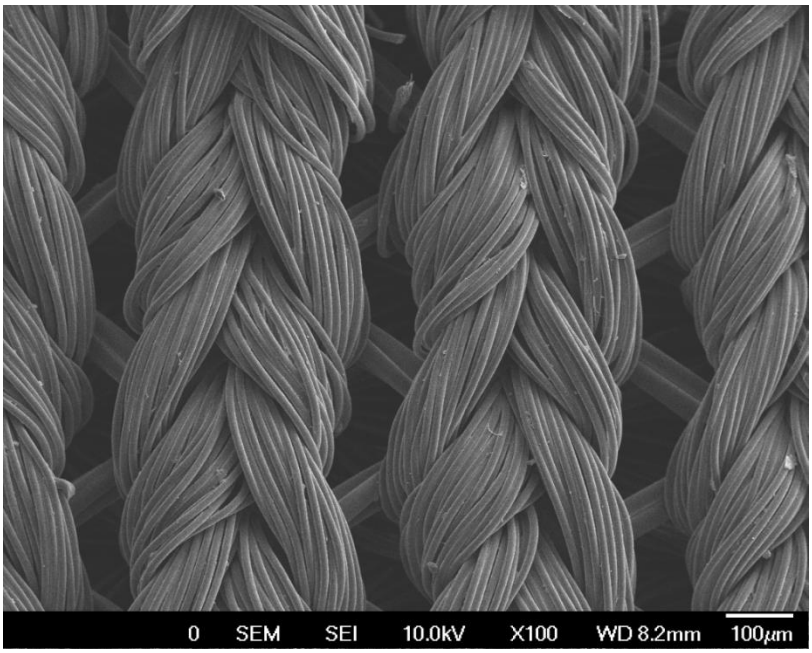

Figure 4.66: SEM X100 magnification of 10% CleviosPH1000 solution in spandex.

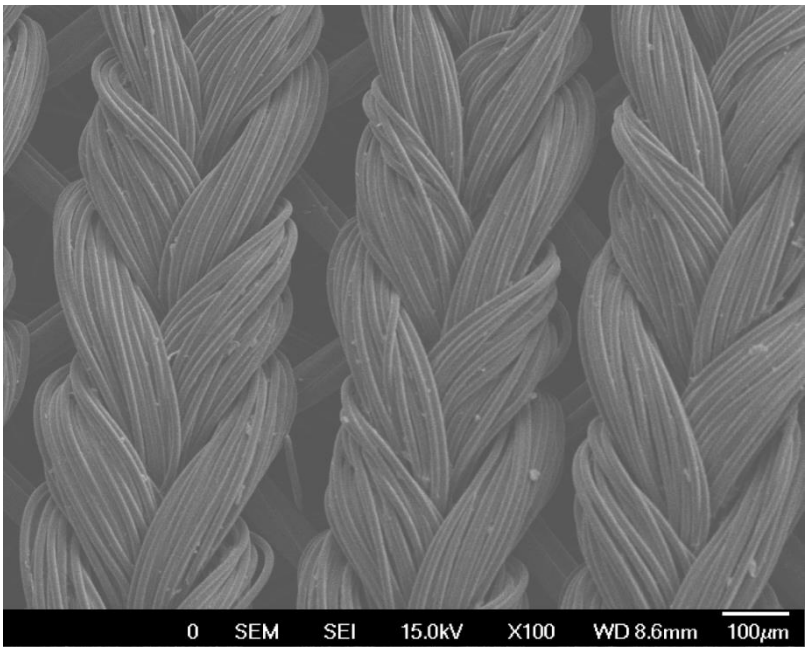

Figure 4.67: SEM X100 magnification of 15% CleviosPH1000 solution in spandex.

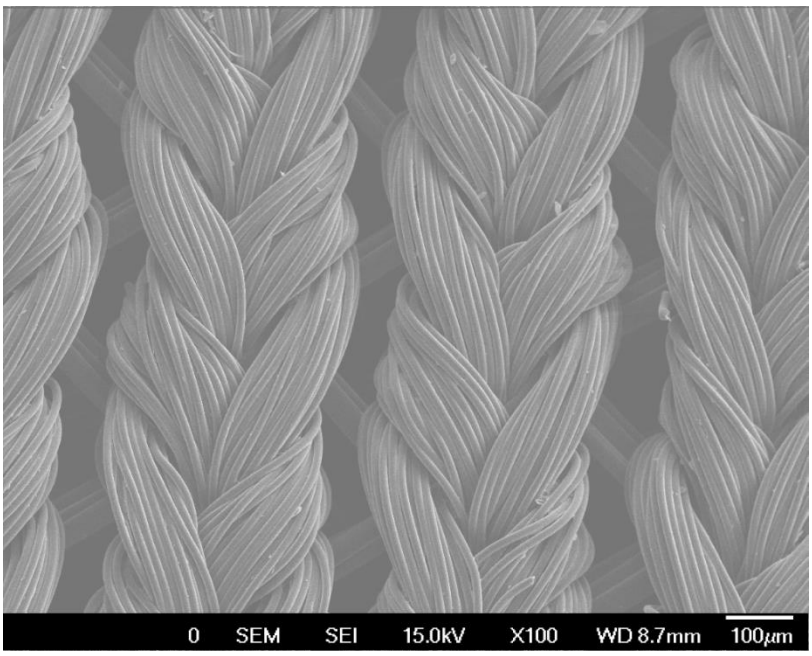

Figure 4.68: SEM X100 magnification of 25% CleviosPH1000 solution in spandex.

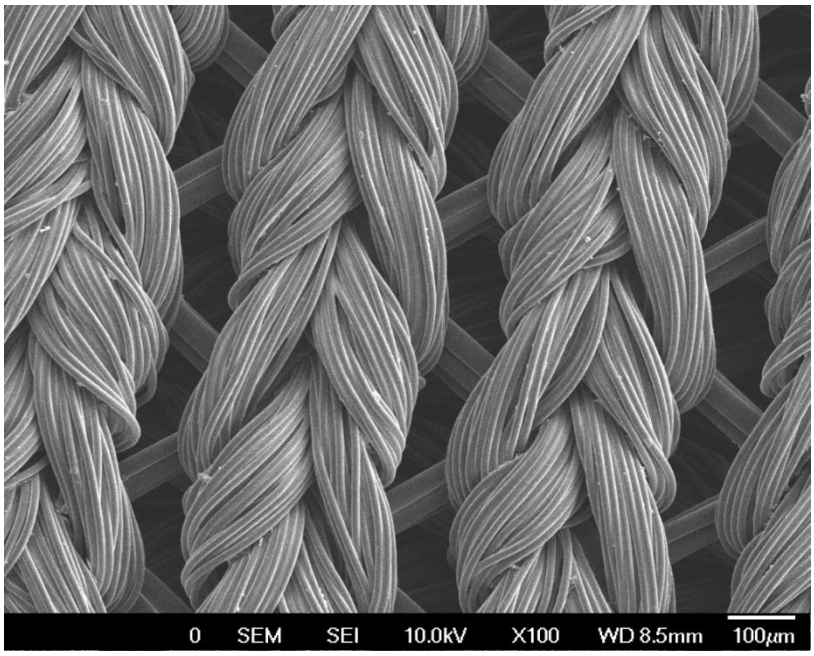

Figure 4.69: SEM X100 magnification of 50% CleviosPH1000 solution in spandex.

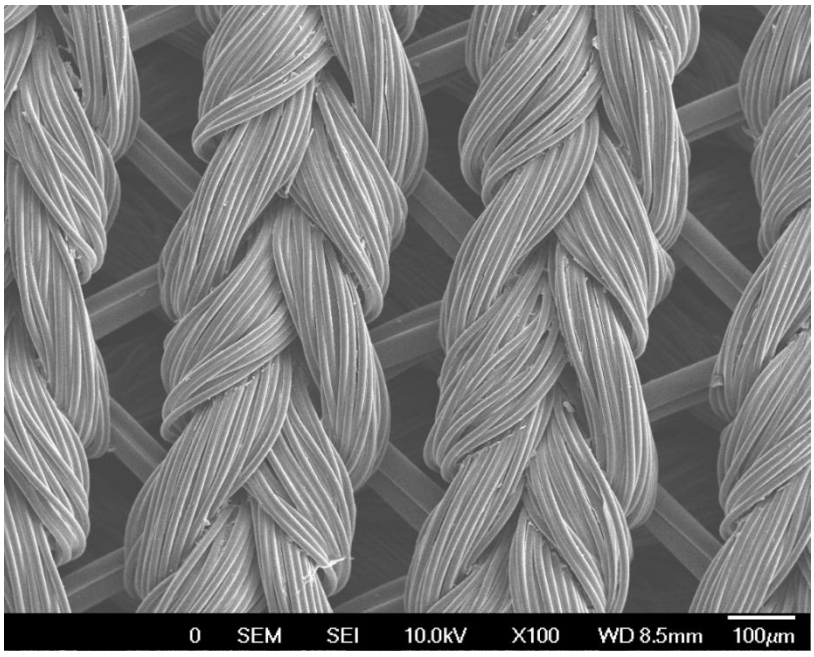

Figure 4.70: SEM X100 magnification of 75% CleviosPH1000 solution in spandex.

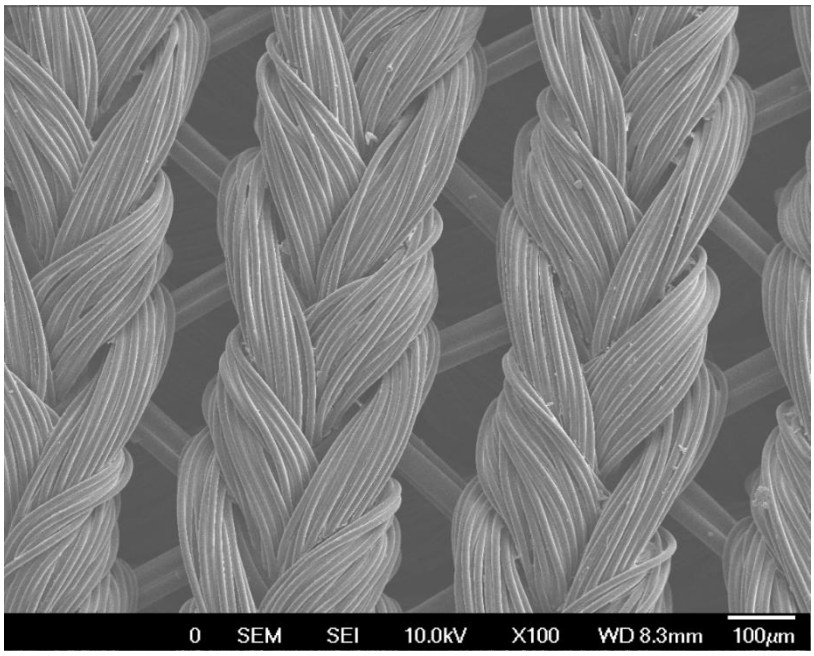

Figure 4.71: SEM X100 magnification of 100% CleviosPH1000 solution in spandex.

The following images are higher magnification to show some of the areas where PEDOT:PSS film was peeling from the fibers. Film thickness were calculated from much higher magnification images of areas where the PEDOT:PSS appeared perpendicular to the screen.

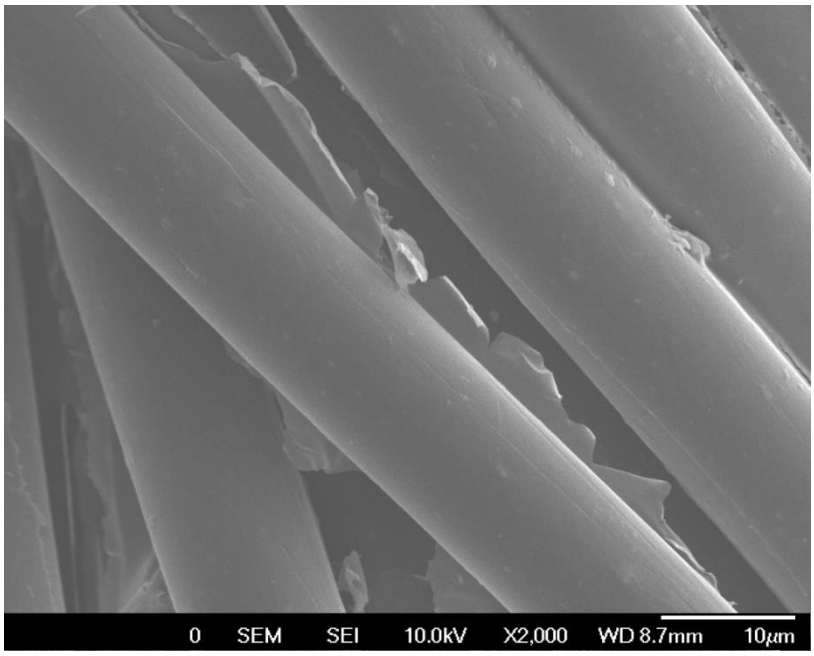

Figure 4.72: SEM X2000 magnification of 10% CleviosPH1000 solution in spandex.

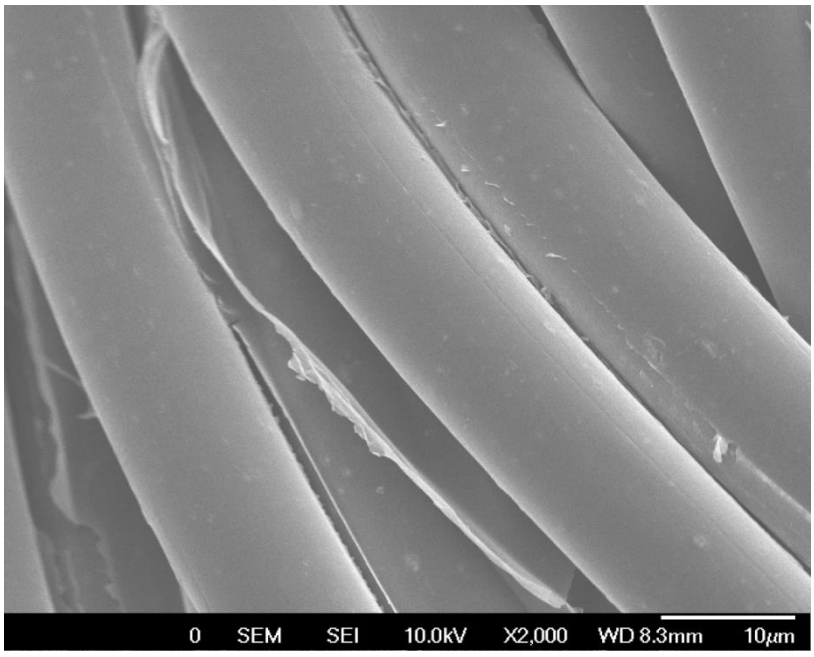

Figure 4.73: SEM X2000 magnification of 15% CleviosPH1000 solution in spandex.

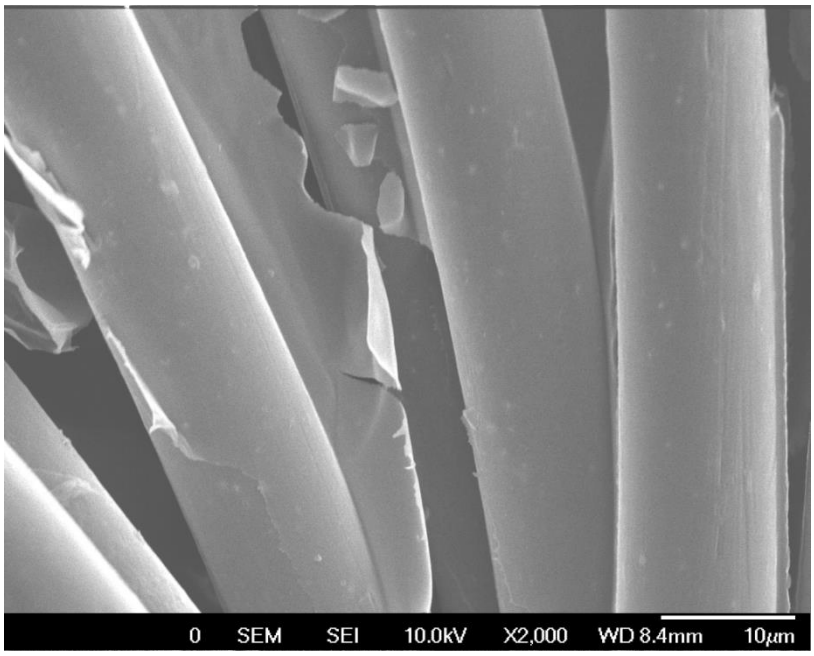

Figure 4.74: SEM X2000 magnification of 25% CleviosPH1000 solution in spandex.

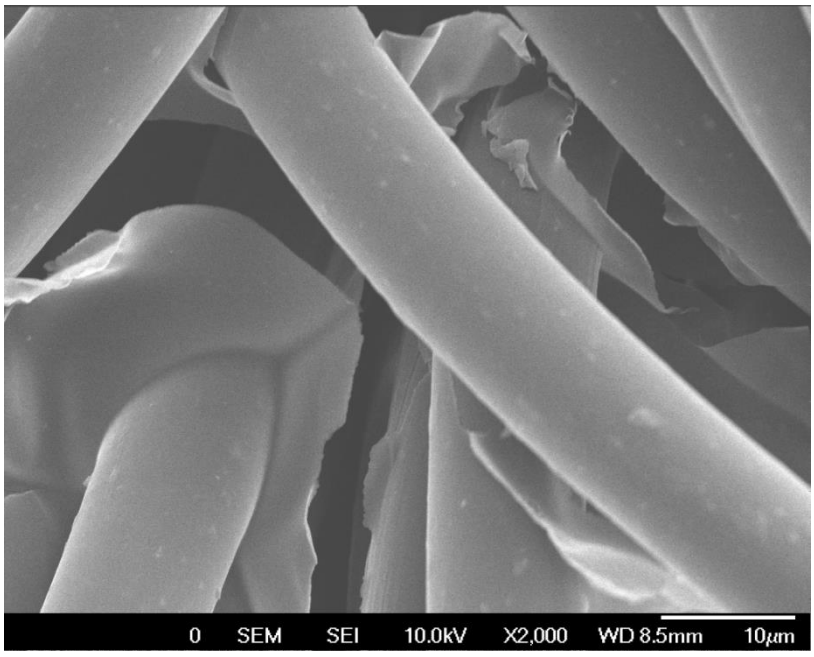

Figure 4.75: SEM X2000 magnification of 50% CleviosPH1000 solution in spandex.

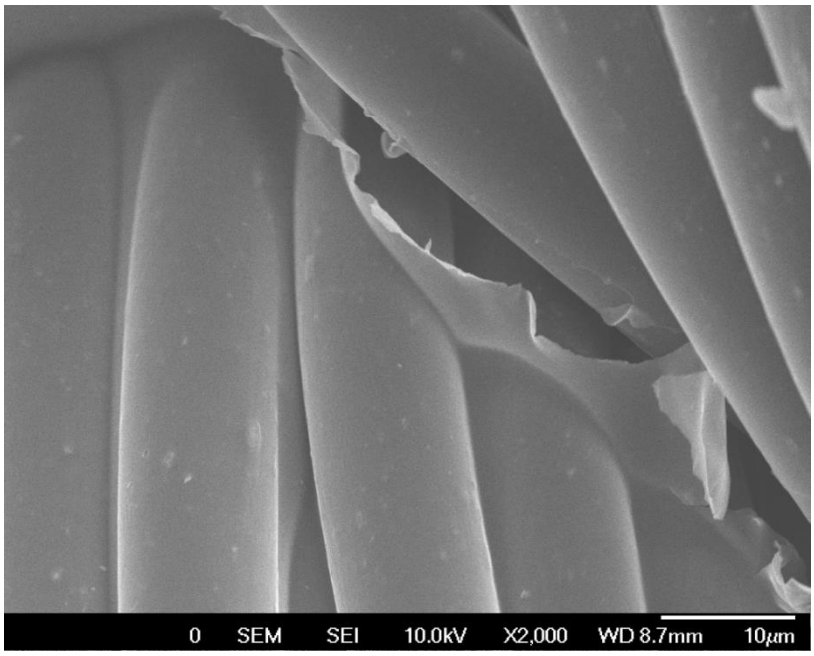

Figure 4.76: SEM X2000 magnification of 75% CleviosPH1000 solution in spandex.

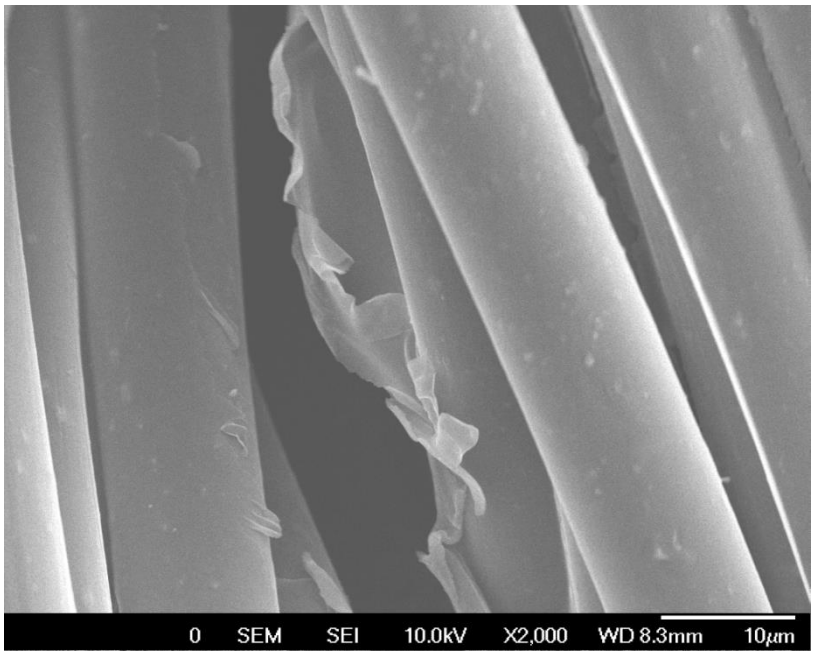

Figure 4.77: SEM X2000 magnification of 100% CleviosPH1000 solution in spandex.

The following image is one of several that was used to determine the film thickness.

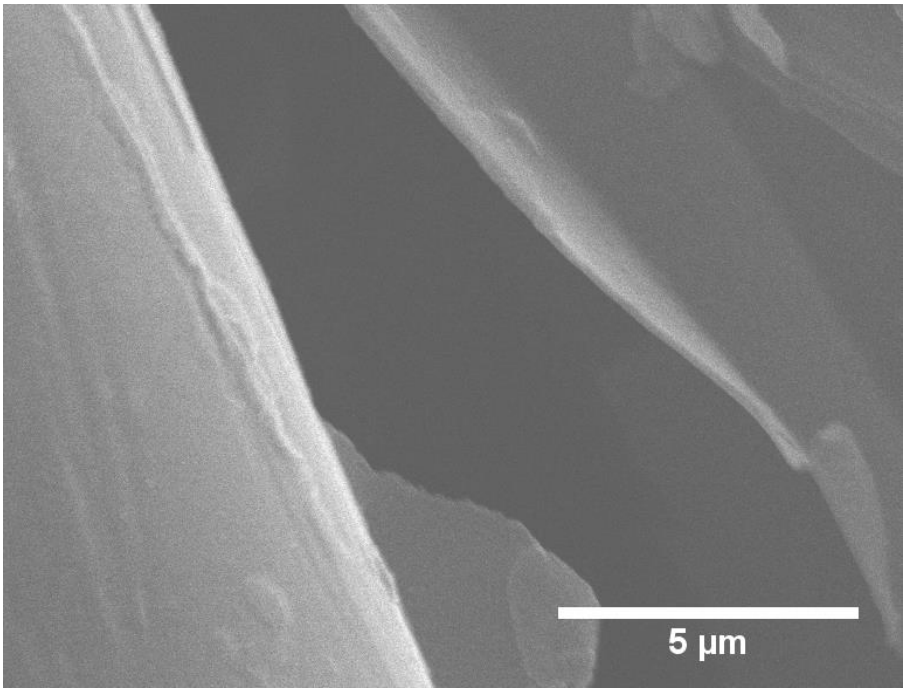

Figure 4.78: SEM X5000 magnification showing the edge of PEDOT:PSS film in 10% CleviosPH1000 sample.

4.5.4 Mechanical Analysis

Dynamic mechanical analysis (DMA) was conducted on the individual layers of the EFD. The unaltered spandex can be stretched up to 150% strain without permanent deformation, and the spandex that has been treated with the 50 wt% PEDOT:PSS solution is reversible up to 50% deformation. At 50% strain, the stress of the treated spandex is increased by 0.2MPa.

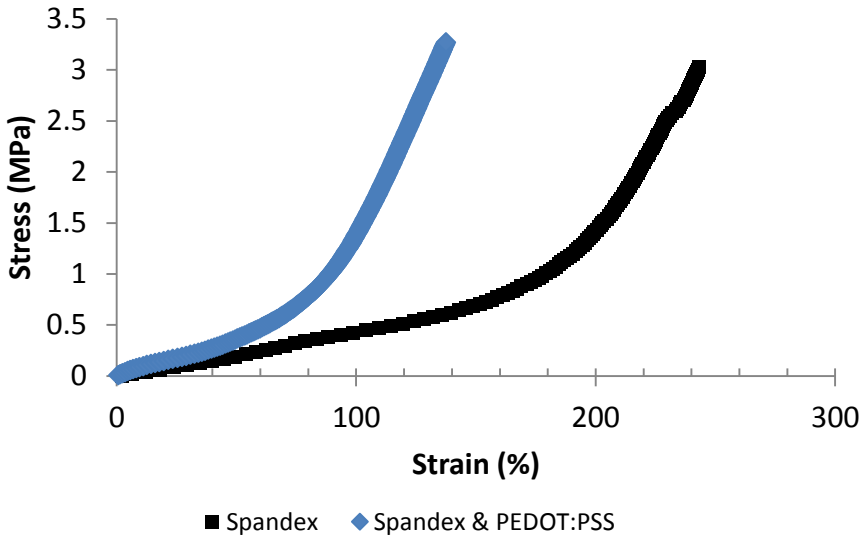

Figure 4.79: Stress/Strain for untreated and treated spandex.

4.6 References

[1] http://www.heraeus-clevios.com/

[2] ELSCHNER, A.; Korchmeyer, S.; Lovenich, W.; Merker, U.; Reuter, K.; Principles and Applications of an Intrinsically Conductive Polymer; *CRC Press* (2002).

[3] The manufacturer's recommendations were obtained at Heraeus's website, http://www.heraeus-clevios.com/en/applications/highlyconductiveclevios/highly-conductive-clevios.aspx

Chapter 5: Resistive Heating of Conductive Fabric

5.1 Introduction

In this chapter, a poly(ethylene terephthalate) (PET) synthetic leather substrate was treated with dimethyl sulfoxide (DMSO) doped poly(3,4-ethylenedioxythiophene):poly(styrenesulfonate) (PEDOT:PSS) and was found to exhibit low sheet resistance and high thermal stability. A study that measured the resistance versus the concentration of conductive material found that saturation was achieved after the addition of only 1 wt. % doped PEDOT:PSS (Section 4.2.5). The treated PET was capable of resistive heating, and reached a maximum temperature of 200°C in less than two minutes when a 5 V potential was applied. Additionally, the fabric was soaked in water and resistively heated, self-drying in approximately 8 minutes. One major advantage of this system is the opportunities that arise in industrial applications, such as wearable technology, from the all-organic nature of the selected components.

5.2 Sample Preparation

The grey PET fabric was cut to 50 mm x 25 mm samples and the initial weight was recorded. The samples were then treated with doped PEDOT:PSS (CleviosPH1000) and dried at 110°C for one hour for each soaking. The final weight was recorded and the weight percent of PEDOT:PSS in each sample was calculated (see section 4.1.2). To achieve a weight percent lower than 2 wt. %, the PEDOT:PSS dispersion was diluted with deionized water and then doped.

Multiple soaking and drying cycles were needed to achieve higher weight percents.

A 25 gauge (0.5 mm diameter) copper wire was threaded through each end of the PET using a syringe need to first punch a hole. Each side had 3.5 stitches and the wires were 45 mm apart. The wire stitches were then covered with silver paste and allowed to air dry overnight.

Samples for resistive heating need to have a power source and a way in which to monitor temperature. A type J thermocouple was adhered to the fabric with a high temperature tape and a Keithley 2700 multimeter was used to monitor the temperature change.

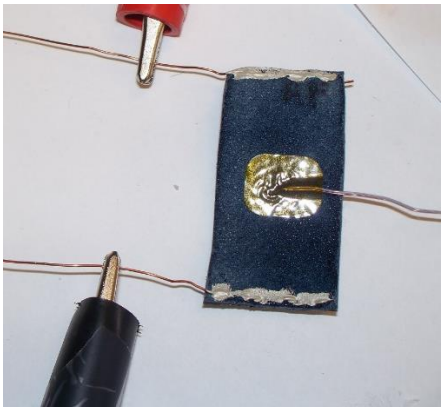

Figure 5.1: Close-up of PET fabric sample detailing connections for resistive heating.

5.3 Resistive Heating of Grey PET

5.3.1 Time to Reach Maximum Temperature & Cool Down

Each resistive heating sample required about the same amount of time to reach maximum temperature and to cool to room temperature once the power source was removed. At the highest temperature reached in these studies (200°C), the time to heat and to cool was 2 minutes. At lower voltages and temperatures, less time was needed.

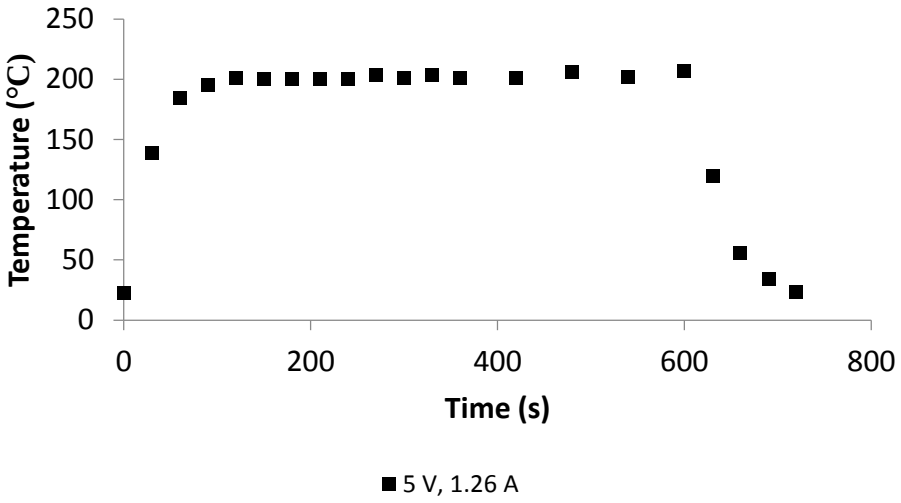

Figure 5.2: 6.51 wt. % sample displaying heating and cooling temperature and time.

5.3.2 Varying PEDOT:PSS Concentration

For Sections 5.3.2.1-5.3.2.5, the fabric samples were resistively heated at 2 V, 4 V, 5 V and in one case 7 V. The corresponding current values are listed in the figure legends.

5.3.2.1 Grey PET with 2.59 Wt. %, 7.3 Ω/sq.

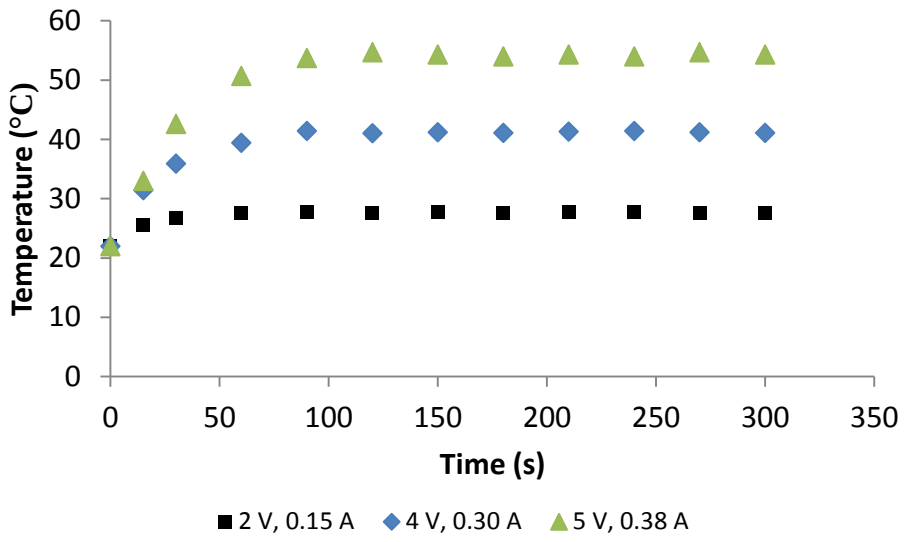

Figure 5.3: Resistive heating a 2.59 wt. % grey PET sample.

5.3.2.2 Grey PET with 3.18 Wt. %, 3.9 Ω/sq.

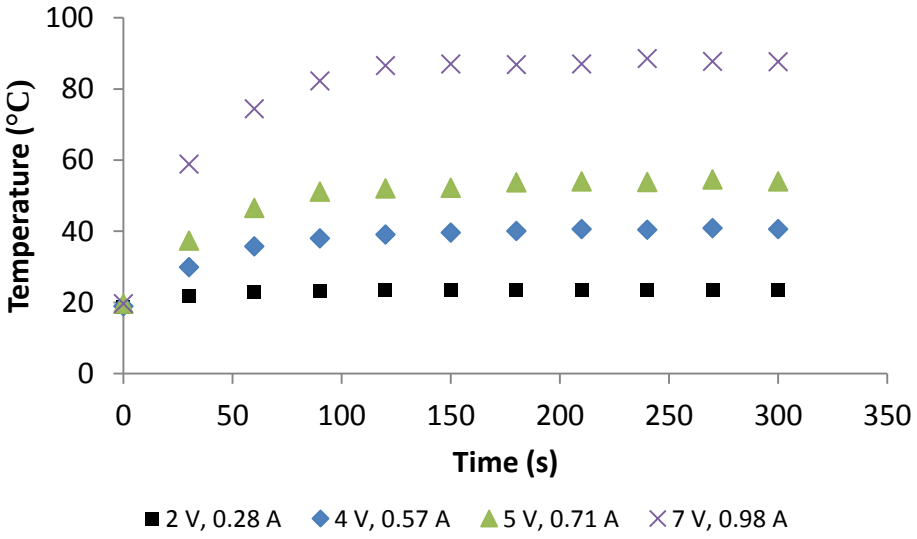

Figure 5.4: Resistive heating a 3.18 wt. % grey PET sample.

5.3.2.3 Grey PET with 4.16 Wt. %, 3.7 Ω/sq.

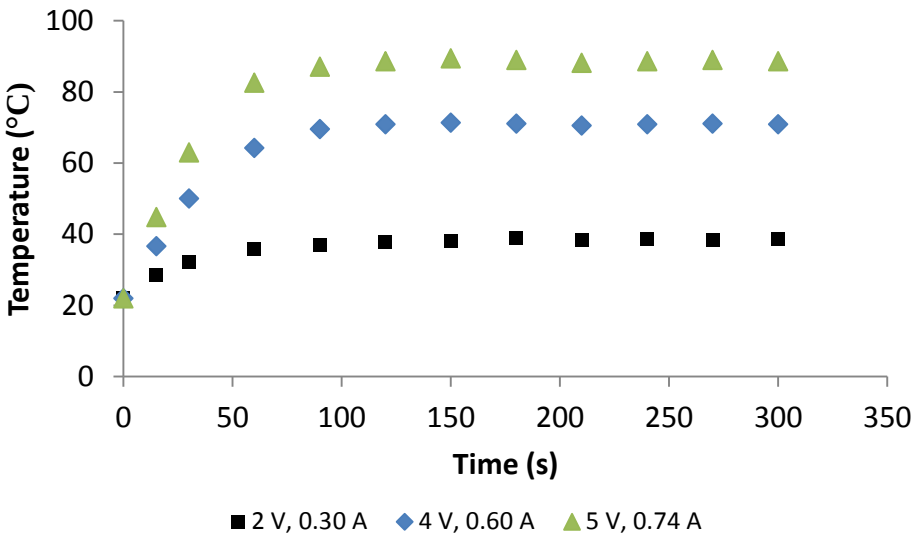

Figure 5.5: Resistive heating a 4.16 wt. % grey PET sample.

5.3.2.4 Grey PET with 6.96 Wt. %, 1.76 Ω/sq.

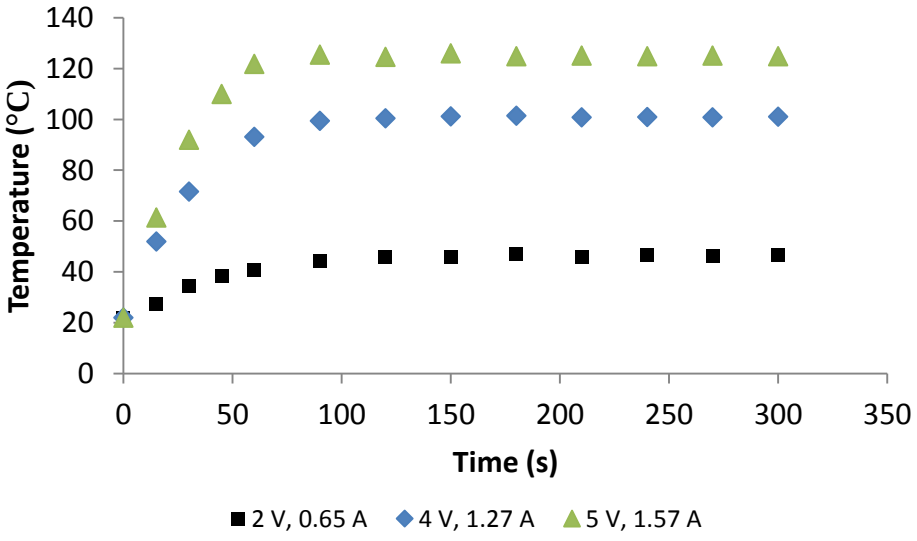

Figure 5.6: Resistive heating a 6.96 wt. % grey PET sample.

5.3.2.5 Grey PET with 7.56 Wt. %, 1.78 Ω/sq.

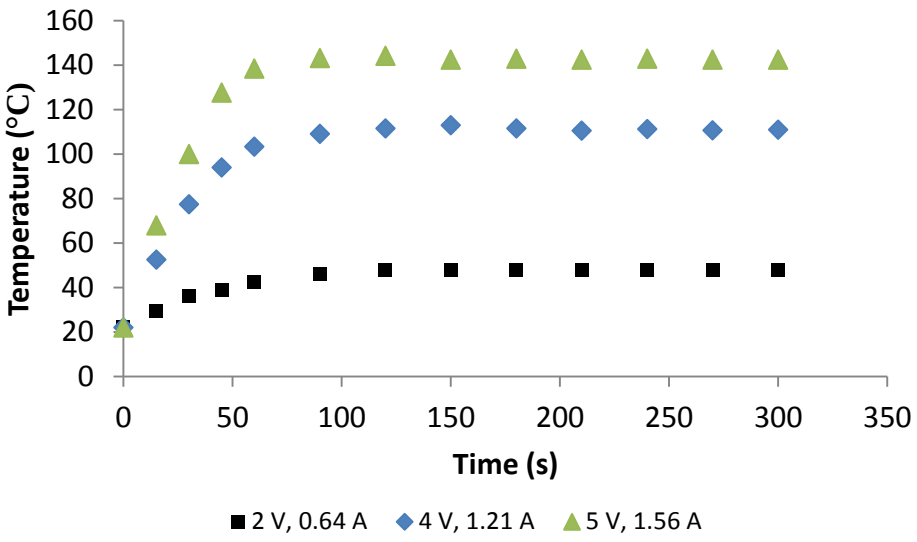

Figure 5.7: Resistive heating a 7.56 wt. % grey PET sample.

5.3.2.6 Combined Graphs for Comparison

Each of the concentrations in the previous sections are compared at 2 V, 4 V, and 5 V in the following figures. ΔT (difference between measured temperature and room temperature) was used to account for the difference in daily room temperature.

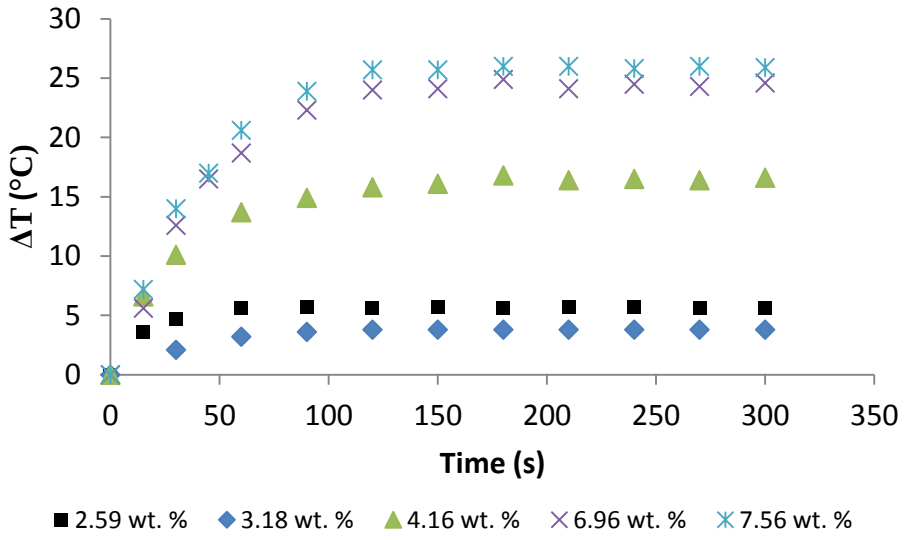

Figure 5.8: Combined concentrations at 2 V.

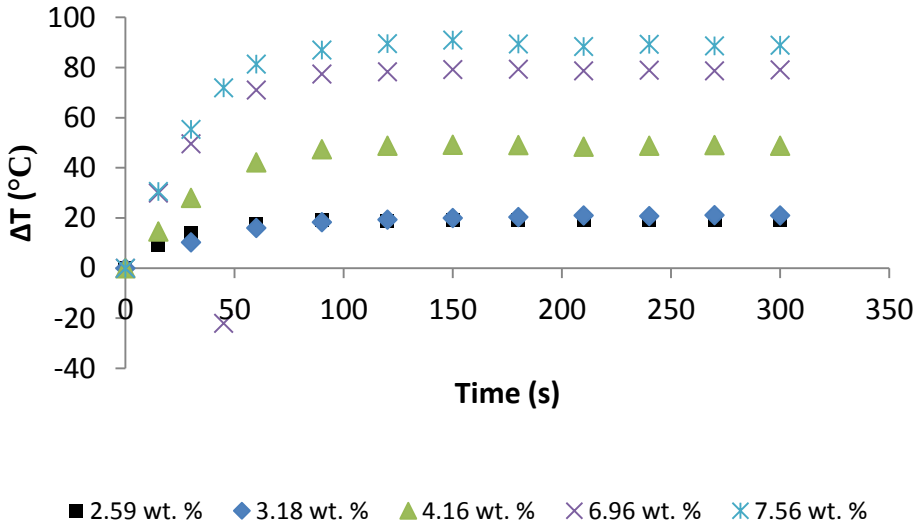

Figure 5.9: Combined concentrations at 4 V.

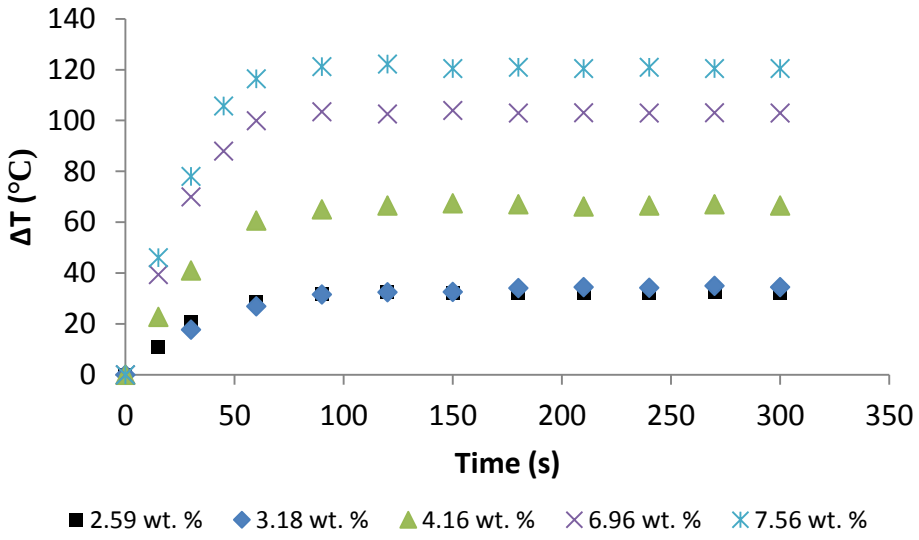

Figure 5.10: Combined concentrations at 5 V.

The sample with 3.18 wt % PEDOT:PSS heats to a lower maximum temperature at 2 V than the 2.59 wt % sample and is very similar at 4 V and 5 V. This was likely due to contact differences between the copper wires and the fabric.

The power consumption at 2 V, 4 V, and 5 V for each concentration are plotted in Figure 5.11. There is a linear trend for each sample.

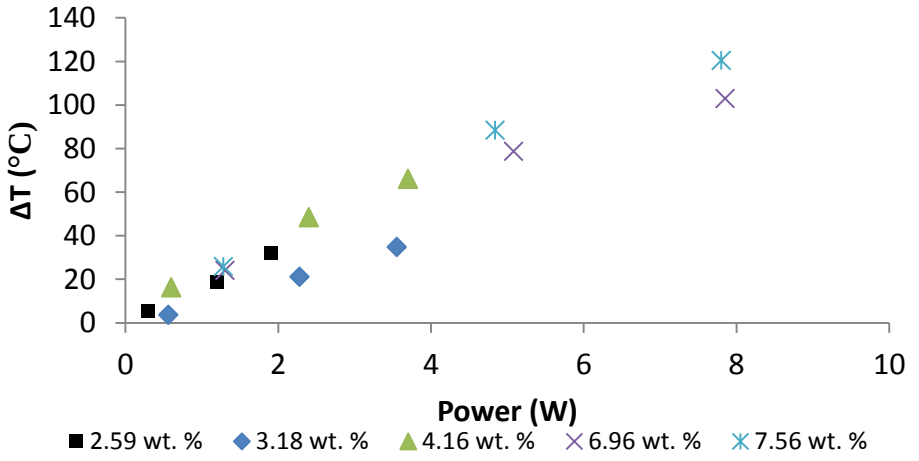

Figure 5.11: Power requirements for 2 V, 4 V, and 5 V at each concentration.

The specific power for each concentration was also calculated, however the trend looks nearly identical to Figure 5.11.

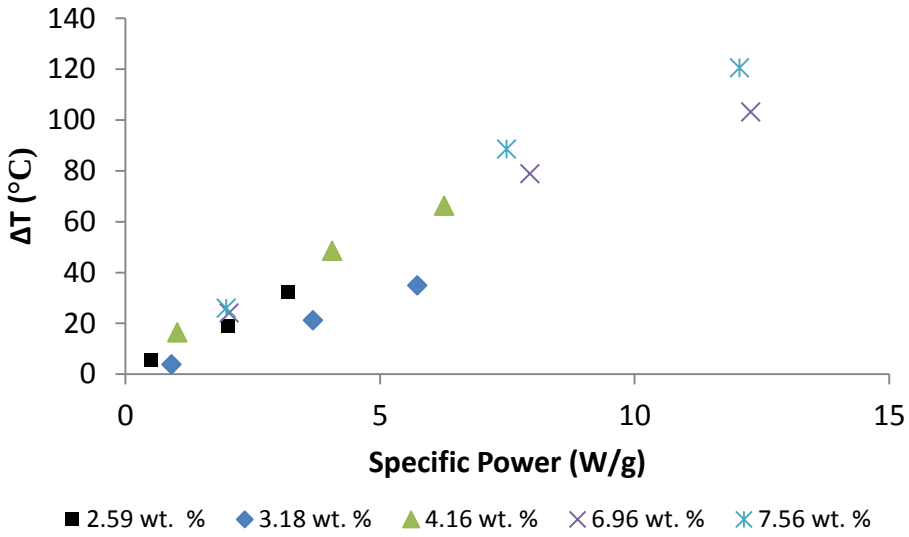

Figure 5.12: Specific power requirements for 2 V, 4 V, and 5 V at each concentration.

5.3.3 Longevity

The resistive heating samples at 5 V typically lasted between 10 – 20 minutes, at which point the samples would smoke and sometimes burn in half near one of the copper wires. Since the samples are not near the breakdown current,[1] the failure must be due to degradation of one of the fabric components. From TGA data, the PET is stable up until 300°C, which is consistent with literature.[2] However, at temperatures above 250°C, PSS degrades via rupture of the sulfonate group from styrene.[3,4] Since there is a temperature gradient across the resistive heating samples (confirmed with an IR camera), it's most likely that the

areas near the copper wire were at much higher temperatures, causing the degradation that led to failure.

For example, a 6.78 wt. % sample with no prior resistive heating was tested at 5 V. The sample began at 1.17 A, reached a maximum temperature of 145°C (in the middle), and lasted 48 minutes before burning in half towards one of the electrodes.

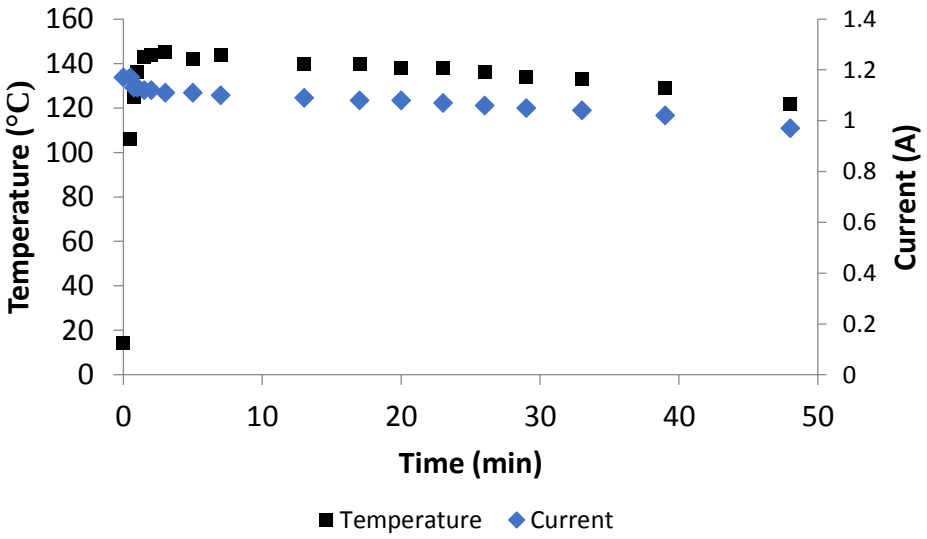

Figure 5.13: 6.78 wt. % sample longevity test at 5 V.

At lower voltages, the grey PET samples are extremely stable and have maintained temperatures up to 50°C for days with no detrimental effects on current.

5.3.4 Wire Distance

Two 1” x 1” sample were cut from a 3.72 wt. % piece of treated grey PET and prepared for resistive heating. The first was resistively heated at 1 V, 2 V, 3 V, 4 V, and 5 V to determine the maximum temperature (Table 5.1).

Voltage (V)	Current (A)	Maximum Temperature (°C)
1	0.19	26.9
2	0.38	52.0
3	0.58	99.4
4	0.76	150.0
5	0.92	190.0

Table 5.1: Maximum temperatures for a 3.72 wt % 1” x 1” square.

The second 1” x 1” square was held at 50°C to determine longevity at a lower temperature and voltage. The sample required 1.6 V and 0.34 A and remained constant for 8 hours, at which time the power was disconnected.

A 2” x 2” square at the same concentration didn’t reach 50°C until 3 V (0.78 A) was applied. This indicates that besides using the PEDOT:PSS concentration and voltage to control the temperature, the distance between the electrodes can also be used.

5.3.5 Maximum Possible Temperature

The maximum temperature reached on a grey PET sample was 200°C for a 6.51 wt. % PEDOT:PSS concentration. Grey PET samples with a higher concentration of PEDOT:PSS were unable to replicate these results.

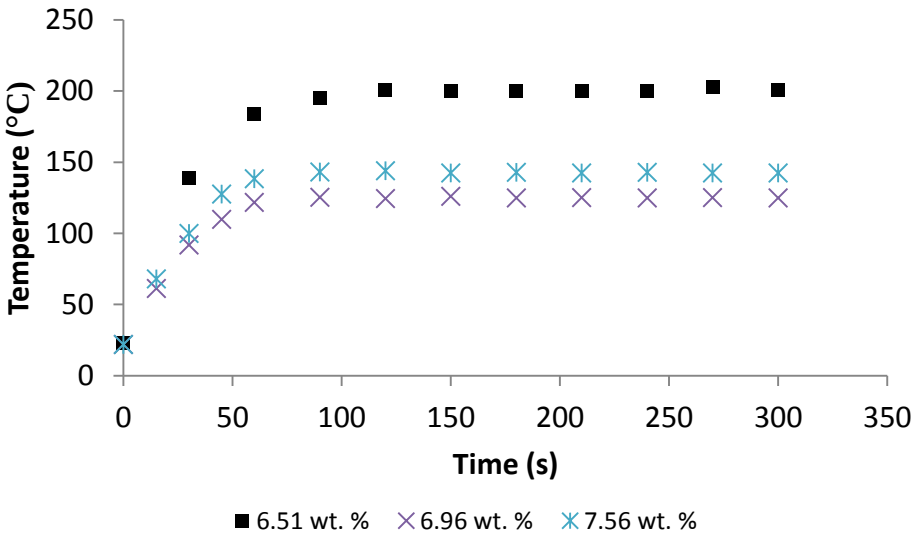

Figure 5.14: Maximum temperature at 5 V of high concentration samples.

The difference in maximum temperature was likely due to differences in contact between the copper wire and the fabric. Furthermore, the fabric has to be maneuvered to stitch the copper wire, so it's possible that the PEDOT:PSS film was damaged when the fabric was bent, thus disrupting the continuity of the charge across the fabric.

5.3.6 Improving Contact

Silver paste was added to the back of the 6.96 wt. % sample to compare the resistive heating results with the previous results (Figure 5.6) that only had silver

paste on the front. The current did not change with the additional silver paste, but the maximum possible temperature at each voltage went up by at least 10°C.

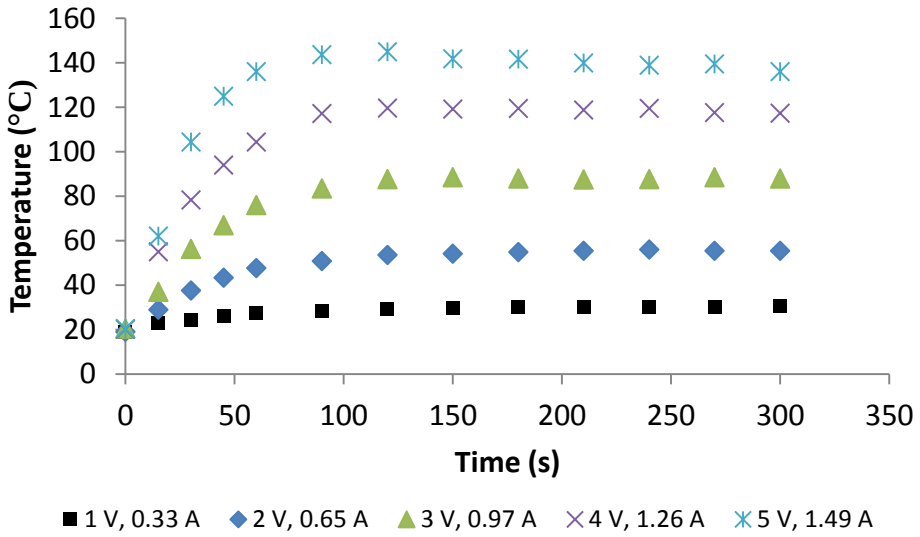

Figure 5.15: Addition of silver paste increases maximum temperature.

A comparison of the power requirement for the device before and after the addition of the extra silver paste can be seen in Figure 5.16.

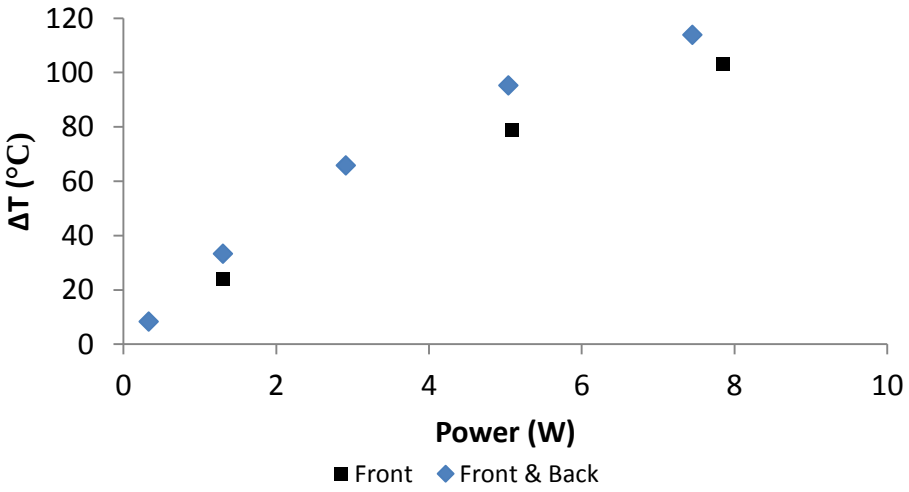

Figure 5.16: Power required for a sample with silver paste on the front vs. the front & back.

There are several other ways in which contact with the fabric could be enhanced. The method used to stitch the copper wire could be improved upon, as well as trying a higher gauge (thinner) wire. A copper coated thread may also be an option for sewing the electrode connection. Copper tape did not work for resistive heating.

5.3.7 Resistively Heating Water & Drying

The PET sample with 7.56 wt. % PEDOT:PSS (Ω/sq.) was placed in a petri dish with 25 mL of water. A thermocouple was used to measure the water temperature. Leads were attached to the copper wires and 5 V was applied. The sample increased the water temperature by 6 °C over 10 minutes. Some silver paste detached from the fabric when soaked.

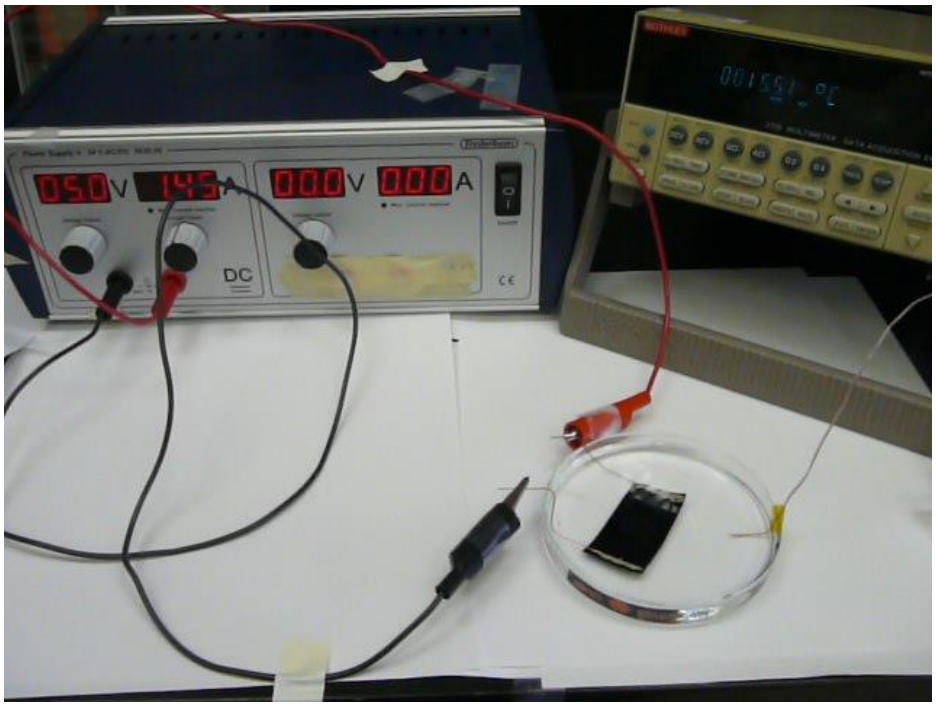

Figure 5.17: Setup for resistively heating water.

Next, the wet PET sample (7.56 wt% & 1.78 Ω/sq) was placed on the table and 5 V was applied. The drying was visible via the color change across the fabric sample. The sample was completely dry in 8 minutes.

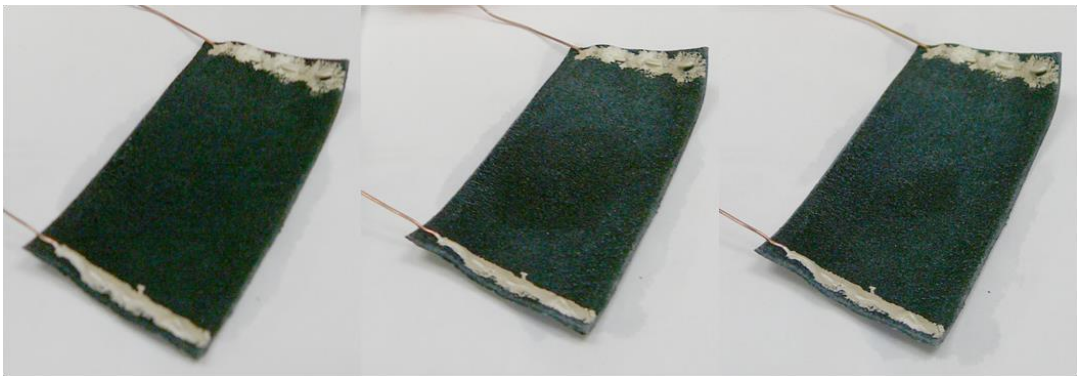

Figure 5.18: Visual of resistive heating used for drying.

The current dropped permanently to 1.27 A after the sample was wet. The current did not increase to the previous dry current value of 1.56 A after the self-drying was complete.

Another sample with 6.08 wt. % PEDOT:PSS was used in the next attempt to boil water. An aluminum pan with 5 mL of water was placed on top of the fabric sample and then placed on the lab counter. At 5 V (1.11 A), the water reached 40°C in 5 minutes. The fabric was then taped to the pan, but the temperature did not increase. Next, the fabric was wrapped around a vial, which heated the water to 50°C.

Due to heat dissipation, water was never successfully boiled. An insulating layer may help direct the heat transfer towards the water.

5.3.8 Resistive Heating by Battery

The PET sample with 4.16 wt. % PEDOT:PSS was attached to a 1.25 V battery using electrical tape. The temperature in the center of the fabric was measured using a thermocouple and a multimeter was used to check the current and voltage. The current for this voltage and sample was 0.00033 A and the sample heated 3°C in 2 minutes. Multiple AA batteries, a larger battery, or a higher concentration of PEDOT:PSS would be more effective at heating the fabric.

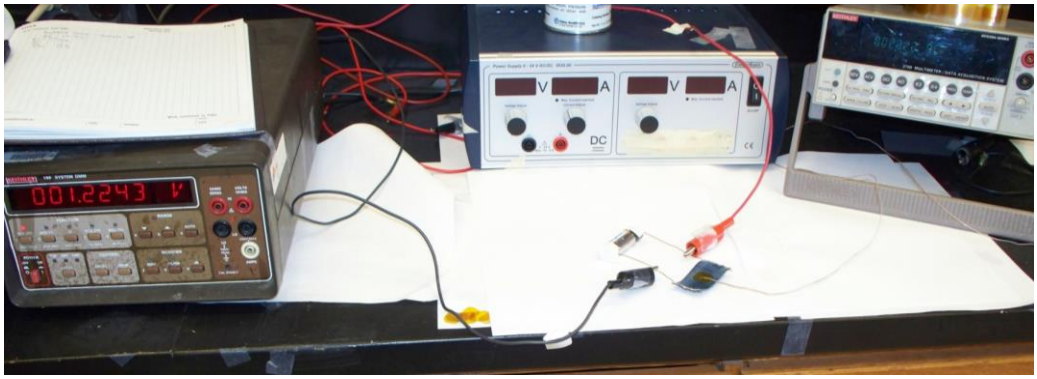

Figure 5.19: Setup for resistive heating by battery.

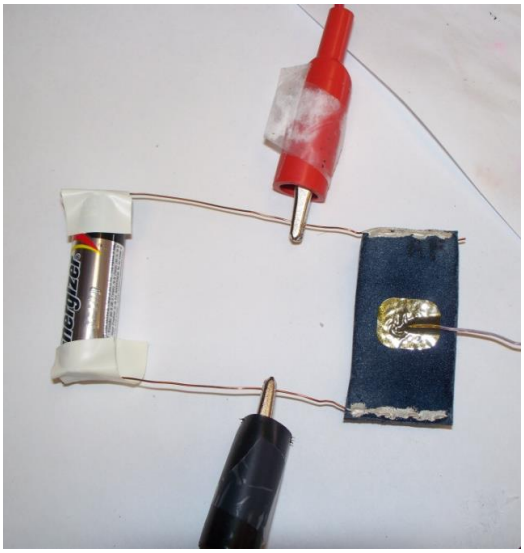

Figure 5.20: Close-up of connections for resistive heating by battery.

5.3.9 Resistive Heating to Induce Thermochromic Color Change

Resistive heating of a fabric could be used to induce a thermochromic color change.

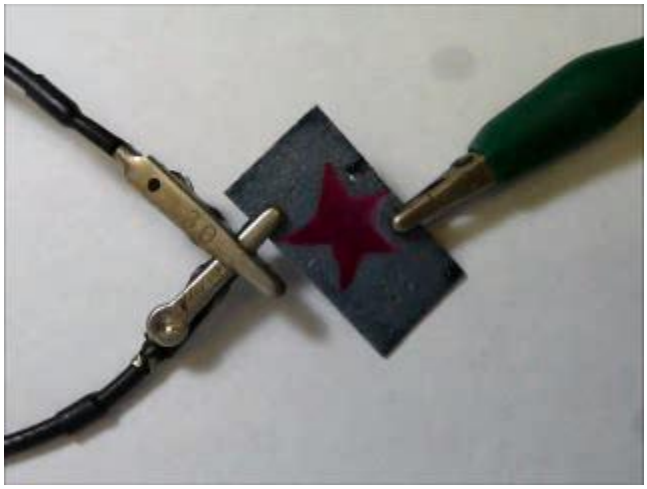

Figure 5.21: Simple thermochromic resistive heating setup.

5.4 Resistive Heating Alternative Fabrics

Several alternative fabrics were tested for resistively heating ability. The non-melted black PET, grey PET, and a stitched polyester fabric proved to be the most capable.

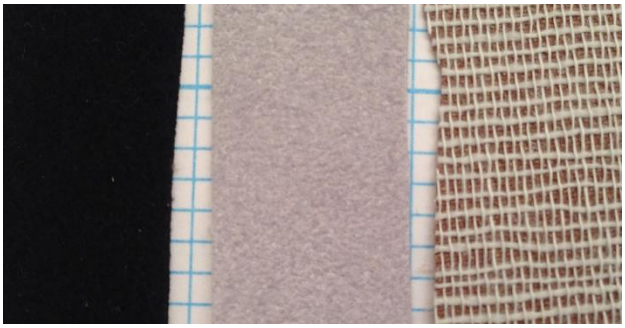

Figure 5.22: Black PET, grey PET, and polyester stitch.

Each fabric was treated once with a solution of CleviosPH1000 doped with 5% by weight DMSO and dried at 110°C for 1 hour.

Figure 5.23 displays the resistive heating capabilities of the polyester fabric with different color stitching and 4.41 wt. % and 10.7 Ω/sq.

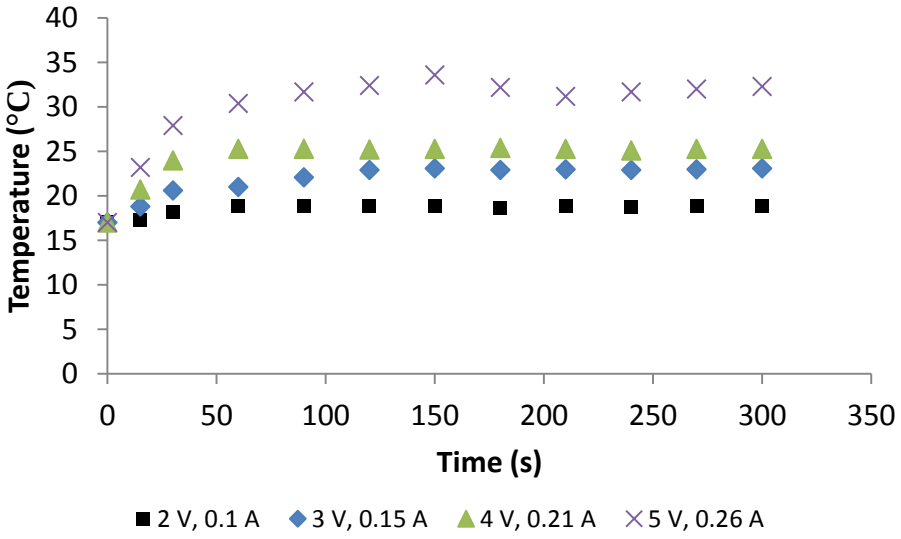

Figure 5.23: Resistively heating a polyester fabric with one PEDOT:PSS treatment.

Figure 5.24 displays the resistive heating capabilities of the non-melted black PET with 5.94 wt. % and 9.0 Ω/sq.

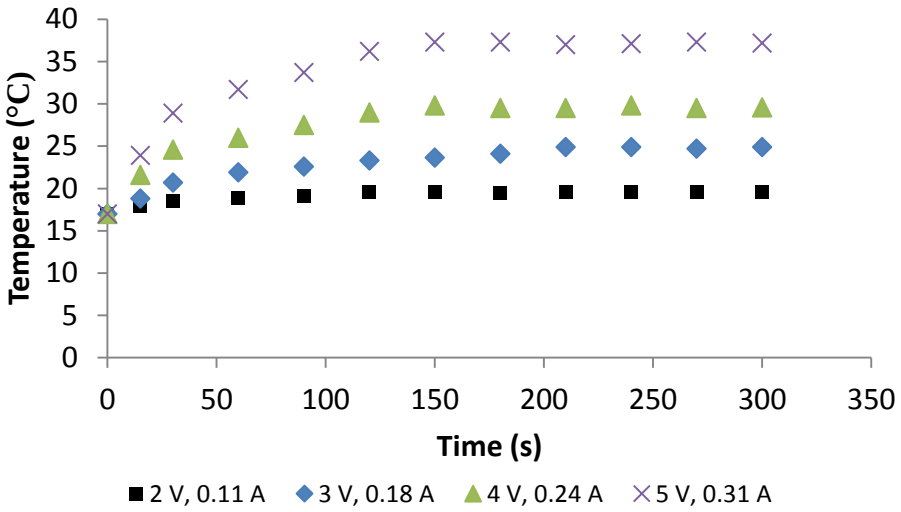

Figure 5.24: Resistively heating black PET with one PEDOT:PSS treatment.

For comparison, a grey PET sample with 2.97 wt. % and 8.2 Ω/sq. was resistively heated (Figure 5.25).

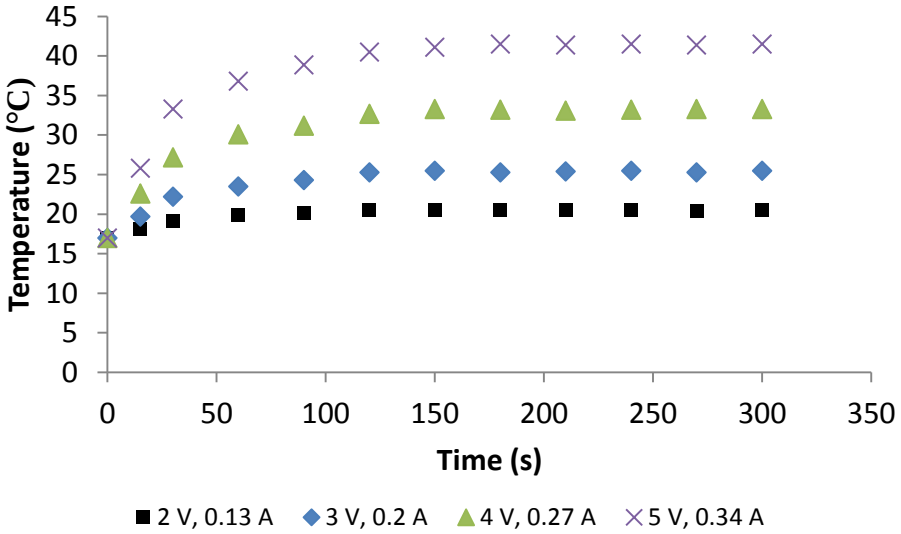

Figure 5.25: Resistively heating grey PET for comparing one PEDOT:PSS treatment to other fabrics.

The grey PET was still the best fabric for resistively heating, although the black PET was close. The polyester stitch fabric did not maintain temperature as well as the PET fabrics.

The Nylon mesh was unable to resistively heat. At 2 V and 0.03 A, a sample with 5.3 wt. % failed after just 30 seconds. A higher weight % might produce better results, but it's likely that the breakdown current for this fabric is low. It was also difficult to stitch the copper wire without tearing the fabric.

5.5 References

[1] Alamer, F.; Thesis. 2014

[2] Samperi, F.; Puglisi, C.; Alicata, R.; Montaudo, G.; *Polymer Degradation and Stability* **83** (2004) 3-10

[3] Friedel, B.; et. al.; *Macromolecules* **42** (2009) 6741-6747.

[4] Greczynski, G.; Kugler, T.; Salaneck, W. R. Thin Solid Films 1999, 354, 129–135.

Chapter 6: Electrochromic Fabric Devices

6.1 Introduction

The nascent field of organic electrochromic fabric devices (EFDs) has rapidly advanced in the past few years,[1] inching ever closer towards commercializable technologies including adaptive camouflage and wearable displays. EFDs are a small subset within the fields of stretchable, flexible, and textile electronics, which have garnered great attention in past few years.[2, 3, 4, 5, 6, 7, 8] A number of proof-of-concept EFDs have been demonstrated in the literature,[9,10,11,12,13,14,15,16,17] but were either electrochemically switched in an electrolyte bath, or used ITO-coated substrates or metal electrodes for one side of the device. In 2010, the Sotzing group published the first all-organic electrochromic device[18] fashioned from two pieces of PEDOT:PSS-impregnated spandex;[19] this device, however, used a salt-based crosslinked polymeric solid electrolyte matrix and therefore did not withstand stretching or deformation. Herein, an oligomeric polyurethane doped with ionic liquid is used to alleviate this problem and create the first stretchable EFD. In line with the Sotzing group's previous work in this field, we sought to develop the simplest fabrication procedures possible to ensure amenability with manufacturing processes. The conductive spandex described previously and within this article is made by soaking commercially-available spandex in an aqueous dispersion of PEDOT:PSS, and allowing it to air dry overnight. Furthermore, electrochromic polymer films are often prepared in cumbersome electrolyte baths[20] or with an in-situ polymerization procedure,[21] however, we continue to use soluble alkylsilane-containing precursor polymers that are spray-

coated onto the conductive fabric substrates, and are oxidatively converted chemically with solutions of $FeCl_3$.

6.2 Preparation of Conductive Spandex

For the following studies, a commercially available aqueous dispersion of PEDOT:PSS was employed to impart conductivity to the spandex. Solutions of CleviosPH1000, a 1-1.3 weight % dispersion of PEDOT:PSS, are further diluted with deionized water before soaking the spandex. To ultimately quantify the amount of PEDOT:PSS in each spandex sample, they were weighed before treatment then again after soaking and drying, and the difference was used to calculate the weight % (Section 4.1.2). A saturation curve, conductivity at each concentration, and film thicknesses can be found in Section 4.5. The spandex was dried in air to avoid hydrolytic degradation of the nylon component. Everything in this chapter uses a conductive solution made from 50% by weight CleviosPH1000 and 50% by weight deionized water, doped with 5% by weight DMSO, unless otherwise stated.

When making an electrochromic fabric device, it is important to consider the color of the fabric. If the fabric is too dark (high concentration of PEDOT:PSS), the electrochromic may not show up well. If the fabric is too light (low concentration of PEDOT:PSS), the device will be slower, but the electrochromic will show up better. The 50% CleviosPH1000 solution was used because it had enough conductivity to work well but it was also light enough to see a color change. Alternatively, a lower conductivity grade of PEDOT:PSS could be used, such as Orgacon S300.

6.3 Precursor Polymer

6.3.1 Synthesis of PBEDOT-T-Si[Octyl]$_2$

The processable precursor polymer PBEDOT-T-Si[Octyl]$_2$ was synthesized by deprotonating 1 equivalent of bis(3,4-ethylenedioxythienyl)thiophene[22] with 2 equivalents of n-butyllithium in a dry ice/acetone bath, and reacting with 1 equivalent of dioctyldichlorosilane. The mixture was allowed to stir for 3 days at room temperature, before precipitation in n-pentane and thorough ACN washing. The synthesis and characterization of this polymer has been thoroughly detailed in a previous publication by this group.[23]

6.3.2 Using the Precursor

The precursor polymer is oxidatively polymerized chemically or electrochemically, which cleaves the carbon-silicon bond (Figure 6.1). The resulting polymer is blue in the oxidized state and red in the reduced state (Figure 6.2). The precursor is used as the electrochromic for EFDs because it is soluble and can be spray coated onto the fabric and then polymerized.

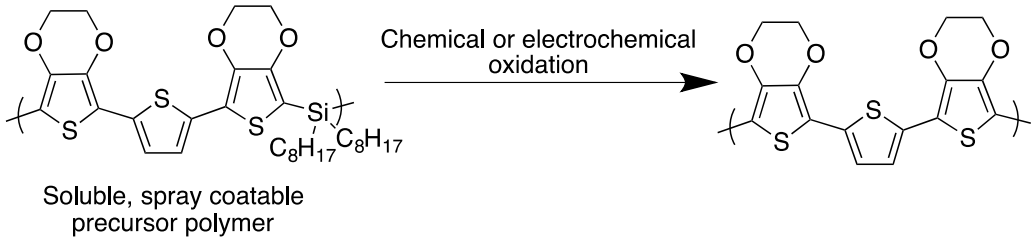

Figure 6.1: Precursor Structure.

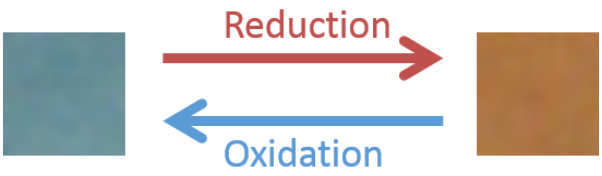

Figure 6.2: Depiction of Precursor Color Change.

To spray coat the precursor, it is dissolved in a low boiling point solvent such as dichloromethane (DCM) and filtered into the spray coating vial. The solution is spray coated onto one spandex electrode using high pressure air. The precursor is converted with a solution of $FeCl_3$ and ACN, then washed with ACN. After 30 minutes, the fabric is dry and the device can be assembled.

6.4 Initial Electrochromic Fabric Devices (EFDs)

6.4.1 Normal Gel EFDs

The first EFDs in the Sotzing group used the “normal gel” recipe from the window type devices, and were photoinitiated. This gel was made from 5g propylene carbonate (PC), 5g poly(ethylene glycol) diacrylate (PEGDA), 1g lithium trifluoromethanesulfonate and 17.5mg 2,2-dimethoxy-2-phenyl-acetophenone (initiator) (See section 2.1.2). The mixture was then sonicated. UV light cleaves the carbon-carbon bond in the initiator and the free radical then initiates PEGDA (Figure 6.3 and Figure 6.4).

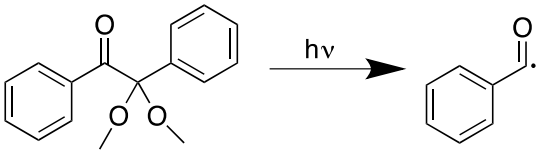

Figure 6.3: Initiation of 2,2-dimethoxy-2-phenyl-acetophenone.

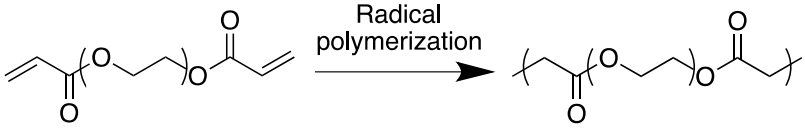

Figure 6.4: Polymerization of PEGDA.

Gels are a good solution for an electrolyte in fabric devices, because while they are mostly liquid, they behave like solids due to a three-dimensional cross-linked network within the liquid. Varying the types and amounts of chemicals in the gel electrolyte gives different properties, such as stretching and flexibility.

Since PEDOT:PSS itself is electrochromic, an electrochromic fabric device can be made according to Figure 6.5. In this device, the PEDOT:PSS acts as the conductive material which is impregnated into the fabric, but it also acts as the electrochromic layer. The electrolyte layer in a fabric device isn't trapped in the middle, but rather the whole device is saturated with electrolyte due to the porous nature of the fabric electrodes.

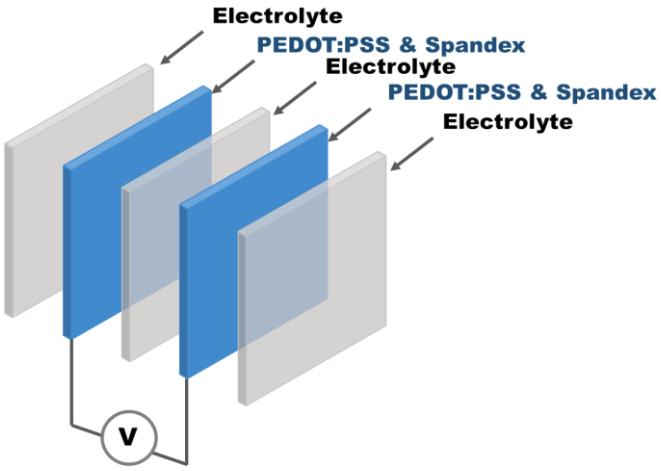

Figure 6.5: PEDOT:PSS EFD schematic.

For Figure 6.6, grey PET was treated with Orgacon S300 and doped with 5% DMSO and air dried overnight. Each piece of PET was soaked with the normal gel and cured in a UV oven and then cured together. The color change depicted is from the PEDOT:PSS.

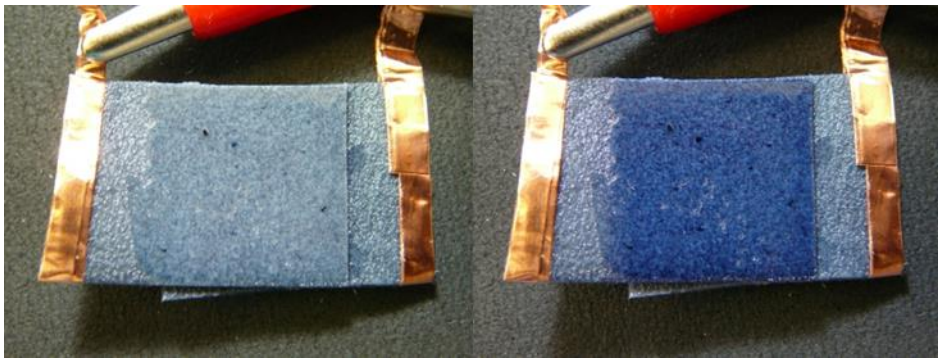

Figure 6.6: PEDOT:PSS color change with normal gel.

Previous devices in the Sotzing group used D-sorbitol to dope the PEDOT:PSS, however when that was replicated, the D-sorbitol precipitated from the fabric, leaving white spots.

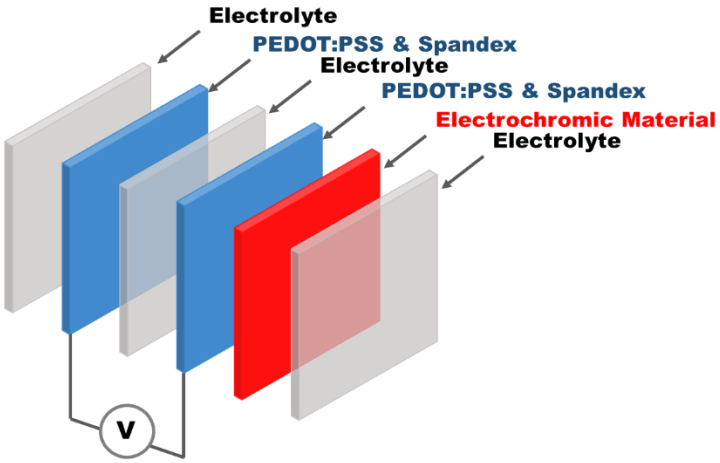

Figure 6.7: Precursor EFD schematic.

For a device containing precursor, the schematic looks like that depicted in Figure 6.7. For this type of EFD, the fabric is treated with PEDOT:PSS and then an electrochromic material is deposited onto one of the fabric electrodes. In this chapter, the only electrochromic material considered is the precursor polymer described in Section 6.3. The precursor is dissolved in DCM, filtered, then spray coated onto a piece of treated fabric. The precursor is then oxidatively polymerized using a solution of $FeCl_3$ and ACN, and then washed with ACN. Once dry, the device can be assembled.

A precursor device with normal gel is depicted in Figure 6.8. For this EFD, the Nylon mesh was soaked once with Orgacon doped with 5% DMSO and dried overnight. The precursor was then sprayed onto one piece of Nylon and converted. Normal gel was drop coated onto each piece separately and cured, followed by curing the pieces together.

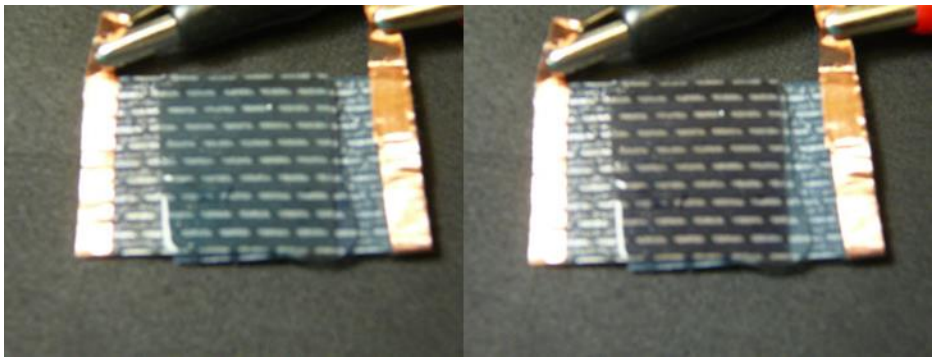

Figure 6.8: Precursor on Nylon with normal gel.

For the following device, two pieces of spandex that were 1” x 1” were treated with Orgacon doped with 5% DMSO. The precursor was applied to one piece of spandex and the device was assembled using the normal gel.

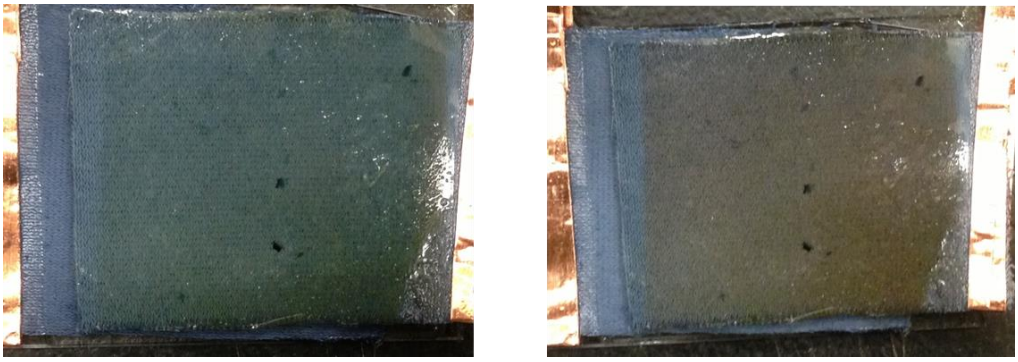

Figure 6.9: Precursor on spandex with normal gel.

While the normal gel is a good match for a window type electrochromic device, it is not flexible or stretchable, making it unsuitable for an EFD. When the Nylon and PET fabrics are bent, cracks appear in the normal gel. For an EFD using spandex, a stretchable electrolyte would be ideal. Additionally, the precursor slightly dissolved into the normal gel matrix, turning the gel a light yellow color.

6.4.2 Devices Made with Diluted CleviosPH1000

Devices were made with the diluted solutions of CleviosPH1000 and normal gel, which was removed from the top of the devices with a razor blade. The device made with the 25% CleviosPH1000 solution was slow and had only a very light PEDOT:PSS electrochromic color change. The device made with the 50% CleviosPH1000 solution was quick and had a noticeable PEDOT:PSS color change (Figure 6.10). The device made with the 75% CleviosPH1000 solution was quick but had poor contrast (Figure 6.11). The device made with 100% CleviosPH1000 had no discernable color change.

Figure 6.10: Spandex EFD made with a 50% CleviosPH1000 solution and normal gel.

Figure 6.11: Spandex EFD made with a 75% CleviosPH1000 solution and normal gel.

6.4.3 Stretchable Gel EFDs

The stretchable gel in this section was a variation of the normal gel. The mixture contains 3g propylene carbonate, 7g PEGMA, 1g LITRIF, and 17.5mg of 2,2-dimethoxy-2-phenylacetophenone. When this gel is cured, it is able to flex and is slightly stretchable.

For the device in Figure X, Clevios was diluted to a 50% Clevios, 50% deionize water solution and then doped with 5% DMSO. Spandex was treated with this solution and allowed to air dry overnight. The stretchable gel was drop coated onto each piece of spandex separately and cured, then the pieces were cured together.

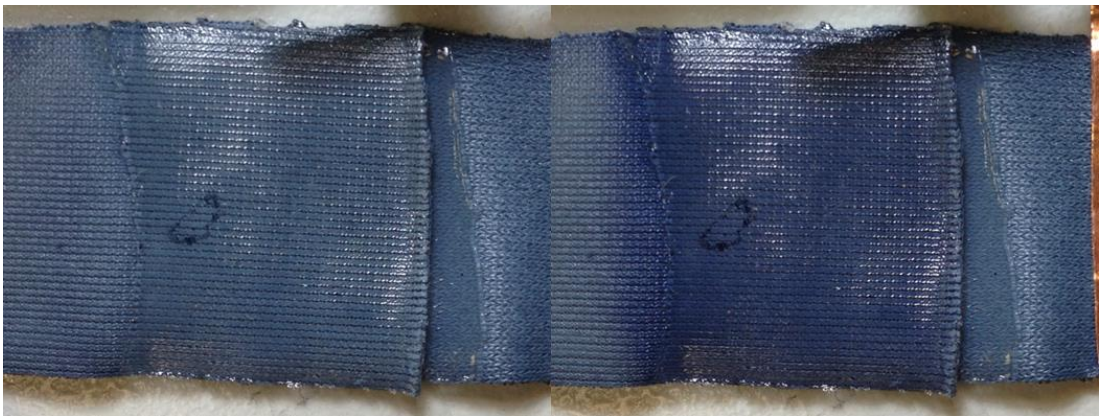

Figure 6.12: PEDOT:PSS EFD with stretchable gel.

A demonstration of the stretchable gel and spandex device being stretched can be seen in Figure X.

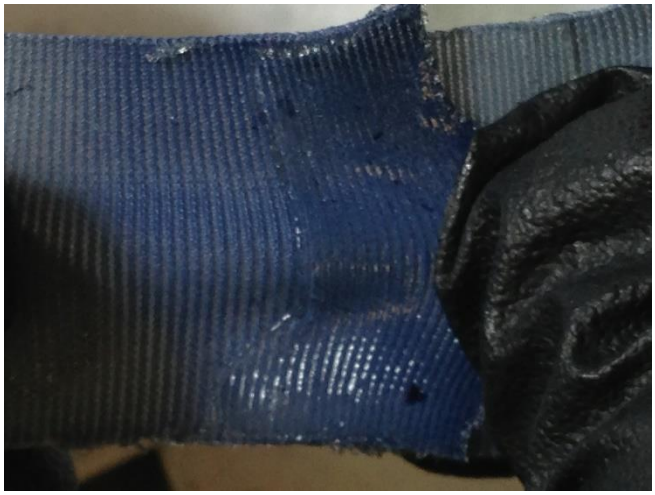

Figure 6.13: Stretching the stretchable gel.

One problem with this stretchable electrolyte is that the spandex loses the feel of spandex. The shine from the gel coating can be seen in the device above. This effect can be lessened by either peeling the top layer off with a razor blade (which would remove a precursor coating), or by carefully adding a lesser amount of gel.

A precursor device was attempted with the stretchable gel, but the precursor dissolved into the gel almost immediately. In Figure 6.14, a slight red tint from the precursor can still be seen in the left image.

Figure 6.14: Precursor and stretchable gel EFD on spandex.

6.4.4 Problems with Photoinitiators in EFDs

The biggest issue with using a photoinitiated electrolyte in an EFD is that fabrics have varying degrees of resistance to UV. The amount of resistance to UV depends on the material, the type of weave, thickness of the fabric, UV absorbing additives, etc.

Each of the fabric devices pictured in Sections 6.4.1 - 6.4.3 were not fully cured together. When the stretchable gel was stretched, the pieces of fabric are pulled apart (seen slightly in Figure 6.13).

Another issue is getting the gel to cure and remain adhered to the fabric. When the fabric pieces are placed on glass, large chunks of electrolyte are easily removed with the glass is removed (Figure 6.15). When glass was replaced with a flexible plastic for curing, this problem was mitigated.

Figure 6.15: Problems photocuring gel on fabric.

6.4.5 Need for a Stretchable Gel & Retaining Feel of Fabric

An EFD was made using only ionic liquid to demonstrate that an electrochromic response occurs (Figure 6.16). This device was made with the 50% CleviosPH1000 solution. The problem with such a device is that the ionic liquid is just that, a liquid. A possible coating could be applied to the fabric to seal in the ionic liquid, but that again would affect the feel of the fabric.

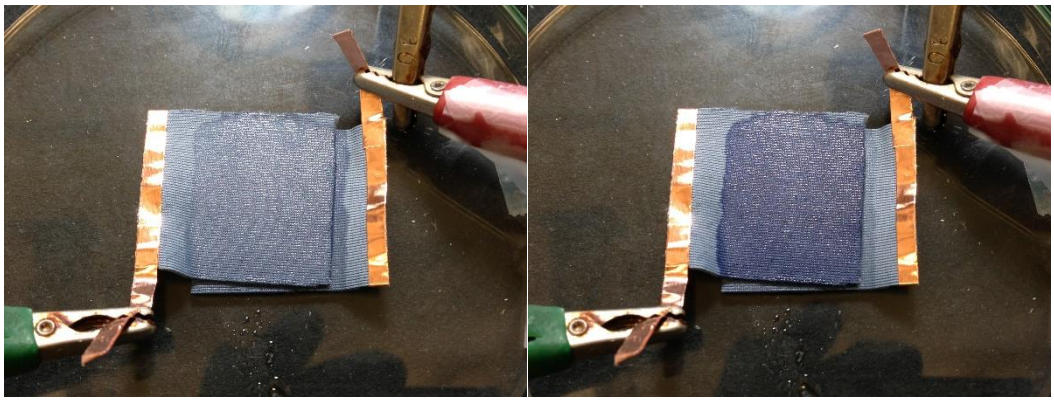

Figure 6.16: 50% CleviosPH1000 device using only ionic liquid.

6.5 Synthesis & Characterization of Polyurethanes

6.5.1 Making a Stretchable Electrolyte

Polyurethanes were examined for use in a stretchable electrolyte for many reasons. They are easily synthesized in high purity, stretchable, transparent, and electrochemically inert in the desired range.

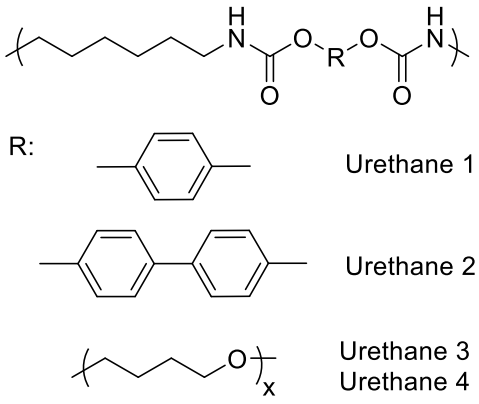

Figure 6.17: Polyurethane gel structures, where, x ≈ 28 (left).

There are many different polymers that could be an appropriate choice, as well as many options for molecular weights and chain extenders. The materials in Figure 6.17 were chosen as a first step towards a stretchable polyurethane electrolyte.

6.5.2 Synthesis of Polyurethanes

For the stretchable electrolyte matrix, polyurethanes were synthesized with and without aromatic chain extenders, and were compared with respect to ionic conductivity and ability to stretch. The polyurethanes were synthesized by reacting the 5 mmol of the corresponding diols and 5 mmol HDI in 10 mL DMAc. Polyurethanes 1 and 2 used hydroquinone and 4,4’-biphenol, respectively, as chain extenders (CE) in a 1 CE: 1 Poly(THF) : 2 HDI ratio. Polyurethane 3 was synthesized with equimolar amounts of Poly(THF) and HDI. Oligomeric urethane 4 was synthesized in a 2 Poly(THF) : 1 HDI ratio. In all cases, a catalytic amount (3 drops) of dibutyltin dilaurate was added to facilitate polymerization. The materials were combined in a flame-dried, nitrogen-purged 3-neck flask equipped

with a gas inlet, rubber septum and glass stopper. They were heated in an oil bath at 70°C for 1 hour before the chain extenders were added. The reaction was allowed to proceed for an additional 3 hours, before quenching with methanol (2 mL), precipitation in methanol (~100 mL) and filtration with a Büchner funnel, followed by copious washing with methanol.

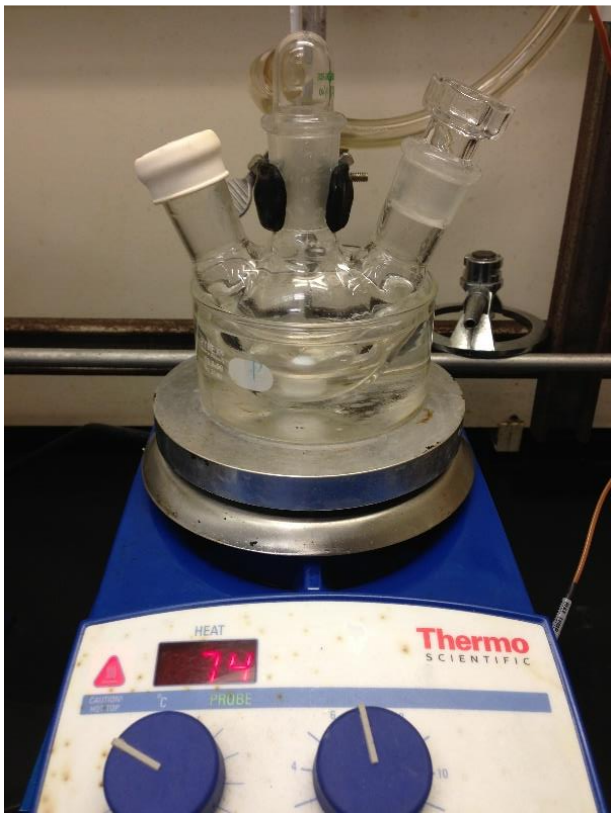

Figure 6.18: Setup for polyurethane synthesis.

Figure 6.19: Polyurethanes 1 (top left), 2 (top right), 3 (bottom left), and 4 (bottom right) after synthesis.

Thermogravimetric analysis (TGA) was conducted in nitrogen using a TA Instruments TGA Q500, at a heating rate of 10°C/min from room temperature to 600°C. Differential scanning calorimetry (DSC) was conducted in nitrogen using a TA Instruments DSC Q100 at a heating/cooling of rate 10°C/min. The samples were first heated to 100°C to clear the thermal history, then were cooled to -25°C. The presented glass transition and melting temperatures (Table 6.1) were obtained on the second heating scan, from -25°C to 250°C.

All polyurethanes had a melting point around 20°C, which corresponds to the Poly(THF) used in the synthesis. Polyurethane 2 displayed a glass transition temperature at 107°C and a melting point of 203°C. All other polymers did not

show glass transition temperatures or melting points. Upon testing the first three polyurethanes, it was found that they lacked the ability to stretch enough to accommodate the high strain of the spandex used in the device. Polyurethane 4 was synthesized as a 2:1 diol/diisocyanate oligomer to mitigate this problem, and was ultimately selected as the most suitable candidate because of its superior elasticity.

Polyurethane	T_d (°C) 3% Weight Loss	Ionic Conductivity (S/cm) Liquid	M_n (g/mol)	M_w (g/mol)
1	221	1.51E-04	8700	23790
2	238	1.82E-03	20920	49580
3	198	1.00E-03	38290	83900
4	278	1.11E-03	3850	8220

Table 6.1: Degradation temperature, ionic conductivity and molecular weight data for synthesized polyurethanes.

The ionic conductivity was also measured. For each device, 125 mg of polyurethane was first dissolved in 1.25 mL DMAc, followed by the addition of 20 mg of BMIM. The mixture was thoroughly stirred until homogeneity was achieved. The polyurethane/ionic liquid solution was placed in a stainless steel cell with a diameter of 2 cm and depth of 5.442 mm. The frequency was increased between 100 Hz and 1 MHz at an amplitude of 20 mV using a 4284A Precision LCR Meter. The impedance (Z) and degrees (Θ) were measured and

the conductivity was calculated from $\sigma = \frac{L}{AR}$, where *L* is the depth of the cell in cm, *A* is the area in cm^2, and *R* is the resistance in Ω. The resistance is equal to the impedance at high frequency, when Θ approaches zero. Differences in the ionic conductivity are at least partially from tiny differences in the amount of ionic liquid.

6.5.3 EFDs With Polyurethane Gels

For the electrolyte matrix used in the following EFDs, the polyurethanes were dissolved in a small amount of dimethylacetamide (DMAc), and 1-butyl-3-methylimidazolium hexafluorophosphate (BMIM) ionic liquid was added to yield a 0.1M solution.

Figure 6.20: 50% CleviosPH1000 device with polyurethane 1 electrolyte.

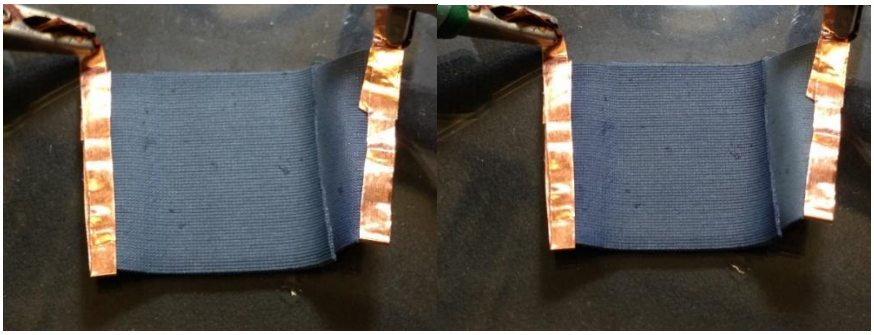

Figure 6.21: 50% CleviosPH1000 device with polyurethane 2 electrolyte.

Polyurethane 3 was too high of a molecular weight to fully dissolve in DMAc and then appeared jelly-like when used in a device. The devices made with the first three polyurethanes all worked while the electrolyte was saturated with DMAc, but as the solvent evaporated the devices became rigid and stopped working. However, the urethanes were not as stretchable as the stretchy gel even when saturated. Additionally, the spandex electrodes did not stick together while the urethanes were wet, but did stick together as the electrolyte dried. Tetraglyme was used instead of DMAc, however the polyurethanes appeared somewhat yellow in this solvent, possibly from interactions between the leftover tin catalyst and the solvent.

Figure 6.22: DMAc (left) versus Tetraglyme (right) polyurethane gel.

Next, an oligomeric urethane was made to increase the stretchability of the electrolyte. The device made with polyurethane 4 was able to stretch even as the electrolyte dried, making it a good choice for an EFD.

Figure 6.23: Orgacon PEDOT:PSS device in oxidized (left) and reduced (right) states with polyurethane 4 electrolyte.

6.6 Preventing the Electrodes from Pulling Apart

6.6.1 Sewing by Hand

In order to be able to stretch an EFD without pulling the fabric pieces apart, the fabric electrodes were sewn together. Several devices were stitched by hand to find out if the stitches would cause a short in the device. The first device, made with the stretchable gel, only partially switched. Another device with precursor and a polyurethane 1 tetraglyme electrolyte also only partially switched. At this point, it was unclear whether the stitching caused a short in the device by interfering with charge transfer or by causing fibers in the spandex electrodes touch.

Figure 6.24: Stitching on a 50% CleviosPH1000 device with stretchable gel.

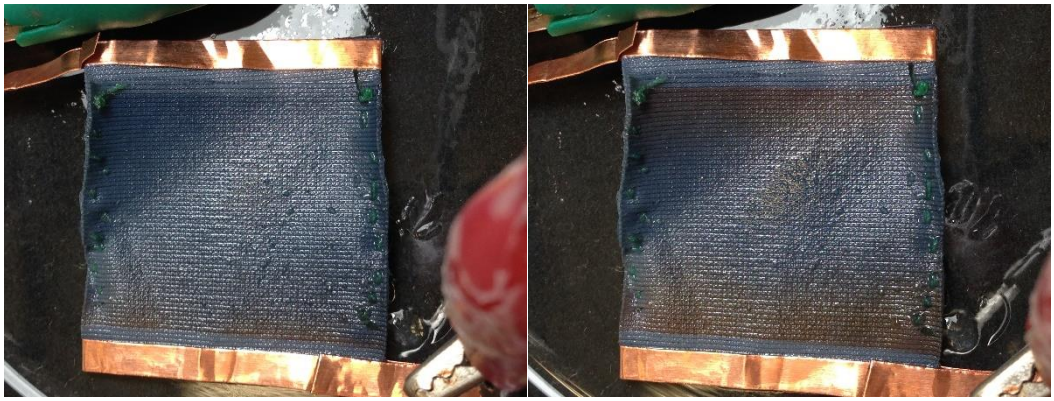

Figure 6.25: Precursor spray coated on a 50% CleviosPH1000 device with polyurethane 1 and tetraglyme electrolyte.

A device made with the normal gel was stitched in an *X* pattern and completely switched. There was no shorting around the stitches, indicating that sewing a device does not interfere with charge transfer. Since the normal gel has a more defined layer between the spandex electrodes, materials were explored to use as a middle layer in an EFD.

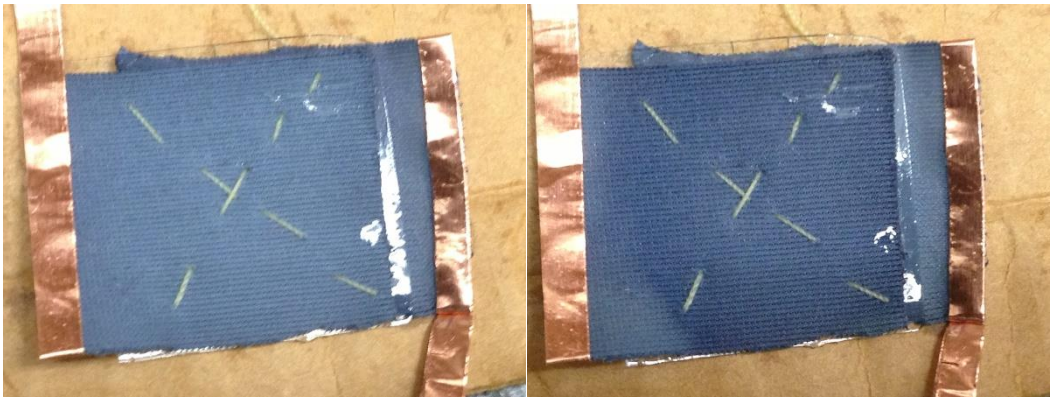

Figure 6.26: Stitching on a 50% CleviosPH1000 device with normal gel.

6.5.2 Sewing Machine & Adding a Middle Layer

A Brother CS-6000i electric sewing machine was purchased to sew the fabric together. Additionally, several stretchable fabrics were sewed inbetween the spandex electrodes to prevent shorting. When a third layer of spandex was placed between the spandex electrodes, the device did not work, suggesting the layer was too thick. Next, pantyhose and tights were tried but the devices still shorted. Finally, a polyester trouser sock was used as the middle layer, which successfully stopped the shorting.

Figure 6.27: Trouser sock.

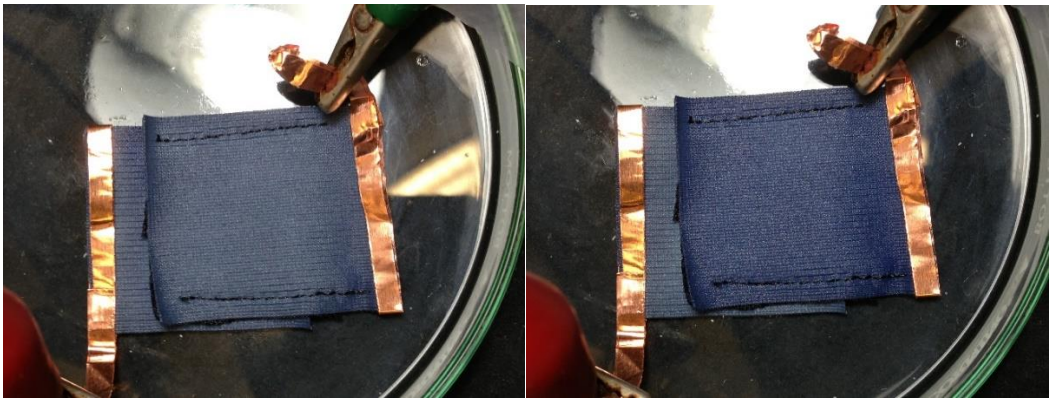

Figure 6.28: Sewn 50% CleviosPh1000 device in oxidized (light blue, left) and reduced (dark blue, right) states with polyurethane 4 electrolyte and polyester middle layer.

6.6 Preparation of Stretchable, All-Organic EFD

With the new middle layer and the precursor added to a sewn device, the schematic changes to that depicted in Figure 6.29.

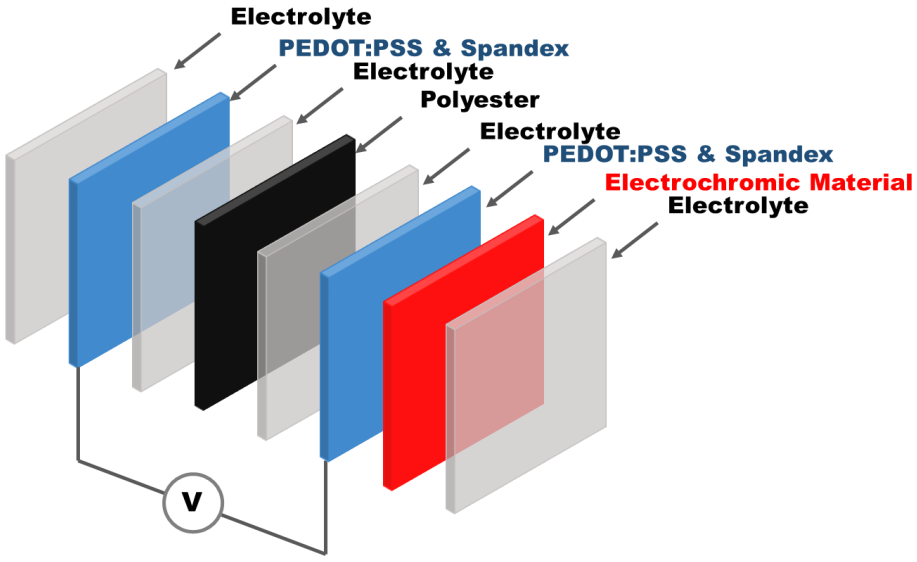

Figure 6.29: Schematic of sewn precursor EFD.

Two pieces of PEDOT:PSS-soaked spandex were sewed together with a thin piece of stretchable polyester fabric between them to prevent the electrodes from touching, leading to a short circuit. Solutions of the precursor polymer poly(bis[3,4-ethylenedioxythiophene]-thiophene-dioctylsilane) (PBEDOT-T-Si[Octyl]$_2$) were prepared in DCM, and were spray coated onto one side of the assembled device. The precursor polymer was oxidatively converted to fully conjugated polymer by spray coating with a solution of $FeCl_3$ in ACN, and was thoroughly washed with ACN. The device was allowed to dry for 30 minutes, after which copper tape was wrapped around the end of each spandex electrode. Each step of the device assembly can be seen in Figure 6.30.

Figure 6.30: Device assembly steps: conductive spandex (top left), spandex electrodes and middle layer sewed together (top right), spray coated with precursor (bottom left), converted precursor (bottom right).

To complete the assembly, the device was saturated with the polyurethane 4/ionic liquid solution, and was connected to a CHI 400A potientiostat; the device switched from the neutral to oxidized states between -2 and 2V. The first device was made with 40 mg of precursor and only a faint change in color could be seen (Figure 6.31).

Figure 6.31: EFD in the neutral (top left), oxidized (top right) and neutral stretched (bottom) states.

The next EFD was made with 80 mg of precursor. The device successfully switched for 5 charging/discharging cycles before deleterious effects on the color swing were noted. The Lu'v' coordinates were determined using a colorimeter,

and for the neutral state were L=26.2, u'=0.1892, v'=0.4701, while the coordinates for the oxidized state were L=26.6, u'=0.2341, v'=0.5061.

Figure 6.32: EFD in the neutral (red) and oxidized (blue) states.

6.7 Looking Foward

6.7.1 Dying the Spandex

A yellow dye (Figure 6.33) was added to the fabric to test the change in electrochromic color. The dye was mixed into the PEDOT:PSS solution before saturating the fabric.

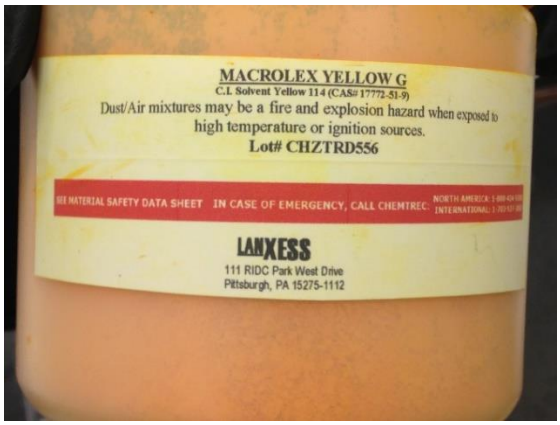

Figure 6.33: Yellow dye.

The first device was assembled with normal gel, however the gel never properly cured, possibly due to extra UV absorbance or blocking from the addition of the yellow dye.

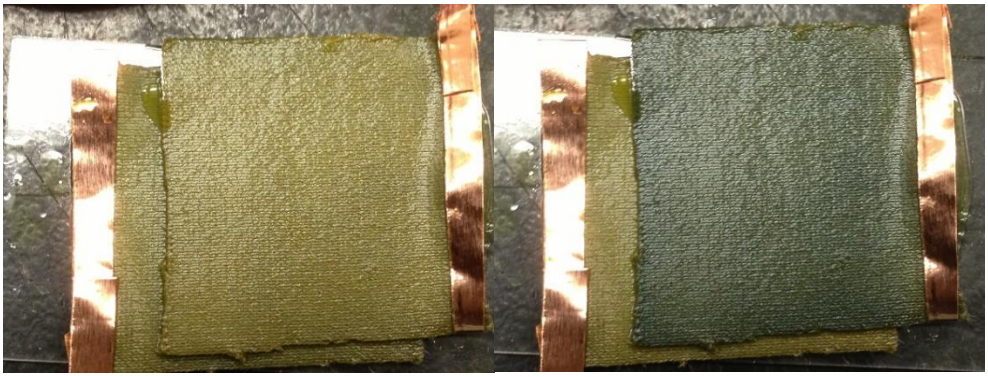

Figure 6.34: Dyed EFD with 50% CleviosPH1000 and partially cured normal gel.

The next device was assembled with a flexible gel very similar to the normal gel, however it pulled the dye out of the fabric.

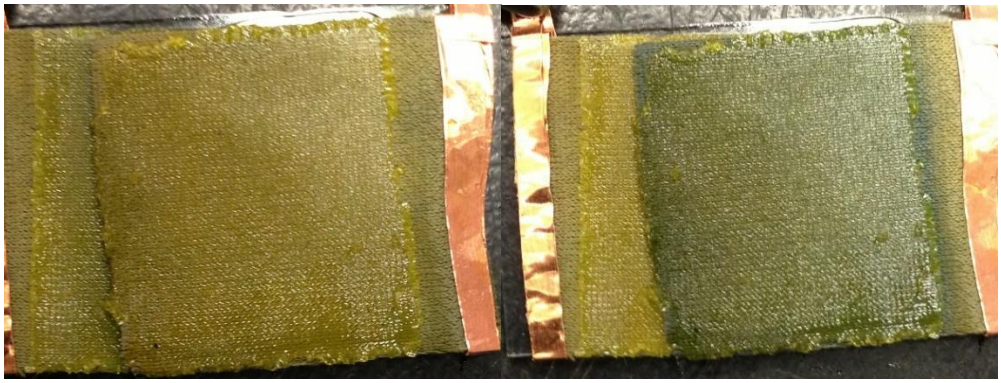

Figure 6.35: Dyed EFD with 50% CleviosPH1000 and flexible gel.

This could be an alternative to an additional electrochromic material with the right concentration of dye and the right electrolyte.

6.7.2 Problems with the Current EFD

The current method of assembling an EFD is not without its flaws. When there is too much space between the stitching or the fabric isn't perfectly flat when sewing, there is often poor contact between the spandex electrodes, leading to an area that does not electrochromically switch in the middle of the device.

Devices made with the normal and the stretchable gel still worked a month later. Because the polyurethane electrolyte is not a crosslinked network, the EFD experiences charge dissipation and has a very short lifespan. Adjusting the polyurethane electrolyte to include small amounts of a crosslinking agent could help increase the lifespan of an EFD. The balance with including crosslinks in the

electrolyte would have to be found for retaining the feel of the fabric, yet allowing for a longer working period.

6.8 References

[1] Kline, W.M.; Lorenzini, R.G.; Sotzing, G.A. *Color. Technol.* 2014, 130, 1-8

[2] Kim, J.; You, J.; Kim, B.; Park, T.; Kim, E. *Adv. Mater.* 2011, 23, 4168-4173

[3] Pang, C.; Lee, C.; Suh, K.Y. *J. Appl. Polym. Sci.* 2013, 3, 1429-1441

[4] Jensen, J.; Krebs, F.C. *Adv. Mater.* 2014, doi: 10.1002/adma.201402771

[5] Chen, X.; Lin, H.; Deng, J.; Zhang, Y.; Sun, X.; Chen, P.; Fang, X.; Zhang, Z.; Guan, G.; Peng, H. *Adv. Mater.* 2014, doi: 10.1002/adma.201403243

[6] Shim, B.S.; Chen, W.; Doty, C.; Xu, C.; Kotov, N.A. *Nano Lett.* 2008, 8, 4152-4157

[7] Kim, D.H.; Rogers, J.A. *Adv. Mater.* 2008, 20, 4887-4892

[8] Jost, K.; Dion, G.; Gogotsi, Y. *J. Mater. Chem. A* 2014, 2, 10776-10787

[9] Beaupré, S; Dumas, J.; Leclerc, M, *Chem. Mater*. 2006, 18, 4011-4018

[10] Zhang, Q.; Xin, B.; Lin, L. *Advd. Mater. Res.* 2013, 651, 77-82

[11] Kelly, F.M.; Meunier, L.; Cochrane, C.; Koncar, V. *Displays* 2013, 34, 1-7

[12] Kelly, F.M.; Meunier, L.; Cochrane, C.; Koncar, V. *J. Display Technol.* 2013, 9, 626-631

[13] Meunier, L.; Kelly, F.M.; Cochrane, C.; Koncar, V. *Indian J. Fibre Text.* 2011, 36, 429-435

[14] Li, X.; Zhao, G.; Qian, J.; Fu, Z. *J. Chin. Univ.* 2009, 30, 1052-1054

[15] Li, X.; Qian, J.; Fu, Z. *J. Beijing Inst. Clothing Technol.* 2009, 29, 12-17

[16] Molina, J.; Esteves, M.F.; Fernández, J.; Bonastre, J.; Cases, F. *Eur. Polym. J.* 2011, 47, 2003-2015

[17] Mokhtari, J.; Nouri, M. *Fibers Polym.* 2012, 13, 139-144

[18] Invernale, M.A.; Ding, Y.; Sotzing, G.A. *ACS Appl. Mater. Interfaces* 2010, 2, 296-300

[19] Ding, Y.; Invernale, M.A.; Sotzing, G.A. *ACS Appl. Mater. Interfaces* 2010, 2, 1588-1593

[20] Sonmez, G.; Shen, C.K.F.; Rubin, Y.; Wudl, F. *Angw. Chem. Int. Ed.* 2004, 43, 1498-1502

[21] Ding, Y.; Invernale, M.A.; Mamangun, D.M.D.; Kumar, A.; Sotzing, G.A. *J. Mater. Chem.* 2011, 21, 11873-11878

[22] Sotzing, G.A.; Reddinger, J.L.; Katritzky, A.R.; Soloducho, J.; Musgrave, R.; Reynolds, J.R. *Chem. Mater.* 1997, 9, 1578-1587

[23] Invernale, M.A.; Ding, Y.; Mamangun, D.M.D.; Yavuz, M.S.; Sotzing, G.A. *Adv. Mater.* 2010, 22, 1379-1382

Appendix

This section was created based on requests for clarification from the advisory committee during the final defense. This section contains supplementary information for Chapters 5-6.

Direct Current vs Alternating Current

All of the experiments in this thesis were conducted with direct current. The question was raised as to whether alternating current would change the resistive heating properties or lessen the over-polarization sometimes present in electrochromic devices.

The difference between direct current (DC) and alternating current (AC) is the direction in which the electrons flow. In DC, the electrons flow steadily in a single direction whereas in AC, electrons keep switching directions. Direct current (DC) is most commonly used in small electronic devices, such as computers, telephones, and automotive systems. Batteries, fuel cells, and solar cells all produce DC in that the positive and negative terminals are always positive and negative, respectively, and current always flows in the same direction between those two terminals. Alternating current is the distribution method used for the transmission of energy from power plants into homes. For example, the current direction in AC alternates 60 times per second in the U.S.

If AC was used in the resistive heating experiments at a high enough frequency, the results would be the same, assuming the RMS (root mean square) value of the supplied voltage is the same. However, at a lower frequency, and due to the

sinusoidal shape of the current, reaching a maximum temperature via resistive heating would take longer. It's also possible that the longevity of the devices may be increased as less time is spent at potentially oxidizing voltages.

If AC were used in an electrochromic device, the over-polarization problem might be mitigated. However, if a device requires a certain amount of charge to switch, it could take longer to reach that level of charge in AC with a low frequency.

Copper vs. Other Metals

Copper was used to make connections via wires in the resistive heating samples and as tape in the EFDs. The resistivity is used to compare metals because it is a property that is inherent to the material. Conversely, the resistance is the property of a material that resists electron flow, so a longer material would have more resistance than a short one. The material with the lowest resistivity (most conducting) is silver, followed by copper, aluminum, tungsten, iron, and platinum. This means that if silver were used instead of copper in these devices, there would be less contact resistance.

Charge in EFDs

The charge for three devices is shown below in Figure A.1. All three devices are spandex devices with the polyester middle that have been sewn together. The curve labeled "PEDOT:PSS" is the charge required for only the PEDOT:PSS device to switch. The curve labeled "40 mg" is a precursor device made with 40 mg of precursor, and the curve labeled "80 mg" is a precursor device made with 80 mg of precursor.

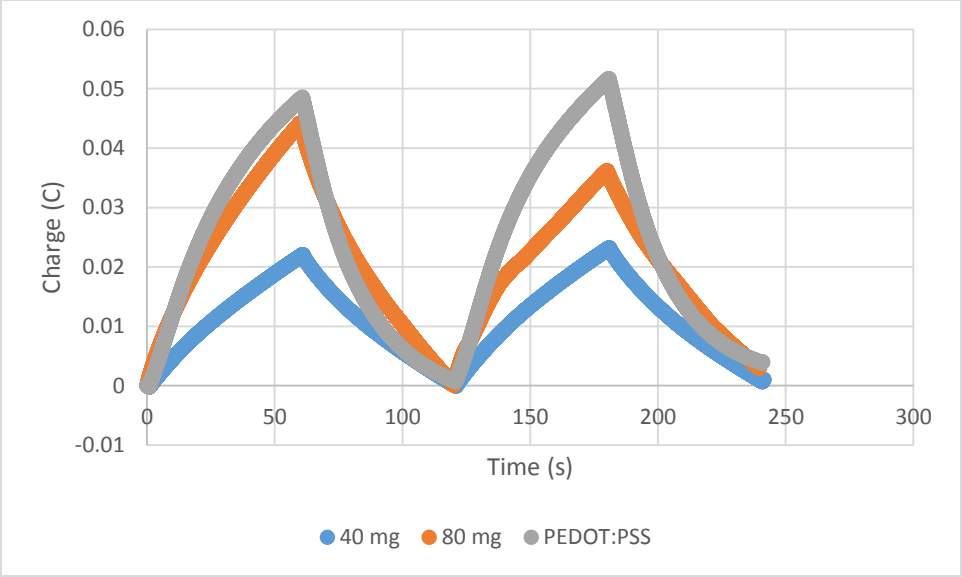

In the PEDOT:PSS device, the PEDOT:PSS is changing color as well as carrying the charge. In the precursor devices, the PEDOT:PSS has been coated with the electrochromic material and now only needs to transport charge. Additionally, the 80 mg device requires more charge than the 40 mg because it has a thicker layer of electrochromic polymer.